PRO-INFLAMMATORY TRANSFORMING GROWTH FACTOR BETA SIGNALLING AS A THERAPEUTIC TARGET FOR REPETITIVE MILD TRAUMATIC BRAIN INJURY

by

Ellen VF Parker

Submitted in partial fulfilment of the requirements
for the degree of Doctor of Philosophy

at

Dalhousie University
Halifax, Nova Scotia
July 2019

For the first people to make neuroscience matter to me

My grandmothers,

Reta Grace Ferguson and Betty Anne Parker

TABLE OF CONTENTS

LIST OF TABLES

LIST OF FIGURES

ABSTRACT

Traumatic brain injury (TBI) occurs in an estimated 50-60 million people annually, making it a major global health concern. Despite growing awareness of the risks associated with repetitive mild traumatic brain injury (rmTBI) and concussion, there remain significant unknowns regarding the mechanisms underlying the acute and delayed complications of these events. Moreover, there are currently no approved therapies for the treatment or prevention of the pathological sequelae of rmTBI.

This thesis sought to investigate the role of pro-inflammatory transforming growth factor beta (TGFβ) signalling in rmTBI and evaluate its potential as a novel treatment strategy for rmTBI-associated complications. To address these questions, I established and characterized a rodent model of rmTBI that recapitulates the clinical spectrum of outcomes that are commonly observed following concussion and mild brain trauma (Chapter 2). To further characterize this heterogeneity, retrospective grouping of animals as "sensitive" to the acute neurological consequences of rmTBI versus those "resilient" to these effects was performed. This approach revealed that acute neurological outcomes of rmTBI were not predictive of delayed deterioration, suggesting that the mechanisms underlying chronic neurological consequences of rmTBI occur in the absence of overt acute neurological signs. In Chapter 3, the mechanisms underlying acute sensitivity to rmTBI were explored. I showed that pathological increases in blood-brain barrier dysfunction (BBBD), TGFβ signalling, reactive gliosis, and neuroinflammation following rmTBI are associated with a more severe clinical outcome (sensitivity) during the acute phases of injury. Thus, I tested the effect of two TGFβ antagonists, IPW and losartan, as therapeutic approaches for the treatment and prevention of rmTBI-associated complications (Chapter 4). While slight differences in effects were observed for each of these treatments, I found that antagonism of TGFβ signalling was successful in improving acute outcomes, including post-impact convulsions and early recovery following injury. Further, antagonism of TGFβ signalling protected the integrity of the blood-brain barrier and prevented delayed neurological and cognitive complications of repetitive injury. Together, my findings highlight the potential of TGFβ antagonism as a future therapeutic strategy for complications of rmTBI.

LIST OF ABBREVIATIONS USED

ACRM	American Congress of Rehabilitation Medicine
ANOVA	Analysis of variance
ATP	Adenosine triphosphate
BBB	Blood-brain barrier
BBBD	Blood-brain barrier dysfunction
CAD	Canadian dollars
CCI	Controlled cortical impact
CDC	Centers for Disease Control and Prevention
CHI	Closed head injury
CISG	Concussion in Sport Group
CNS	Central nervous system
COX	Cyclooxygenase
CSF	Cerebrospinal fluid
CTE	Chronic traumatic encephalopathy
DAI	Diffuse axonal injury
DAMP	Damage-associated molecular pattern
DCE-MRI	Dynamic contrast-enhanced magnetic resonance imaging
DOD	Department of Defence (USA)
DPI	Dots per inch
DTI	Diffusion tensor imaging
EEG	Electroencephalogram
FPI	Fluid percussion injury
Fps	Frames per second
GCS	Glasgow Coma Scale
GFAP	Glial fibrillary acidic protein
HMGB1	High-mobility group box protein 1
Iba-1	Ionized calcium binding adaptor molecule 1
IL	Interleukin
IP	Intraperitoneal
IPW	IPW-5371
IV	Intravenous
LOS	Losartan
MAPK	Mitogen-activated protein kinase
MMP-9	Matrix metalloproteinase 9
MPa	Megapascal
MR	Magnetic resonance
MRI	Magnetic resonance imaging
MWM	Morris water maze
NIH	National Institutes of Health

LIST OF ABBREVIATIONS USED (Cont.)

PFA	Paraformaldehyde
RAGE	Receptors for advanced glycation end products
RES	Resilient
RIPA	Radioimmunoprecipitation assay buffer
rmTBI	Repetitive mild traumatic brain injury
ROS	Reactive oxygen species
RT-qPCR	Real-time quantitative polymerase chain reaction
SCAT	Sideline concussion assessment tool
SD	Spreading depolarization
SDS-PAGE	Sodium dodecyl sulfate polyacrylamide gel electrophoresis
SEM	Standard error of the mean
SENS	Sensitive
SHAM	Sham control
SIS	Second impact syndrome
SM	Sensorimotor
Smad	Mothers against decapentaplegic homolog
TBI	Traumatic brain injury
TBST	Tris-buffered saline with tween
TGFβ	Transforming growth factor beta
TLR	Toll-like receptor
TNFα	Tumor necrosis factor alpha
USD	United States dollars
VA	Veterans Affairs (United States Department of)
VEH	Vehicle control
WHO	World Health Organization

ACKNOWLEDGEMENTS

Dr. Alon Friedman: Thank you. For fostering a research environment in which I was challenged every day and for giving me the space to grow scientifically with your guidance. Also, thank you for helping me develop a tougher shell than when I walked into 12H and your office for the first time. As you know, an endless supply of coffee, Welch's, and sarcasm kept me going.

Committee members and others: Dr. Sultan Darvesh, Dr. Alexander Easton, Dr. Ramon Diaz-Arrastia, Dr. Kazue Semba, Dr. William Baldridge – thank you for your time, your guidance, and your support.

Kay Murphy (lab mom extraordinaire): I have said it many times before – you are the best teacher I have ever had. Your ability to know precisely when to challenge and when to comfort is unparalleled. Your belief in me never faltered, even if mine did. Thank you most of all for teaching me about myself. Many memorable laughs, snacks, and jibjabs were had. I won't forget our moments together from when we were kids: you were my literal arms and legs. I could not and would not have done this without you.

Fellow members of the Friedman lab: Refa't, Lyna, Jim, Shayna, Olumide, Pooyan – thank you for your support of me and this work, your many contributions and patience did not go unnoticed. A special shout out is warranted to the incredible past and present undergrads who have contributed countless hours to this project. Jill, Klara, Griffin, Isabelle – perhaps without knowing it, or perhaps out of pity, you each gave me a valuable gift: you made the lab fun for me. Thank you. I can't wait to see where each of you go from here (but first, there is more work to do).

The Israeli contingent and others: Ofer, Noa, Jonathan, Evyatar, Dan, Erez, Yonatan, Dror, and Karl. One of the most enjoyable parts of this experience has been meeting you, sharing ideas, and collaborating together. Thank you for your continued guidance and inspiration.

The Berkeley group: Dr. Daniela Kaufer. Vlad, Aaron, Jessica, Lynn, Ally, Shawn, and others. Thank you for welcoming me into your lab with open arms and providing me with every tool, tip (pipette or otherwise), and trick needed to complete my experiments. And although the science was good, the boba was best.

The staff of Animal Care: Belinda, Allison, Sue, Barb and others. Thank you for your support of this project and for gracefully tolerating the steady expansion of the Friedman lab. Also special thanks to Bud from his ever-growing fan club. Needless to say, we could not do our work without your expertise.

My best friends: Sophie, thank you for being everything I could have asked for in a best friend. I am forever grateful for the piggy tails of '99 that brought us together. Tareq: None of this madness would have been possible without you and I can't seem to decide if that's good or bad. You are my favourite witch, tailleur vigne, and dead one. Versalove, MMP, Sport, and Mary's bologna will continue, don't worry. Helena and Caila: we were apart, but I felt your love behind me each day. You all amaze me.

My parents: Ever my biggest cheerleaders and sounding board, this would not have been possible without you. Mom, only you could be so present (between the heartbeats) with me even from afar. Dad, you put me together again with many necessary cottage "rehabs" and pep talks throughout this process. Ulla, your laughter and overall positive outlook kept me going more than you know. Thank you all for inspiring me, making me laugh, and supporting me without hesitation every step of the way. I could not have gotten luckier to have you as my family.

And finally, Hayden: Your unwavering support of my goals appears to have no bounds. I am so grateful for you and so proud of the person that you are. I can't wait for us to find a balance between Terra Nova and Paradise Falls to call our own. I'll meet you there.

CHAPTER 1:
INTRODUCTION

1.1 Overview: Traumatic Brain Injury

The brain is a highly complex structure composed of a vast array of cells, including neurons, astrocytes, microglia, oligodendrocytes, and ependymal cells. It is estimated that there are approximately 85 billion neurons in the adult brain, with an equal number of glial cells (Herculano-Houzel, 2009). These numerous cells are supplied by a rich vasculature with incredible density: the total length of capillaries in the brain is approximately 600 kilometers long (Zlokovic, 2005). Additionally, a continual bath of cerebrospinal fluid (CSF) circulates within the ventricles, subarachnoid space, and brain parenchyma (Brodbelt and Stoodley, 2007). Surrounded by the meninges and encased by the skull, this remarkable density of cellular, vascular, and fluid components form the structure of the brain. Critically, each of these components are subject to pathological impairment when traumatic brain injury (TBI) occurs.

The Centers for Disease Control and Prevention (CDC) defines TBI as the impairment of normal brain function due to external trauma of the head. This trauma can result when the head is suddenly shaken or impacted due to an external mechanical force or penetrating injury (CDC). The application of these forces can lead to shearing and compressive strain of brain tissue, which can directly and rapidly impair function and may lead to lasting structural and functional complications.

1.2 Epidemiology of TBI

TBI is a major global health concern: an estimated 50-60 million new cases of TBI occur each year, resulting in hospitalization or death in approximately 10 million people annually (Cassidy et al., 2004; Hyder et al., 2007; Roozenbeek et al., 2013; Maas et al., 2017). The CDC estimates that 1.7 million Americans sustain a TBI annually, of which 1.4

million are treated in emergency care settings (Roozenbeek et al., 2013). In Canada, approximately 50,000 people sustain a TBI every year and it is estimated that over 190,000 Canadians are currently living with complications due to a previous TBI (Caro, 2011).

Mild TBI is the most common form of TBI and is thought to comprise as many as 90% of TBI cases (Blennow et al., 2016; Maas et al., 2017). In contrast, severe TBI is far less common but has a high mortality rate of 30-40% (Maas et al., 2017). For survivors of initial injury, lifelong disability is common following severe TBI. As such, TBI is a major contributor to global neurological disability (Roozenbeek et al., 2013; Maas et al., 2017). Survivors of TBI often experience significant physical, psychiatric, emotional, and cognitive disabilities. These challenges contribute to immeasurable disruptions in the lives of patients and their family members and pose significant costs to society (Maas et al., 2017). TBI costs the international economy $400 billion USD annually, which is estimated to be equivalent to 0.5% of the entire annual global output (Maas et al., 2017). In Canada, TBI is associated with a cost of $7 billion CAD owing to health care costs and life years lost (Caro, 2011).

1.3 Classification of TBI

TBI is a highly heterogeneous disorder that is typically classified by one of three systems: injury severity, physical mechanism, or pathophysiology (Saatman et al., 2008; Namjoshi et al., 2013).

1.3.1 Injury Severity

Clinically, TBI is often categorized by severity by using classification criteria relating to multiple factors including level of consciousness, amnesia, neurological

changes, and neuroimaging results (Blennow et al., 2016). The most commonly used tool to assess clinical severity of TBI is the Glasgow Coma Scale (GCS) (Teasdale and Jennett, 1974). The GCS assesses the level of consciousness of a patient by using a 15-point clinical scoring scale for behaviour relating to motor responsiveness, verbal ability, and eye opening (Blennow et al., 2016). The GCS broadly stratifies patients into categories of "mild", "moderate", or "severe" injury and allows for rapid symptom classification to facilitate diagnosis, treatment, and prognostic assessment (Shlosberg et al., 2010; Blennow et al., 2016). A maximum GCS score of 15 is possible and is assigned to a patient with minimal impairments in consciousness, although patients with a GSC score of 15 may still present with other neurological impairments, such as amnesia or confusion. Clinically, GCS scores ranging from 13 to 15 indicate a mild TBI, scores of 9 to 12 indicate a moderate TBI, and scores from 3 to 8 indicate a severe TBI (Teasdale et al., 2014).

Response Parameter	6	5	4	3	2	1
Eye Opening	-	-	Spontaneous	To Speech	To Pressure	None
Verbal	-	Oriented	Confused	Words	Sounds	None
Motor	Obeying commands	Localizing	Normal flexion	Abn. Flexion	Extension	None

(Adapted from Teasdale et al., 1974)

Table 1.1: The Glasgow Coma Scale

While widely used clinically and in research, the GCS has notable limitations. The GCS does not account for different populations affected by TBI and low GCS scores in children have been shown to be poor predictors of outcome (Lieh-Lai et al., 1992). Additionally, the GCS does not consider underlying pathological mechanisms of injury

severity and is often administered under clinical circumstances in which medications such as anesthetics, analgesics, and sedatives are involved. These limitations can alter the utility of the GCS and, from a research perspective, may hinder the translation of preclinical treatment strategies into successful clinical trials (Saatman et al., 2008; Shlosberg et al., 2010). Further, the utility of the GCS has been questioned for head injuries sustained in the context of sport, as these can be below the detection level of the GCS (Johnston et al., 2001; McCrory et al., 2013). Additionally, sports-related TBIs can have a fluctuating and variable time course of symptom presentation, further complicating accurate and consistent diagnosis with the GCS.

1.3.2 Physical Mechanism of Injury

Another approach to classifying TBI is by the physical mechanism of injury, such as closed-head, penetrating, or blast TBI. Blast injuries are a major cause of TBI in military personnel and can result from the initial blast wave of an explosion, acceleration and deceleration forces resulting from the blast, or from particulate matter striking the head (Goldstein et al., 2012; Rosenfeld et al., 2013). Penetrating injuries occur when the skull is fractured and there is perforation of the meninges due to high-pressure tissue penetration (Santiago et al., 2012). Penetrating TBIs are typically severe and require immediate medical attention (Black et al., 2002; Kazim et al., 2011). Closed-head injuries occur due to the application of mechanical forces to the brain and are the most common form of TBI in the general population (Kumar and Loane, 2012). These forces can be statically applied to a constrained head, such as in the case of a skull-crush injury, although these injuries are relatively uncommon in comparison to the application of dynamic forces to the head (Ommaya and Gennarelli, 1974; Tortosa et al., 2004).

The transmission of dynamic forces to the head can result from direct head contact or from inertial loading of the head (Cernak, 2005). Direct head contact injuries (in which physical contact is made to the head) can vary in the applied forces experienced during impact, such as in impact velocity, acceleration, duration, and magnitude. These dynamic forces can lead to translation and rotation of the head, which can further contribute to brain injury. Depending on the severity of impact, skull fracture, contusions, hematoma, and hemorrhage can ensue following direct head contact (Cernak, 2005; McAllister, 2011). Inertial loading of the head (in which the head undergoes relative motion compared to the body) involves acceleration and deceleration forces which often have translational and angular components (McAllister, 2011). Importantly, angular acceleration of the head can cause shear, tensile, and compressive strain during rotational motion (Gennarelli et al., 1982; Smith and Meaney, 2000; Meaney and Smith, 2011). In some cases, these forces can result in diffuse axonal injury (DAI) in which there is widespread damage to white matter tracts following TBI (Strich, 1956; Adams et al., 1982; Gennarelli et al., 1982; Adams et al., 1989).

Most closed-head TBIs involve both direct contact and inertial forces (Zhang et al., 2004). In the context of sport, this is often due to direct contact to the head or through impact to the body which can lead to inertial loading of the head. Both of these mechanisms can produce a dynamic combination of linear and acceleration forces experienced by the brain which can manifest clinically as focal or diffuse injuries (Rowson and Duma, 2013).

1.3.3 Injury Pathophysiology

TBI can be classified according to the time course of injury progression and underlying pathophysiological mechanisms that take place following injury. In particular,

primary injury refers to immediate and unavoidable damage to the integrity of brain structures that occurs at the earliest time following impact, whereas secondary injury refers to the ongoing and evolving process of damage that ensues following injury (Greve and Zink, 2009).

Primary injury in TBI can be classified based on the presence of focal or diffuse injury. Focal injuries include contusions, lacerations, hematomas, hemorrhage or brain herniation and can occur when forces acting on the skull compress underlying brain tissue at the site of impact (coup) or opposite to this site (contre-coup) (El Sayed et al., 2008; Andriessen et al., 2010). The pathology and neurological deficits that result from focal brain injury are related to the location and severity of impact (Andriessen et al., 2010). In contrast, diffuse brain injury can involve DAI, diffuse vascular injury, cerebral swelling and ischemia (Andriessen et al., 2010). Diffuse injuries arise when the head undergoes rapid acceleration and deceleration movements which cause the brain tissue to move relative to the skull and itself, leading to widespread brain dysfunction (Davis, 2000).

Secondary injury following TBI can develop as a result of events initiated by the primary injury and many common mechanisms are shared between these (Greve and Zink, 2009). The secondary injury phase can last for days to months post-impact and may involve edema, inflammation, and cell death (Pavlovic et al., 2019).

1.4 Sports and Mild TBI

Sports are a major cause of mild traumatic brain injury. In particular, contact sports such as boxing, football, hockey, lacrosse, soccer, and rugby, are all associated with an increased risk for TBI (Lincoln et al., 2011; Jordan, 2013). Sports-related TBI is particularly prevalent among young people. In the US, children and young adults younger

than 19 years of age accounted for two-thirds of emergency room visits for sports-related TBI between 2001 and 2012 (Coronado et al., 2015). Additionally, results from an 11-year prospective study observed 2651 concussions across 11 million athlete-exposures (defined as a single practice or game), which suggests an incidence rate of 24 concussions per 100,000 exposures (Lincoln et al., 2011). These figures only capture patients who sought medical attention for their injuries, and as such, likely highly underrepresent the true number of sport-related injuries sustained by athletes. It has been estimated that 75% of concussed individuals do not seek medical attention (Willer and Leddy, 2006).

1.4.1 Definition of Mild TBI

There are currently no established biomarkers for mild TBI and thus diagnosis depends on clinical criteria. There is no universally-accepted definition of mild TBI or concussion and the definitions of these terms and their interpretations are under continual revision by various groups (Carroll et al., 2004; Chancellor et al., 2019).

A number of organizations have proposed guidelines for the clinical diagnosis of mild TBI. In 1993, The American Congress of Rehabilitation Medicine (ACRM) proposed that a mild TBI is defined as a "traumatically induced physiological disruption of brain function" and is diagnosed due to the presence of at least one of the following criteria: (1) loss of consciousness for less than 30 minutes, (2) post-traumatic amnesia lasting less than 24 hours, (3) any alteration in mental state at the time of the event (e.g. dizziness, disorientation, confusion), and (4) focal neurological deficits (with a GCS from 13 to 15) that may or may not be transient in nature (Kay et al., 1993).

In 2004, the World Health Organization (WHO) proposed an operational definition of mild TBI as "an acute brain injury resulting from mechanical energy to the head from

external physical forces", and added onto the ACRM diagnostic criteria that the manifestations of mild TBI cannot be due to drugs, other conditions (e.g. intubation, facial injuries, psychological trauma), or due to penetrating injury (Carroll et al., 2004).

In 2009, the United States Department of Veterans Affairs (VA) and Department of Defense (DoD) published clinical practice guidelines for the management of concussion-mild TBI (VA/DoD, 2009). These guidelines were updated in 2016 and defined a TBI as a "traumatically induced structural injury and/or physiological disruption of brain function as a result of an external force". The updated VA/DoD report indicates that any period of loss or decreased level of consciousness following exposure to an external force can be considered a TBI. Additionally, they noted that any post-traumatic amnesia, an alteration in mental state (e.g., confusion, disorientation), neurological deficits (e.g., weakness, loss of balance, aphasia), or the presence of an intracranial lesion can also be considered a TBI (VA/DoD, 2016).

1.4.2 Sports-Related TBI

The expert panel for the International Consensus Conference on Concussion in Sport Group (CISG), met in 2001, 2004, 2008, 2012, and in 2016, and continues to provide refinements to the definition of sports-related TBI and concussion (Aubry et al., 2002; McCrory et al., 2005; McCrory et al., 2009; McCrory et al., 2013; McCrory et al., 2017a). Currently, the CISG defines sports-related concussion as "a traumatic brain injury induced by biomechanical force" and provides several common features which can be used clinically to denote concussion (McCrory et al., 2017a). The CISG states that sports-related concussion can be caused by a "direct blow to the head, face, neck, or elsewhere on the body" leading to the transmission of an impulsive force to the head. The CISG notes that

sports-related concussion typically results in the rapid onset of impaired neurological function that resolves spontaneously and is short-lived, although this is not always the case. The CISG also indicates that acute clinical symptoms of concussion "largely reflect a functional disturbance" and as such, standard structural neuroimaging tests are often unremarkable. Finally, the CISG suggests that sports-related concussion may or may not involve loss of consciousness. Clinically, concussion can present with coordination impairments, behavioural changes, cognitive impairments, sleep disturbances, headache, and amnesia (McCrory et al., 2017a; Chancellor et al., 2019).

Evaluations of sports-related concussions are currently based on multimodal assessments, such as the Sideline Concussion Assessment Tool (SCAT). The SCAT is designed for use by health care providers and has undergone a series of revisions in recent years by the CISG. The current SCAT5 version incorporates a variety of multimodal tests, including the GCS, Maddocks questions to assess orientation, medical background questions, evaluation of symptoms and cognitive performance, and balance and coordination tests (Echemendia et al., 2017b). The SCAT5 is intended for evaluating athletes aged 13 and older, and a Child SCAT5 for athletes 12 and under was developed in 2012 (Davis et al., 2017). Additionally, the Concussion Recognition Tool 5 is available for individuals who are not health care professionals, such as coaches and parents (Echemendia et al., 2017a).

1.4.3 Complications of Repetitive Mild TBI

Following a single mild TBI, an acute "window of vulnerability" may exist during which time the brain has an increased susceptibility to subsequent injury. If additional

injuries are sustained during this period, prolonged recovery from injury can occur (Guskiewicz et al., 2003; Slobounov et al., 2007).

Additionally, a history of exposure to repetitive mild TBI (rmTBI) (likely over a longer duration of time) is a risk factor for the development of several neurodegenerative conditions, such as Alzheimer's disease (Mortimer et al., 1991; Jellinger et al., 2001), Parkinson's disease (Ben-Shlomo, 1997; Goldman et al., 2006), amyotrophic lateral sclerosis (Chen et al., 2007), and chronic traumatic encephalopathy (CTE) (Omalu et al., 2005; Omalu et al., 2006; McKee et al., 2009; McKee et al., 2010; McKee et al., 2013; McKee and Robinson, 2014). There remain significant unknowns regarding the development of these conditions following exposure to repetitive head impacts, however it is possible that repetitive injuries could trigger the overproduction and aggregation of proteins leading to neurodegenerative disease (Gavett et al., 2010). Of all of the aforementioned neurodegenerative diseases, CTE is the only one to be exclusively described in individuals with a history of repetitive head injury, typically in former contact-sport athletes (Gavett et al., 2010). Clinically, CTE symptoms include irritability, impairments in executive function, memory loss, cognitive deficits, and dementia (Stern et al., 2013). Currently, diagnosis of CTE can only be made using post-mortem tissue, with the defining neuropathological hallmark of CTE being perivascular accumulation of phosphorylated tau, neurites, and astrocytic tangles in the neocortex and at the depths of cortical sulci (McKee et al., 2015; McKee et al., 2016).

1.5 Experimental Models of TBI

Much of our current understanding of the pathophysiological mechanisms underlying TBI are due to the use of animal models. Animals models are essential tools for the

investigation of human disease, allowing causal mechanisms of disease to be characterized through interrogation of mechanistic pathways. Additionally, animal models are critical to the establishment of novel diagnostic and therapeutic interventions (Wojnarowicz et al., 2017). In particular, rodent (e.g. rat and mouse) models are extensively used in medical research and are the most commonly used animal models in TBI research (Namjoshi et al., 2013).

As discussed previously, human TBI is a highly heterogeneous disorder and no single rodent model can replicate the entire spectrum of human TBI pathophysiology. Animal models of TBI can be grouped into two broad categories: open head injury models, and closed head injury models (Xiong et al., 2013). In open head injury models, the dura mater is exposed via a craniotomy and the traumatic force is applied directly to the surface of the dura. These models involve little to no head movement as a result of the trauma and include the fluid percussion injury (FPI) model and the controlled cortical impact (CCI) model (Namjoshi et al., 2013).

The FPI model involves the rapid injection of fluid onto the surface of the dura via propulsion of fluid using a pendulum contacting a reservoir to produce an impact pulse. The pulse can be modulated by varying the input parameters to produce a range of injury severities. The location of impact is determined by the experimenter and is typically administered onto the dura which is exposed laterally over the parietal cortex (lateral FPI) or medially between the bregma and lambda suture lines (medial FPI). FPI leads to a variety of injury responses including DAI, subarachnoid hemorrhage, and cell loss (Thompson et al., 2005; Xiong et al., 2013). FPI models produce a relatively high mortality rate (likely due to apnea) and variability that may be associated with the location of the craniotomy and impact pulse.

In contrast, CCI models of TBI deliver an impact to exposed dura using a piston driven by weight-drop (Feeney et al., 1981), pneumatic (Dixon et al., 1991; Smith et al., 1995), electromechanic (Onyszchuk et al., 2007), or electromagnetic (Brody et al., 2007) forces. CCI leads to rapid compression of brain tissue, leading to focal damage including neuron loss, intracranial hemorrhage, edema, and increased intracranial pressure (Saatman et al., 2006). Modifications to injury severity are produced by varying the location of the impact, the impactor tip size and shape, and the impact velocity and depth. The major advantage of CCI models is their high level of injury reproducibility. However, in addition to the requirement of a craniotomy, the tissue damage that is produced by CCI models is often not consistent with mild injury (Marklund and Hillered, 2011).

In closed head injury (CHI) models of TBI the trauma is delivered through the skull by direct impact, such as via a weight or piston striking the skull, or by non-impact methods such as blast injuries. Blast injuries are modelled through the generation of blast waves from compressed gas or explosives are directed at the animal's head (Goldstein et al., 2012). The most common and simplest form of administering a CHI using direct impact involves dropping a weight of known mass from a specific height onto the skull of the animal (Marmarou et al., 1994; Chen et al., 1996). Injury severity can be modified by varying the mass and height of the falling weight, and the impact itself can be administered at various anatomical locations, usually laterally or at the midline between bregma and lambda. Most CHI models involve surgical exposure of the skull (but no craniotomy), however some models involve the delivery of impacts without any surgical preparation (Marmarou et al., 1994; Kane et al., 2012).

Various methods to stabilize the head of the animal during impact have been used in CHI models. For example, the Maramarou method involves placing the animal prone on a

piece of foam padding prior to impact, allowing for some movement of the head as it is struck and the foam compresses underneath. Alternatively, Kane et al. (2012) modified this approach in mice so that the animal's body is fully supported on a suspended piece of aluminum foil that breaks upon impact. This allows the animal to undergo unrestrained movement during impact before falling onto a piece of foam padding below. This model was described by the authors to produce a mild concussive injury after a single impact. The model described in this thesis characterizes the use of this approach in rats under conditions of repetitive injury (see Chapter 2).

In comparison to open head injury models, the major advantage of CHI models is that most humans who experience TBI do not have skull fractures and instead sustain closed-head impacts. Further, CHI models are less invasive and are simpler to employ due to the lack of surgical preparation required. Some limitations of CHI models include the variability of administered impacts. For example, in weight-drop models it can be difficult to control the weight immediately after initial impact which can result in secondary impacts being delivered due to rebound effects (Namjoshi et al., 2013), although the modification proposed by Kane et al. (2012) avoids this issue.

Overall, the selection of an appropriate model of TBI depends on what features of TBI are intended to be investigated. Specifically, injury context (such as closed-head or blast injuries) versus injury consequences (such as focal or diffuse injury) must be carefully considered during model selection (Wojnarowicz et al., 2017). When appropriately selected, each of the animal models described in this section can provide useful insights into the various aspects of human TBI.

1.6 The Blood-Brain Barrier

1.6.1 Function and Structure

Homeostatic regulation of the brain extracellular environment is imperative to the maintenance of normal brain function. For example, concentrations of ions (such as Na^+, Ca^{2+}, and K^+) must be tightly controlled in the brain to permit normal neuronal function. Further, the metabolic demands of the central nervous system (CNS) are such that the brain accounts for approximately 20% of oxygen consumption for the entire body, despite comprising only 2% of total body mass (Rolfe and Brown, 1997; Attwell et al., 2010), highlighting the requirement of a dense vasculature to supply large amounts of oxygen and remove waste. The brain is also sensitive to many chemicals that do not necessarily harm peripheral structures in the body but can be highly neurotoxic. To ensure proper brain function, highly specialized control over the extracellular environment, the ability to meet dynamic metabolic demands, and protection from harmful substances is needed. These functions are met by a unique anatomical and physiological barrier between the peripheral blood supply and neural tissue, called the blood-brain barrier (BBB) (Abbott et al., 2010).

At its most basic structural level, the BBB is formed by brain endothelial cells that line the cerebral microvasculature. Brain homeostasis is maintained by close regulation of the passage of substances at the blood-brain interface by way of properties which are unique to the endothelial cells of the BBB. Compared to the periphery, endothelial cells of the BBB have increased numbers of mitochondria (Oldendorf et al., 1977), lack basement membrane fenestrations (Fenstermacher et al., 1988), and have minimal pinocytic activity (Sedlakova et al., 1999). A single endothelial cell spans the perimeter of brain capillaries, and adjacent endothelial cells are connected via transmembrane proteins (such as junctional

adhesion molecules, occludins, and claudins) and cytoplasmic accessory proteins (such as zonula occludens and cingulins). These structural attachments between endothelial cells generate tight junctions which are critical for the integrity and functionality of the BBB, and which are involved in the dynamic regulation of paracellular transport across the barrier (Kniesel and Wolburg, 2000).

The endothelial layer is surrounded by a network of cells including pericytes and astrocyte foot processes, which form a continuous layer separating brain tissue from the blood vessels. Around penetrating vessels and venules in the brain, perivascular macrophages involved in immune functions of the CNS can be found adjacent to the endothelial cell layer. From a functional perspective, the contact of neurons, astrocytes, microglia, macrophages, pericytes, endothelial cells, blood vessels, and the extracellular matrix all form a dynamic entity called the neurovascular unit (Abbott et al., 2006; Serlin et al., 2015).

The BBB provides a barrier to the free exchange of large ions or solutes between the blood and the brain, although gaseous species such as O_2 and CO_2 and lipid-soluble molecules (such as ethanol) can cross freely via lipid-mediated diffusion (Abbott et al., 2010). Nevertheless, significant molecular and cellular interaction occurs between the brain and the periphery, and as such the BBB is able to dynamically regulate the passage of substances between these compartments. As discussed previously, paracellular transport between endothelial cells of the healthy BBB is limited owing to tight junctions between adjacent cells. Instead, transcellular-mediated transport of substances across the BBB is used to shuttle required molecules from the circulation into (and out of) the brain. These transport pathways include carrier-mediated mechanisms, ion pumps, caveolae, peptide

transport systems within endothelial cells, and active transport by ATP-binding cassette transporters (Abbott et al., 2010).

1.6.2 Blood-Brain Barrier Dysfunction

Compromise to the integrity of the BBB results in poor regulation of molecules and ions which would otherwise have been restricted in their interaction with the brain. This can lead to the imbalance of ions and metabolic products in the interstitial fluid of the brain, which can cause abnormal neuronal signalling. Additionally, increased extravasation of peripheral immune cells can occur following BBB dysfunction (BBBD). Importantly, pro-inflammatory cytokines such as interleukin (IL) -6, IL-1β, and transforming growth factor beta (TGFβ) - 1 (Ivens et al., 2006; Levy et al., 2015) have been shown to influence endothelial tight junctions, which can impair the ability of the BBB to maintain the narrow range of extracellular homeostasis that is required for the brain to function properly.

Dysfunction of the BBB has been implicated in many neurological diseases, including stroke (Gursoy-Ozdemir et al., 2012), epilepsy (Marchi et al., 2007; Friedman et al., 2009; Janigro, 2012), multiple sclerosis (Minagar and Alexander, 2003; Correale and Villa, 2007), and Alzheimer's disease (Zlokovic, 2011; Sweeney et al., 2018). Significant evidence from clinical and basic research suggests that TBI can also result in the impairment of BBB integrity (Shlosberg et al., 2010).

BBB breakdown following TBI that directly results from the traumatic impact itself is termed primary BBB damage. This can involve shearing of the endothelial microvasculature leading to changes in the regulation of the BBB, cerebral blood flow, and metabolic processes (Rodríguez-Baeza et al., 2003; Shlosberg et al., 2010). Primary BBB damage can lead to a variety of complications, including the development of an ischemic

zone and associated tissue hypoxia. These changes may, in turn, facilitate more BBB breakdown, further contributing to the pathogenic cycle of BBBD following TBI.

In contrast, the precise mechanisms underlying secondary BBBD remain largely unknown, although both paracellular leakage and increased transcellular transport through endothelial cells have been proposed (Shlosberg et al., 2010; Knowland et al., 2014; Andreone et al., 2017). The delayed phase of BBBD following TBI typically emerges in hours to days following the initial trauma and may be the result of increased numbers of endothelial caveolae, which can expose the brain to blood constituents that would otherwise be sequestered by an intact BBB (Nag et al., 2007; Nag et al., 2009). Further, decreased expression of tight junction and adhesion proteins may also lead to increased BBB permeability following TBI (Yeung et al., 2008).

Dysfunction of the normal vascular response to neuronal activity (i.e. neurovascular coupling), changes in tight junction proteins, chronic inflammation, and impaired homeostatic regulation of the brain's extracellular space can all contribute to long-term complications of BBBD. These alterations can lead to edema, cell death, altered cellular connectivity, and neurodegeneration (Shlosberg et al., 2010).

While BBBD has long been described in the context of moderate to severe TBI, there is increasing evidence that BBB breakdown may be a key pathogenic event in the context of sports-related mild TBI. In one study involving college American football players, disruption of white matter assessed by diffusion tensor imaging (DTI) was significantly correlated to peripheral markers of BBBD (Marchi et al., 2013). Additionally, our group recently conducted a study to investigate changes in BBB integrity in amateur American football players using dynamic contrast-enhanced magnetic resonance imaging (DCE-MRI). This study revealed that 40% of imaged football players showed significant BBB

pathology compared to non-contact sport (track) athlete controls (Weissberg et al., 2014). Recent evidence in animal studies indicates that BBBD can arise following mild impacts (Li et al., 2016; Tagge et al., 2018). Further, BBBD may be highly relevant to the development of long-term sequelae of repetitive head trauma, as a major pathological hallmark of CTE is the perivascular accumulation of phosphorylated tau around small blood vessels, suggesting a vascular role in the development of CTE (McKee et al., 2015; McKee et al., 2016). Impaired tight junction integrity and BBBD has also been described in post-mortem tissue from patients with CTE, further substantiating this hypothesis (Doherty et al., 2016).

1.7 Neuroinflammatory Response to TBI

As with many neurological diseases, the neuroinflammatory response to TBI can have both beneficial and deleterious effects on disease progression. While inflammation is necessary for debris clearance and initiation of healing and regenerative responses following injury, it can also lead to neuronal death and degeneration when it becomes chronic (Simon et al., 2017). While historically the inflammatory response to TBI was thought to arise exclusively from peripheral immune mediators entering the brain following injury, our understanding of the immune function of the brain has increased significantly. The complexity of peripheral and central cellular and molecular mediators of immunity are now recognized as critical components underlying disease pathophysiology (Simon et al., 2017). Interestingly, inflammatory gene expression profiles in models of mild and severe TBI have been shown to be remarkably similar, suggesting that the underlying inflammatory response may be common to a broad range of injury severities (Lagraoui et al., 2012).

Primary injury resulting from TBI can lead to disruption of cellular membranes and the release of damage-associated molecular patterns (DAMPs), which can act as immunogens triggering inflammasome and innate immune activation (Jassam et al., 2017). The prototypical endogenous DAMP, high-mobility group box protein 1 (HMGB1), has been shown to be significantly increased in the CSF of patients following severe TBI and has been associated with a worse outcome following TBI in children (Au et al., 2012; Laird et al., 2014). In response to DAMP release, pro-inflammatory cytokines such as IL-6 and IL-1β are upregulated by glial cells, such as microglia. Microglia are the resident innate immune cells of the CNS and have been shown to be active as early as 72 hours following human TBI (Engel et al., 2000; Beschorner et al., 2002; Gentleman et al., 2004). Microglial activation has been shown to persist for many years following a single moderate-to-severe TBI (Johnson et al., 2013) and perivascular microgliosis was recently described following experimental mild TBI (Tagge et al., 2018).

Acute trauma also leads to increased release of reactive oxygen species (ROS) by mitochondria, triggering inflammasome activation (Chu et al., 2013; Suliman and Piantadosi, 2016). Inflammasomes are multiprotein complexes which regulate the activation of pro-inflammatory caspases and cytokines, contributing to inflammation following TBI (Mortezaee et al., 2018). In addition to the activation of microglia, the various inflammatory triggers that arise due to trauma can elicit responses from neutrophils, astrocytes, monocytes and macrophages, and peripheral T-cells (Corps et al., 2015). These cells are involved in important neuroprotective mechanisms including phagocytosis, neurotransmitter clearance, cytokine release, antigen presentation, and tissue repair. However, chronic activation of these immune mediators can become maladaptive and lead to deleterious outcomes such as edema, hypoxia, as well as neuronal death following mild

TBI (Shultz et al., 2012; Aungst et al., 2014; Corps et al., 2015). There is increasing recognition that lasting neuroinflammation may contribute to chronic neurodegeneration and cognitive impairments following TBI (Shultz et al., 2012; Johnson et al., 2013; Aungst et al., 2014).

1.8 Transforming Growth Factor Beta Signalling

1.8.1 Basic Mechanisms

The TGFβ signalling pathway plays an important role in many cellular responses, including cell growth, proliferation, apoptosis, differentiation, and immune response (Shi and Massagué, 2003). Mediators of TGFβ signalling, such as endogenous TGFβ cytokines, bind to TGFβ receptors on the cell membrane which results in the assembly of TGFβ receptor type I and TGFβ receptor type II serine/threonine kinases, which typically exist as homomeric dimers prior to ligand binding (Derynck and Zhang, 2003). This proximity allows TGFβ receptor II kinase to phosphorylate the receptor I kinase domain. Once phosphorylated, TGFβ receptor I is able to phosphorylate Mothers Against Decapentaplegic Homolog (Smad) proteins, which act as the major mediators of TGFβ signalling activity (Massagué, 2000; Shi and Massagué, 2003). Phosphorylation of Smad proteins allows them to translocate to the nucleus and assemble complexes that regulate transcription by binding DNA directly or by recruiting transcriptional co-activators or corepressors (Massagué, 2000).

TGFβ signalling can also activate other pathways, including the p38 mitogen-activated protein kinase (MAPK) pathway, which can act independently from Smad. However, the details of the activation and outcomes of Smad-independent TGFβ signalling through MAPK remain poorly characterized (Derynck and Zhang, 2003).

Evidence for TGFβ signalling and the TGFβ1 cytokine having a protective (Zhu et al., 2002; Brionne et al., 2003; Shen et al., 2014) versus harmful function has differed depending on the experimental model. Consistent with many other inflammatory mediators, this is likely because the action of TGFβ1 depends on the condition, timing, and cell type involved (Heinemann et al., 2012). However, TGFβ expression is increased in many brain diseases, including multiple sclerosis, Alzheimer's disease, stroke, tumour, or trauma (Heinemann et al., 2012). TGFβ1 levels have been shown to be increased in the CSF of patients following moderate and severe traumatic brain injury (Phillips et al., 2006). Additionally, TGFβ signalling was recently shown to be upregulated in a neuronal stretch injury and fluid percussion injury model of mild TBI (Patel et al., 2017).

1.8.2 Blood-Brain Barrier Dysfunction and TGFβ Signalling

Work by our group has provided evidence that BBBD can lead to pathological TGFβ signalling (Ivens et al., 2006; Cacheaux et al., 2009; David et al., 2009) (Figure 1.1). Specifically, we have shown in experimental models of BBBD that serum albumin can leak through a permeable BBB and bind to TGFβ receptors situated on astrocytes (Ivens et al., 2006), which can activate TGFβ signalling through the phosphorylation of downstream Smad2 (Cacheaux et al., 2009; Bar-Klein et al., 2014). This can lead to the modification of astrocytic function, including the upregulation of pro-inflammatory cytokines, such as IL-6 and IL-1β (Cacheaux et al., 2009; Levy et al., 2015). Further, changes to astrocytic potassium and glutamate buffering can lead to a reduction in the threshold for neuronal activation and the induction of excitatory synaptogenesis (Ivens et al., 2006; Cacheaux et al., 2009; Bar-Klein et al., 2014; Weissberg et al., 2015).

Additionally, TGFβ signalling itself has been associated with exacerbation of BBB dysfunction in a number of different experimental contexts. For example, in a model of hepatic encephalopathy application of TGFβ1 resulted in suppression of the BBB tight-junction protein, claudin-5, as well as increased expression of matrix metalloproteinase 9 (MMP-9), which can degrade tight junctions (McMillin et al., 2015). Similar observations of the role of TGFβ signalling in increasing the permeability of endothelial cells have been described in lung and retinal endothelial cells (Behzadian et al., 2001; Goldberg et al., 2002). Thus, there is evidence that BBBD can cause an increase in TGFβ signalling, which may, in turn, itself lead to impairment of the integrity of the BBB.

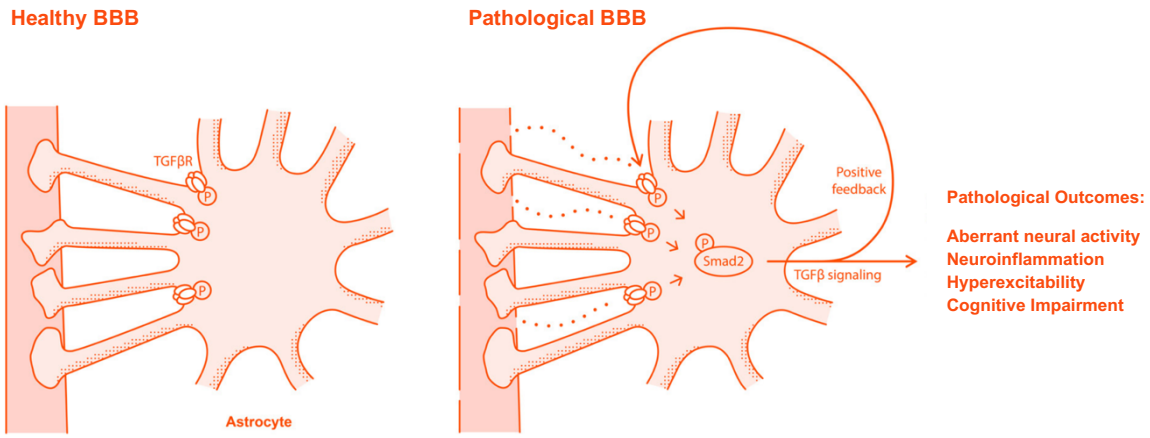

Figure 1.1: Schematic summarizing pathological dysfunction following BBBD leading to albumin-mediated astrocytic TGFβ signalling. BBBD leads to extravasation of serum albumin from the blood into the extracellular space of the brain, allowing albumin to interact with astrocytic TGFβ receptors, initiating TGFβ signalling and pathological changes including aberrant neural activity, neuroinflammation, hyperexcitability, and cognitive impairment. Adapted from Senatorov et al., 2019.

1.9 Rationale and Hypotheses

Significant progress has been made in elucidating the molecular events relating to pro-inflammatory TGFβ signalling in experimental models of direct BBB disruption (for example, through the application of bile salts) (Seiffert et al., 2004; Ivens et al., 2006). However, the role of pro-inflammatory TGFβ signalling in the context of BBBD induced by rmTBI was previously unknown. Further, the viability of TGFβ antagonism as a treatment strategy for rmTBI had not been previously assessed.

The overall hypothesis for this thesis is: rmTBI is associated with a pathological increase in pro-inflammatory TGFβ signalling that can be pharmacologically targeted as a treatment strategy.

The specific objectives of this thesis are:

1. To develop and characterize a rodent model of rmTBI that recapitulates the spectrum of functional outcomes following injury (Chapter 2)
2. To assess BBBD, TGFβ signalling, and neuroinflammation as mechanisms associated with outcome following rmTBI (Chapter 3)
3. To evaluate TGFβ signalling as a therapeutic target in rmTBI (Chapter 4)

CHAPTER 2:
CHARACTERIZATION OF A NOVEL RODENT MODEL OF REPETITIVE MILD TRAUMATIC BRAIN INJURY

2.1 INTRODUCTION

Animal models offer critical tools to increase our understanding of disease and are essential for the translation of basic science findings into advancements for patients (Wojnarowicz et al., 2017). Many investigators of sports-related TBI utilize closed-head impact models, as these models more closely resemble the injury context of mild TBI in athletes. The most commonly used closed-head injury model is the Marmarou weight drop model, which involves dropping a weight onto the intact skull of an animal which has been placed on a foam pad (Marmarou et al., 1994). However, a significant limitation of this approach is the relative lack of rotational motion that is experienced by the animal during impact, which is in contrast to impacts sustained by athletes. As such, a recent experimental adaptation was implemented in mice and in rats to address this (Kane et al., 2012; Mychasiuk et al., 2014; Goddeyne et al., 2015). This adaptation involves suspending the animal on a sheet of tin foil, allowing the animal to undergo substantial acceleration and rotation of the head and body upon impact before falling onto a foam pad below. This approach has been implemented to investigate the effects of a single injury and repetitive injuries in juvenile rats (3 weeks old; Goddeyne et al., 2015) but had not been used to investigate the effects of repetitive head trauma in adolescent rats.

Here we characterize a model of repetitive mild TBI in adolescent rats which produces a heterogeneity of neurobehavioural responses resulting from these injuries. This model incorporates substantial acceleration of the head and rotational motion during impact, enhancing its ability to model sports-related TBI. We investigate acute and delayed neurological events resulting from repetitive injury and show that the spectrum of responses

produced by this model are not due to differences in injury biomechanics, but rather may be due to differential responses to the repetitive impacts themselves.

2.2 METHODS

2.2.1 Animal Care

All procedures were performed in accordance with the guidelines from the Canadian Council on Animal Care and were approved by the Dalhousie University Committee on Laboratory Animals. Eight-week old, adolescent wild-type male Sprague-Dawley rats were purchased from Charles River Canada (St. Constant, Quebec, CA). Animals were double-housed in standard cages and were fed a diet of standard rodent chow and filtered water *ad libitum*. Animals were exposed to a reversed 12:12 light-dark cycle (lights off from 9:00 am to 9:00 pm). Upon arrival to the Carleton Animal Facility, all animals were given one week to adjust to the local environment and lighting conditions before experiments began. All experimentation was performed during the dark (active) phase of the animals' light-dark cycle.

2.2.2 Mild TBI Induction Protocol and Weight-Drop Apparatus

The TBI procedure involved a modified Marmarou weight-drop closed-head model of TBI (Marmarou et al., 1994; Kane et al., 2012; Mychasiuk et al., 2014; Goddeyne et al., 2015) for use in adolescent (9 week-old) rats (McCutcheon and Marinelli, 2009; Sengupta, 2013). All animals were anesthetized prior to impact administration. The anesthesia procedure involved administration of 3.5% isoflurane mixed with oxygen at a flow rate of 2L/minute for a duration of 2 minutes. After 2 minutes, the animals received a firm toe-pinch to confirm no pedal reflex was present, and then received an additional 1 minute of

anesthetic as described above. In the event that there was a positive pedal reflex after pinching, an additional 2 minutes of anesthesia was administered to the animal. Next, the animals were placed ventrally on a surface of tin foil under tension and suspended 0.15 m above a foam collection sponge (Figure 2.1 A). A weight-drop apparatus was constructed in-house using a guide rail system to deliver a controlled force to the midline of the anesthetized animal (Appendix A). TBI administration involved the release of a 500-gram mass that traveled 0.85 m along a guide rail before striking a transfer bolt, which converted the kinetic energy of the falling mass into a concentrated force that travelled through the bolt positioned dorsally on the animals closed skull. The midline impacts were delivered anterior to the lambda suture line (but posterior to bregma) via alignment with the animal's ears as an anatomical reference. This force caused the animal to break through the tin foil, undergo a 180-degree rotation (Figure 2.1 B), and finally land dorsally on the collection sponge below (Figure 2.1 C) (Kane et al., 2012; Mychasiuk et al., 2014; Goddeyne et al., 2015).

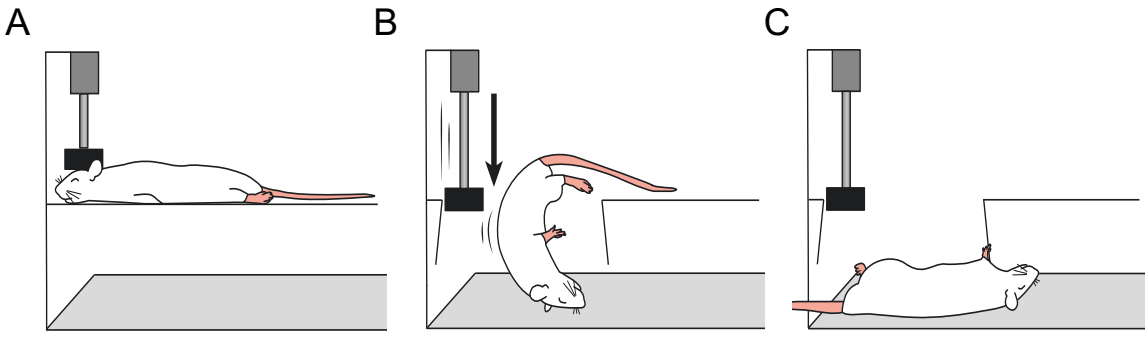

Figure 2.1. Schematic of impact trajectory using modified Maramarou weight-drop method

Immediately following the impact, the animal was placed in a recovery box where it was closely monitored and filmed for 10 minutes post-impact. Isoflurane sham control animals received a sham injury involving the same anesthesia regimen however, they did not receive the impact itself prior to being placed in the recovery box for immediate post-impact monitoring.

2.2.3 Repetitive Mild Traumatic Brain Injury Protocol

The rmTBI protocol involved the administration of one mild TBI (as described in section 2.2.2) per day for up to five consecutive days, for a maximum of five injuries administered to the animal. Animals that deteriorated significantly and did not recover following impact did not receive additional hits.

2.2.4 Pressure Sensitive Film

Pressure sensitive film (Fujifilm PreScale, Ultra Super Low LLLW Two-Sheet Type) was used in a subset of impacts to determine the mean pressure delivered during each impact. The film consisted of two polyester sheets, one coated with a colour-forming material (A-film) and the other with a colour developing material (C-film). These films were positioned together between the impactor and the anesthetized animal's skull immediately prior to impact. The temperature and humidity of the impact room were recorded immediately before impact. Upon impact, the microcapsules in the A-film were broken and transferred to the C-film in a manner proportional to the pressure applied during impact. C-films were archived and scanned after each impact (Epson ET-4500 scanner, 1200 DPI) for analysis using an in-house script (MATLAB® R2018a). This script transformed the mean intensity of scanned C-films into a density value to find the mean

pressure in megapascal (MPa). Corrections to adjust for the effect of temperature and humidity conditions on recorded pixel intensity during each impact were performed.

2.2.5 High Speed Impact Analysis

A subset of impacts were filmed (left side view) at 240 frames per second (fps) and were analyzed using an open-source motion analysis tool (Tracker version 5.0.7, 2019). The left eye of the animal was manually traced through each frame of the impact video to determine the animal's position throughout the impact. The position data were used to calculate the velocity, acceleration, angular velocity, and angular acceleration of the animal's head during the impact using the finite differences method.

2.2.6 Immediate Post-Impact Recovery Analysis

In the immediate seconds following impact, animals were transferred to a recovery box (30 x 30 x 38 cm) constructed from clear plexiglass (1 cm thick). Animals were monitored for 10 minutes post-impact in the recovery box. This period was filmed in red lighting conditions for offline assessment by an observer blinded to condition. Post-impact convulsion occurrence and duration, latency to right, and latency to locomotion were recorded. Additionally, a subset of recovery videos (n = 10) were analyzed to determine the frequency and amplitude of post-impact convulsions that occurred in a subset of animals. This analysis was performed using an open-source motion analysis tool (Tracker version 5.0.7, 2019).

2.2.7 Combined Neurological Assessment

Neurological assessment of rmTBI and sham control animals was performed using three behavioural tests: the open field test, the beam walk test, and the inverted wire mesh

test, as has been described elsewhere (Tagge et al., 2018). Scoring parameters for these tests were adapted for use in rats and were used to provide a rapid assessment of the locomotor and balance abilities of the animals (Table 2.1). All behavioural tasks were filmed (Canon Vixia HF R700) for offline analysis by an observer blinded to experimental conditions. Appendix B shows the breakdown of individual scores on each test following a single mild impact.

2.2.8 Open Field

The open field arena consisted of an open box (60 cm wide x 60 cm long x 50 cm high) constructed from opaque black matte plexiglass. The test was performed in red lighting and animals were given 45 seconds to explore the arena after being placed in the lower left corner of the box. All trials were recorded for offline scoring by an observer blinded to experimental conditions. Scoring for the open field test was done by counting the number of corners visited by the animal during the trial duration. The maximum possible score was 4, and the minimum score was 0 for this test (Table 2.1).

2.2.9 Beam Walk

The beam walk apparatus consisted of a black metal beam suspended by supports, with a dark open target box placed at one end. The beam was 2.5 cm wide, 100 cm long and 85 cm high. The test was performed in regular white lighting and consisted of placing the animal at the open end of the beam, facing toward the dark target box for a duration of one minute. All animals were pre-trained on this task for three days prior to any TBI or anesthesia administration. Beam training involved placing the animal at the open end of the beam and allowing the animal to travel freely on the beam for one minute. If the animal

was successful in crossing the beam and reaching the dark target box, it was removed from the box after the elapsed test time and was returned to its home cage for testing the next day. If the animal was unsuccessful at crossing the beam after one minute, it was prompted by the experimenter to cross the beam and enter the dark target box, where it was left for 30 seconds before removal. This procedure was repeated for three consecutive days to ensure animals would reliably cross the beam prior to any experimental intervention. Scoring for the beam walk test involved using four regularly spaced intervals (25 cm segments) along the length of the beam. The maximum score for this test was 4 points, which was awarded when the animal successfully crossed all 4 segments of the beam and entered the target box. The minimum score for this test was 0, which was assigned if the animal did not move from the starting position or if the animal fell from the beam at any point during the one-minute test (Table 2.1).

2.2.10 Inverted Wire Mesh

The inverted wire mesh apparatus was constructed from a wire grid (2.0 cm^2) that was reinforced with a wooden border around the perimeter of the mesh (total area = 36 cm^2). The inverted wire mesh task was performed in regular white lighting conditions and involved the animal being placed in the center of the mesh apparatus which was then inverted by 180-degrees until the animal was suspended 50 cm in the air above a safety net below. Scoring for this task was determined by the length of time that the animal hung onto the mesh. A maximum score of 4 was given for an animal that held on for 5 seconds or longer and was able to climb over the side of the mesh apparatus to right itself, and a minimum score of 0 was given for an animal that hung on for less than one second (Table 2.1).

Score:	4	3	2	1	0
Test 1: Open Field (45 s)	Visits 4 corners	Visits 3 corners	Visits 2 corners	Visits 1 corner	Visits 0 corners
Test 2: Beam Walk (60 s)	Crosses 4 segments	Crosses 3 segments	Crosses 2 segments	Crosses 1 segment	Crosses 0 segments
Test 3: Inverted Wire Mesh (5 s)	Climbs on top of mesh	Hangs on for ≤ 5 seconds	Hangs on for ≤ 3 seconds	Hangs on for ≤ 1 second	Paralysis
Combined Neurological Score = Test 1 + Test 2 + Test 3					

Table 2.1: Neurological scoring system. Adapted for use in rats, first described for use in mice by Tagge et al. in 2018.

2.2.11 T2-Weighted Magnetic Resonance Imaging

To assess potential structural changes following injury, T2-weighted magnetic resonance imaging (MRI) was performed. A 3 Tesla Agilent system was used in animals under isoflurane anesthesia (1–2%) with a constant oxygen flow (99%, 1 L/h). Breathing was monitored continuously during imaging using a respiration monitor. A standard T2-weighted fast spin echo sequence (repetition time: 2500 ms; echo time: 64 ms; echo train length of 16, echo spacing 8ms; 46 averages; 128 x 128 data matrix, resulting in 0.297 mm in-plane resolution and a slice thickness of 1 mm; acquisition time: 15.3 min) was used.

2.2.12 Morris Water Maze

The Morris water maze (MWM) was used to test spatial learning and memory (Morris, 1984). The maze consisted of a circular aluminum pool (165 cm diameter, 60 cm high). The pool was filled with water to a depth of 34 cm and was made opaque by adding non-toxic black paint (Midnight Black, Tri-Art Acrylic) to the water. The pool water was

allowed to equilibrate to room temperature overnight and the temperature was recorded during testing days (mean 20.5°C). A 30 cm high circular escape platform (12 cm diameter) was positioned in the pool 50 cm away from the edge at a known location. When submerged, the escape platform was not visible at this location due to the opacity of the water. All MWM trials were recorded for offline analysis using an automated animal tracking system (Noldus Ethovision, version 13). Animals were tested under diffuse white lighting conditions to minimize surface reflections, which can interfere with tracking. The immediate surroundings of the pool were marked by large visual cues (55 cm^2) on each of the four walls around the perimeter of the maze and visible from the water surface of the pool. These cues were distinct in colour and in shape and provided visual references for the animals to discern and recall the platform location upon repeated trials.

During testing days, animals were gently released into varied pre-defined and randomized start locations around the perimeter of the pool. The duration of a single trial was 60 seconds, and a series of three trials were completed by each animal at a time, with a "rest" interval of 60 seconds in between each trial. After a series of three trials was completed, the animal was placed in a clean cage on a water-circulating heating pad (37°C) for a minimum of 15 minutes before the next series of three trials was administered. A total of nine trials were administered in this way. Delayed recall was assessed twenty-four hours later by averaging a series of three trials in which the platform was present.

2.2.13 Perfusion and Tissue Collection

Animals were deeply anesthetized by intraperitoneal (IP) injection of sodium pentobarbital (240mg/mL Euthanyl, Bimeda-MTC, Cambridge, ON) at a dose of 100

mg/kg and perfused intracardially with 0.9% saline (pH 7.4). Following decapitation, brains were extracted and photographed with a digital single-lens reflex camera (Nikon D3300).

2.2.14 Statistical Analyses

Statistical analyses were performed using GraphPad Prism version 8.0 for Macintosh (GraphPad Software, La Jolla California USA). Group means with standard error of the mean and sample size were reported. Differences between groups for all tests were reported as exact p-values, and differences were considered statically significant at an alpha level of less than 0.05. When two groups were compared, Student's t-test and Mann Whitney-U test were used for calculating group differences for normally or non-normally distributed data, respectively. When three or more groups were compared, a one-way analysis of variance (ANOVA) was performed. Post-hoc testing was performed using Tukey's post-hoc analysis.

2.3 RESULTS

2.3.1 Single Mild TBI: A Transient Change in Neurological Status with No Gross Structural Brain Damage

Male Sprague Dawley rats underwent baseline neurological assessment and then were anesthetized immediately before a single mild TBI was administered. Ten minutes, two hours, and 24 hours post-impact, animals underwent neurological assessment again to quantify the effect of a single mild TBI on neurological status. Scores from individual behavioural tasks (open field, beam walk, and inverted wire mesh) were summed together to generate a combined neurological score (Figure 2.2 A).

Compared to baseline, animals exposed to a single mild TBI had a significant reduction in their combined neurological score 10 minutes post-impact ($P < 0.0001$, n =

81). This decrease in neurological score persisted at 2 hours post-impact ($P = 0.0012$, $n = 11$). However, when tested 24 hours later, animals exposed to a single mild TBI did not differ in combined neurological scoring compared to baseline ($P = 0.1306$, $n = 81$), indicating a return to baseline test performance one day post-impact (Figure 2.2 A). Sham controls did not differ in combined neurological score across any of the time points assessed ($P = 0.2419$, $n = 29$).

A subset of animals underwent MRI 24 hours after a single mild impact ($n = 4$) or sham anesthesia ($n=2$) was given and a standard T2-weighted fast spin echo sequence was performed. T2-weighted imaging showed no evidence of contusions or hemorrhage in single mild TBI or sham control animals (Figure 2.2 C). Post-mortem analysis of brains removed 24 hours post-impact from animals exposed to a mild TBI ($n = 4$) or sham controls ($n = 2$) showed no evidence of intracranial contusions and no evidence of hemorrhage or skull fracture (Figure 2.2 B). Subcutaneous hematoma on the surface of the skull was common, however no evidence of blood was seen below the layer of the skull upon brain extraction.

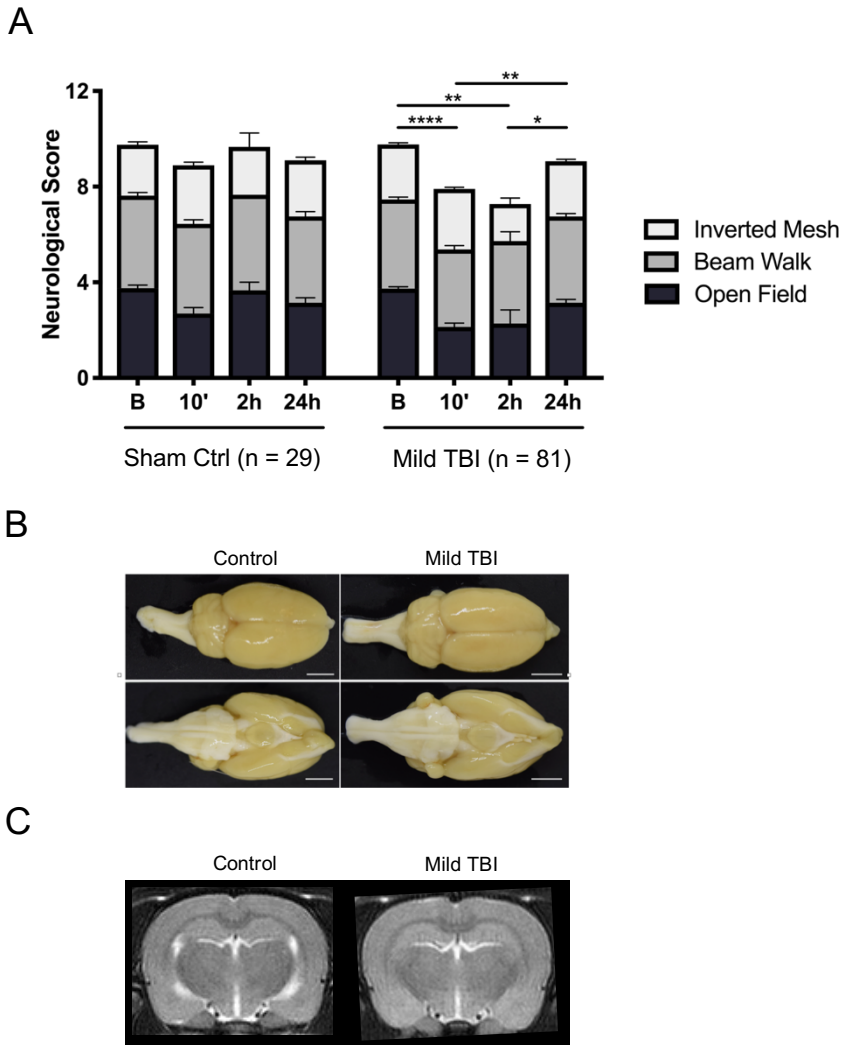

Figure 2.2: A single mild TBI produces characteristics consistent with mild concussive brain injury. (A) Animals exposed to a single mild TBI had a significantly lower combined neurological score when tested ten minutes ($P < 0.0001$, $n = 81$) and two hours ($P = 0.0012$, $n = 11$) following injury compared to baseline. When tested 24 hours later, combined neurological scores did not differ from pre-injury baseline levels ($P = 0.1306$, $n = 81$). Combined neurological scores did not differ at any time point for sham controls ($P = 0.2419$, $n = 29$). **(B)** No gross structural changes were observed in brains extracted 24 hours after a single mild impact or anesthesia was administered. Scale bar = 5 mm. **(C)** T2-weighted imaging conducted in animals 24 hours after a single mild impact was administered ($n = 4$) did not show evidence of intracranial hemorrhage or gross structural damage. Mean ± SEM is shown for A.

2.3.2 rmTBI Leads to Acute Deterioration in a Subset of Animals

Following validation of the model to produce a mild "concussion-like" injury after one impact, we studied the effects of repetitive impacts. One hundred and seventy-four (n = 174) animals underwent baseline neurological assessment prior to commencing the rmTBI protocol. Of these, 137 animals were randomly assigned to the rmTBI group and received one mild TBI per day for up to five consecutive days. Thirty-seven (n = 37) animals were randomly assigned to the sham control group, and received the same treatment as the rmTBI group, but did not receive an impact to the head and instead were only anesthetized. All animals underwent baseline behavioural assessment before each impact was administered to assess their neurological status prior to repetitive injury.

Compared to sham controls, rmTBI-exposed animals had a lower combined neurological score after three impacts were administered ($P = 0.0116$, n = 108; Figure 2.4 A), and this effect was maintained following four impacts ($P < 0.0001$, n = 98; Figure 2.4 A). When tested two days after the fifth impact was administered, partial recovery was observed in rmTBI animals, as their neurological score no longer differed from controls at this time point ($P = 0.1545$, n = 79; data not shown).

There were no deaths observed after a single mild injury (n=137). However, thirteen percent (13%, n = 18) of rmTBI-exposed animals died as a result of the repeated injuries (Figure 2.3 A), with the mortality rate increasing after consecutive impacts (Figure 2.3 B). Of the remaining 87% of animals (n = 119) that survived, some rmTBI animals deteriorated significantly upon repeated injury, while others did not appear to differ from sham controls. Retrospective analysis of the distribution of combined neurological scores for rmTBI animals showed a progressive broadening of the score distribution with consecutive impacts (Figure 2.4 B-D). At baseline (Figure 2.4 B) and after a single impact

(Figure 2.4 C), the distribution of neurological scores appeared similar between sham controls and rmTBI animals. In contrast, a bimodal distribution better characterized the combined neurological scores for rmTBI animals (but not sham controls) after four impacts, indicating substantial differences between animals in response to repeated trauma (Figure 2.4 D).

To better investigate the differential response to injury that was observed between individuals, animals with a combined neurological score below 6 (the trough neurological score value separating the two distributions after four impacts) were retrospectively considered as a distinct group, referred to as "sensitive" (to rmTBI), while animals with a combined neurological score equal to or greater than 6 after four impacts were termed "resilient" (to rmTBI). Additionally, animals that were unable to receive all five impacts (mean n = 3.7 impacts, n = 67) as a result of 1) significant morbidity, or 2) post-impact mortality were also classified as "sensitive" to repeated injury. Overall, 56% of rmTBI-exposed animals retrospectively met the criteria for being "sensitive", while 44% of rmTBI-exposed were classified as "resilient" (Figure 2.4 F).

By definition, classification of the rmTBI-exposed population into sensitive and resilient subgroups showed that sensitive animals have a lower combined neurological score than resilient or sham control animals. After two impacts, sensitive animals had a lower neurological score than sham control animals ($P = 0.0417$; Figure 2.4 E). After three impacts, sensitive animals scored lower than sham control ($P = 0.0006$; Figure 2.4 E) and resilient animals ($P = 0.0063$; Figure 2.4 E). This difference continued after four impacts. When tested two days after the fifth impact, sensitive animals differed significantly from sham control but not resilient animals ($P = 0.0196$; data not shown). In contrast, resilient

animals did not differ in combined neurological score from sham controls at any point during the acute behavioural assessments (Figure 2.4 E).

In addition to differences in neurological score, sensitive animals also lost weight following repetitive injury. Sensitive and resilient animals (n = 67) did not differ in baseline weight prior to impact (P = 0.8798, unpaired t test; Figure 2.5 A). After repetitive injury, sensitive animals showed significantly less daily weight gain than resilient or sham control animals (P < 0.0001; Figure 2.5 B).

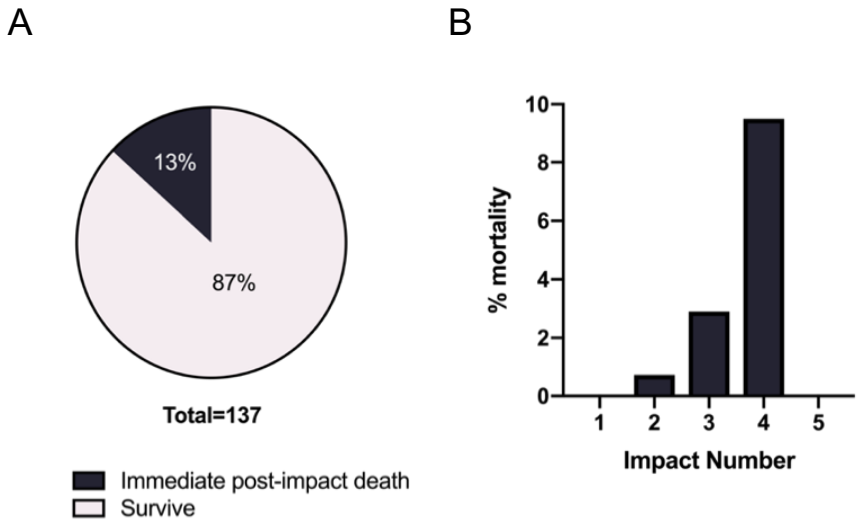

Figure 2.3: Acute mortality following rmTBI. (A) Thirteen (13%) of animals experienced immediate post-impact mortality following exposure to repetitive injury (n = 18 out of 137 animals). **(B)** No mortality was observed after a single mild impact, but the risk of acute mortality increased after repetitive impacts.

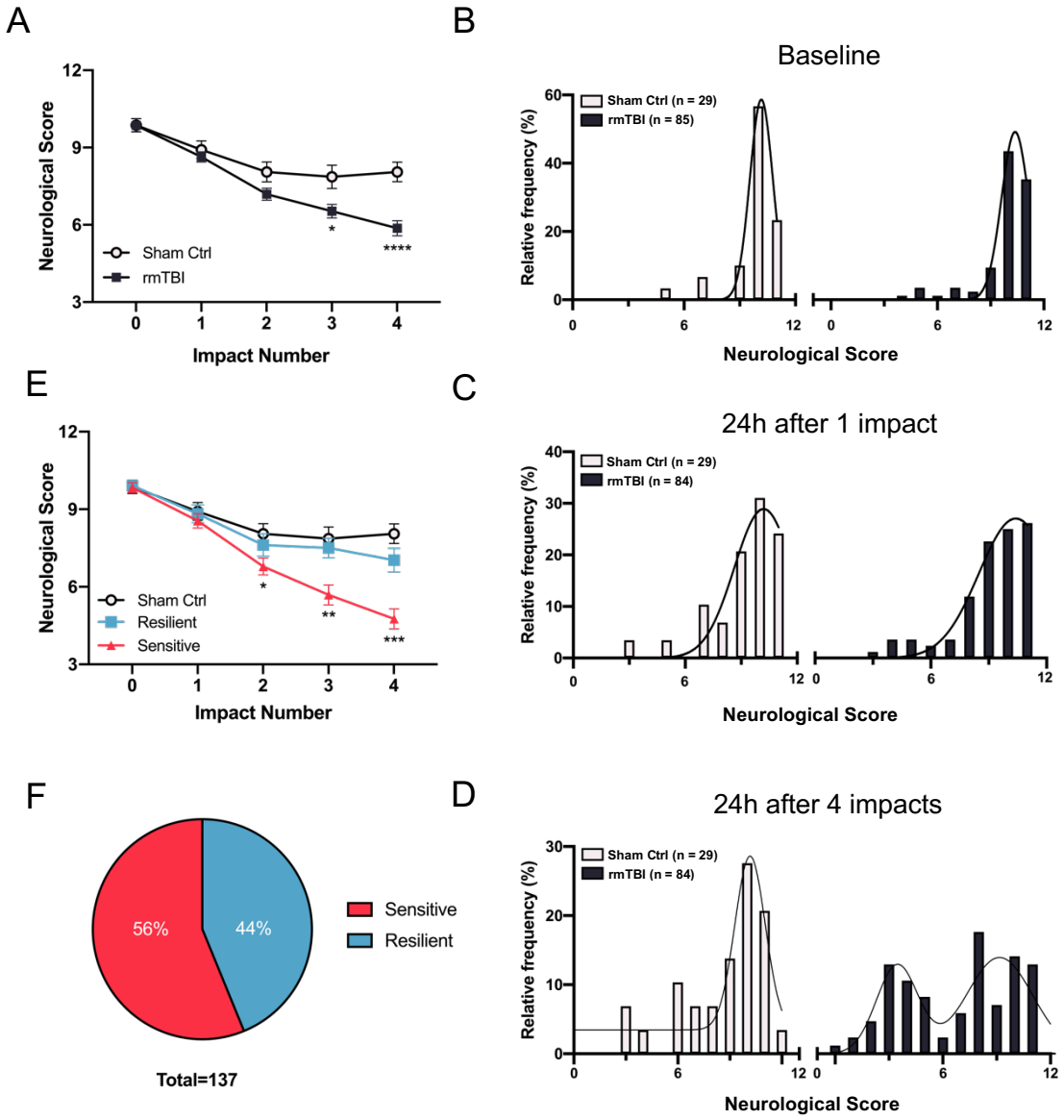

Figure 2.4: Acute characterization of neurobehavioural response to rmTBI. **(A)** Animals exposed to rmTBI had lower neurological scores after three (P = 0.0116) and four (P <0.0001) impacts than sham controls. **(B, C, D)** Relative frequency histograms of scores revealed a bimodal distribution after repetitive impacts. **(E)** Retrospective classification of animals as "sensitive" or "resilient" to rmTBI demonstrates that (by definition) sensitive animals experienced a progressive reduction in neurological score with repetitive impacts. Sensitive animals had a lower neurological score than sham controls after two impacts (P = 0.0417). Sensitive animals scored lower than sham control and resilient animals after three (P = 0.0063) and four impacts (P = 0.0004). **(F)** Overall percentage of sensitive versus resilient animals is shown. See Appendix C for additional details on ratio of sensitive to resilient animals. Mean ± SEM is shown for A and E.

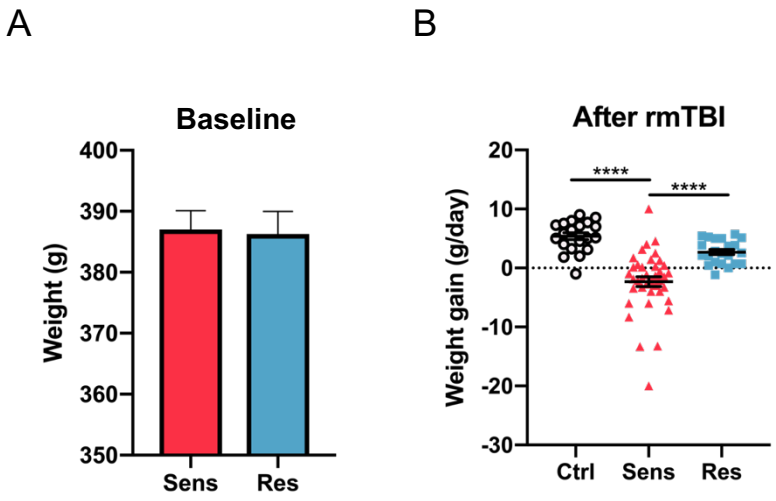

Figure 2.5: Sensitive animals have reduction in weight gain following rmTBI. **(A)** Sensitive (n = 63) and resilient (n = 45) animals did not differ in baseline weight prior to start of experiments (P = 0.8798). **(B)** Following administration of repetitive impacts, sensitive animals (n = 39) showed a reduction in daily weight gain (P < 0.0001) compared to sham control (n = 20) and resilient animals (n = 22), which continued to gain weight during their adolescent phase of growth. Mean ± SEM are shown.

2.3.3 Impact Mechanics Do Not Account for Differential Response to rmTBI

To address the possibility that differences in impact mechanics may underlie the observed differences between sensitive and resilient animals, two quantitative approaches were used. In a subset of rmTBI-exposed animals (n=48), pressure-sensitive film was used to quantify the mean pressure administered during each impact. No differences were found in mean administered pressure between sensitive (n = 37) and resilient (n = 11) animals across all impacts (P = 0.3917; Figure 2.6 A). Additionally, no differences in administered pressure (Figure 2.6 B) were found between sensitive and resilient animals during impact 1 (P = 0.7486), impact 2 (P = 0.6576), impact 3 (P = 0.5195), impact 4 (P = 0.2258), or impact 5 (P = 0.7016).

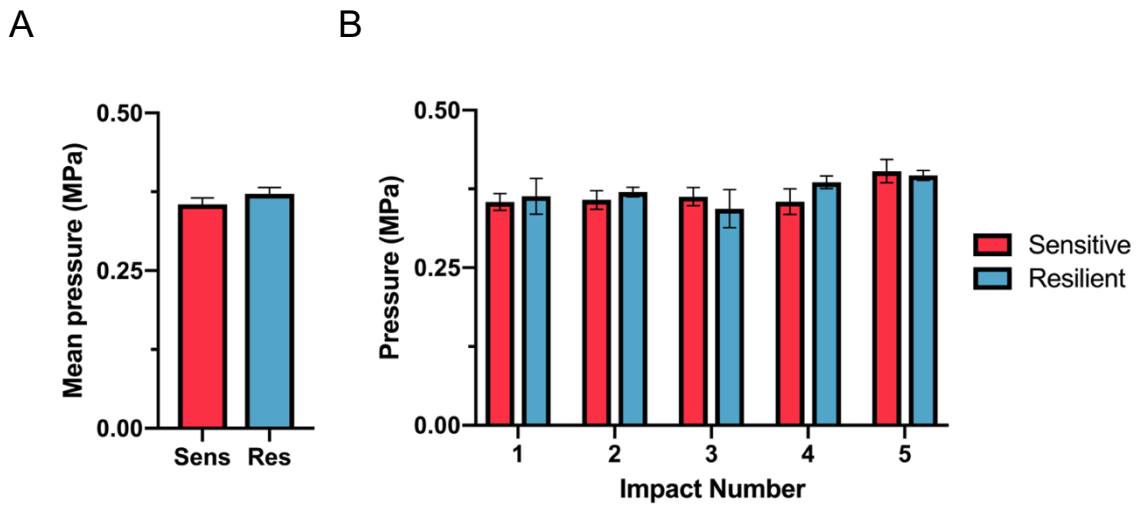

Figure 2.6: Mean impact pressure between sensitive and resilient animals does not differ. (A) The mean pressure across all impacts delivered to sensitive (n = 37) and resilient (n = 11) animals did not differ (P = 0.3917). **(B)** The mean pressure delivered during each individual impact did not differ between sensitive and resilient animals (Impact 1: P = 0.7486, Impact 2: P = 0.6576, Impact 3: P = 0.5195, Impact 4: P = 0.2258, Impact 5: P = 0.7016). Mean ± SEM are shown.

High-speed video footage was recorded for a subset of impacts (n=11) in order to characterize possible differences in various impact features (velocity, acceleration, angular velocity, and angular acceleration) between sensitive and resilient animals. Tracking of impact motion was performed by manually tracing the trajectory of the head of the animal throughout each frame of the impact, using the eye as an anatomical marker. No significant differences were found between sensitive and resilient animals in the average or peak impact velocity, acceleration, angular velocity, or angular acceleration during any of the five administered impacts (Table 2.2). Representative traces and peak values for impact acceleration are shown in Figure 2.7 A - F.

Kinematic Parameter		TBI 1		TBI 2		TBI 3		TBI 4		TBI 5	Mean of all TBIs	
		Sens	**Res**	**Sens**	**Res**	**Sens**	**Res**	**Sens**	**Res**	**Res**	**Sens**	**Res**
Linear Velocity (m/s)		4.2 ± 0.38	4.16 ± 0.21	4.80 ± 0.53	4.87 ± 0.30	5.17 ± 0.46	5.23 ± 0.42	3.99 ± 0.47	4.58 ± 0.67	5.06 ± 0.28	4.5 ± 0.27	4.7 ± 0.19
Linear Acceleration (m/s^2)		442.7 ± 43.7	446.4 ± 32.4	493.5 ± 44.0	462.8 ± 29.0	534.7 ± 38.9	532.2 ± 34.9	430.7 ± 43.4	455.0 ± 87.7	507.4 ± 31.7	475.4 ± 24.0	490.8 ± 16.6
Angular velocity (rad/s)		144.7 ± 6.4	126.8 ± 11.8	141.9 ± 5.9	148.5 ± 7.7	139.9 ± 10.4	146.2 ± 9.4	118.5 ± 14.6	164.7 ± 37.5	139.2 ± 4.7	136.3 ± 5.9	145.1 ± 6.2
Angular Acceleration (rad/s^2)	**Peak 1**	11330 ± 366.1	14100 ± 555.5	14683 ± 395.9	15450 ± 438.5	16122 ± 531.2	16600 ± 654.4	13766 ±1200.2	20090 ±3591.4	14900 ± 621.3	13975 ±1006.4	16228 ±1047.6
	Peak 2	10403 ± 1221.7	14648 ± 1572.8	15967 ± 955.92	16500 ± 1093.2	16893 ± 1622.3	16400 ± 1975.1	12640 ± 5540.3	19663 ± 3198.7	15820 ± 1312.8	13976 ± 1500.5	16606 ± 832.2

Table 2.2. Impact tracking analysis. Peak values for each kinematic parameter evaluated with mean ± SEM are reported. Sensitive and resilient animals do not differ significantly in any kinematic parameter assessed.

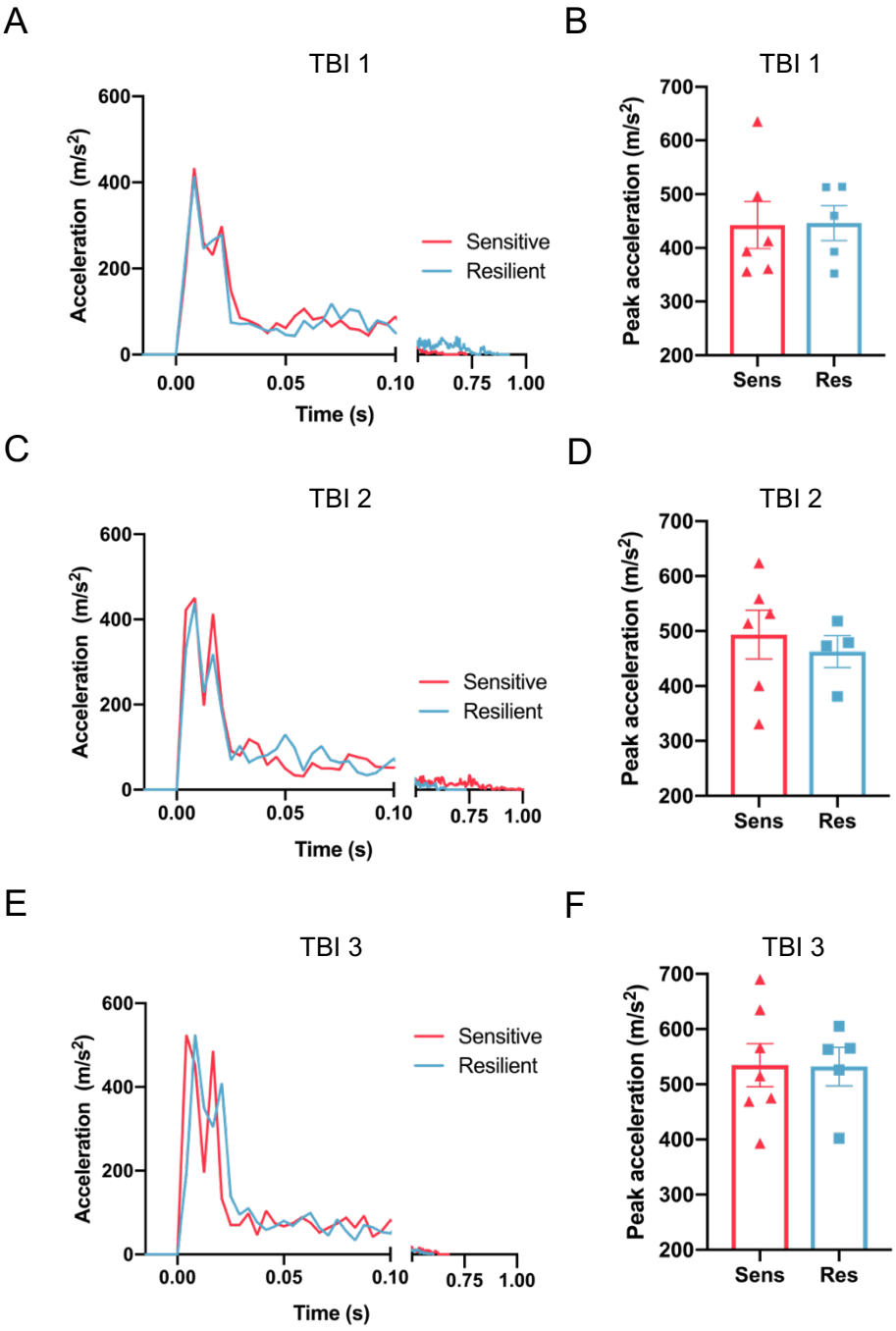

Figure 2.7: Sample of linear acceleration traces for impact tracking analysis. (A, C, E) Impact tracking using high-speed video footage indicated that sensitive (n = 6) and resilient (n = 5) animals do not differ in mean acceleration wave-form appearance or **(B, D, F)** peak values for TBI 1 (P = 0.9307), TBI 2 (P = 0.4762), or TBI 3 (P > 0.9999). Mean ± SEM are shown for B, D, and F.

2.3.4 Sensitive Animals Have Increased Duration of Post-Impact Convulsions and Delayed Acute Recovery

In some animals, we observed convulsions that immediately followed the impact. A subset of post-impact recovery videos for sham control (n = 12) and rmTBI-exposed animals (n = 51) were analyzed for the occurrence of the convulsions. On average, convulsions occurred within 9.1 ± 1.5 seconds of impact, lasted for 22.2 ± 2.4 seconds, and often involved rapid onset of tonic stiffening before rhythmic kicking (tonic-clonic movement) of the hind limbs began. Overall, forty-eight percent (48%) of rmTBI-exposed animals exhibited convulsions, of which 61% were retrospectively classified as sensitive animals and 39% were classified as resilient animals. Additionally, the percentage of animals displaying these movements increased after repeated impacts (Figure 2.8 A), and 70% of animals that exhibited an abnormal post-impact convulsion had another such event after a subsequent impact. A subset (n = 10) of convulsions were analyzed and showed a mean X-amplitude of 5.88 ± 0.75 cm, a mean Y-amplitude of 6.38 cm ± 0.83 cm and a frequency of 1.1 ± 0.10 Hz. No such movements were seen in sham controls. Notably, the duration of the convulsions immediately following impact increased significantly over time for sensitive animals (P = 0.0459, n = 20; Figure 2.8 B), but not for resilient animals (P = 0.1876, n = 12, Figure 2.8 B).

Next, we tested the latency to recover from anesthesia and impact by measuring the righting reflex and the latency to resume spontaneous locomotion. Compared to sham control animals (n = 14), sensitive animals (n = 20) had an increased righting reflex latency after impact 1 (P = 0.0268; Figure 2.8 C) and impact 2 (P = 0.0079; Figure 2.8 C). After impact 3, sensitive animals had a longer delay in regaining the righting reflex compared to resilient (n = 12) (P = 0.0035; Figure 2.8 C) and sham control animals (P = 0.0025; Figure

2.8 C). Likely owing to a substantial reduction in the number of sensitive animals that received additional impacts following TBI 3, no differences in righting latency were found between sensitive (n = 8), resilient (n = 11), and sham control (n = 14) animals after impact 4 (P = 0.0642; data not shown) or impact 5 (P = 0.0872; data not shown).

The time to regain locomotion was also measured following injury and showed similar trends to the righting latency. Specifically, compared to sham control animals (n = 14), sensitive animals (n = 20) had an increased latency to resume locomotion after impact 1 (P = 0.0039; Figure 2.8 D) and impact 2 (P = 0.0447; Figure 2.8 D). After impact 3, sensitive animals had a longer latency to resume locomotion compared to resilient (n = 12) (P = 0.0283; Figure 2.8 D) and sham control animals (P = 0.0023; Figure 2.8 D). Likely due to the substantial reduction in the number of sensitive animals that received additional impacts following TBI 3 (n = 8 for impact 4, n = 2 for impact 5), no significant differences were found in the latency to resume locomotion between sensitive, resilient (n = 11), and sham control (n = 14) animals after impact 4 (P = 0.1092; data not shown) or impact 5 (P = 0.1499; data not shown).

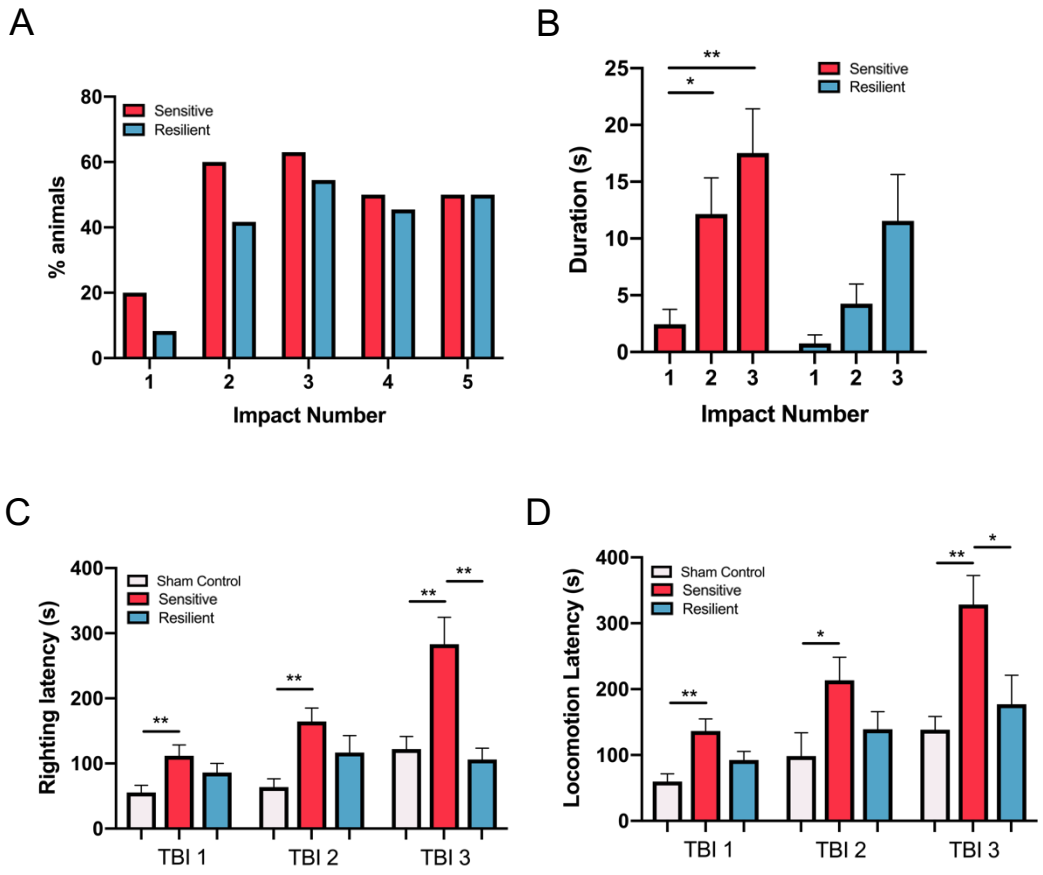

Figure 2.8: Sensitive animals have longer post-impact convulsions and delayed acute recovery with repetitive impacts. **(A)** The percentage of sensitive and resilient animals displaying post-impact convulsions after each impact is shown. Both sensitive and resilient animals displayed these movements, with an increased occurrence over time, which was not significant. Sham controls did not experience convulsions following administration of anesthesia. **(B)** Sensitive animals had a progressively longer convulsion duration with repetitive impacts (P = 0.0459, n = 20), whereas resilient animals did not (P = 0.1876, n = 12). **(C)** Sensitive animals took significantly longer to regain the righting reflex compared to sham controls after TBI 1 (P = 0.0251) and TBI 2 (P = 0.0025). After TBI 3, sensitive animals took significantly longer to regain the righting reflex than sham controls (P = 0.0028) and resilient animals (P = 0.0022). **(D)** Sensitive animals took significantly longer to resume locomotion compared to sham controls (n = 14) after TBI 1 (P = 0.0039) and TBI 2 (P = 0.0447). After TBI 3, sensitive animals took significantly longer to resume locomotion than sham controls (P = 0.0023) and resilient animals (P = 0.0283). Mean ± SEM are shown for B – D.

2.3.5 rmTBI-Exposed Animals are Neurologically and Cognitively Impaired One Month Post-Impact

To assess the delayed complications of rmTBI exposure, a subset of rmTBI (n = 48) and sham control (n = 20) animals were behaviourally tested one month post-impact (Figure 2.9). Compared to sham controls, rmTBI animals had a reduction in neurological score one month post-impact (P = 0.0123; Figure 2.9 A). Interestingly, whereas sensitive and sham control animals did not differ in neurological scoring from one week to one month post-impact, resilient animals deteriorated significantly across these time points (P = 0.0435; Figure 2.9 B). As such, no significant differences in neurological score were found between sensitive (n = 26) and resilient (n = 22) animals one month post-impact (P = 0.3863; Figure 2.9 C).

Additionally, a subset of rmTBI-exposed (n = 13) and sham control (n = 10) animals underwent spatial learning and memory testing using the MWM test one month post-impact (Figure 2.10). This test requires animals to learn the location of a hidden escape platform in a pool of opaque water by using and remembering local visual cues to localize the platform. Animals exposed to rmTBI did not differ from sham controls during the acute learning phases of this task and were able to successfully locate the platform upon repeated trials completed on the same day (Figure 2.10 A). However, when tested 24 hours after the initial trials were given, rmTBI-exposed animals took significantly longer to find the platform than sham controls (P = 0.0411; Figure 2.10 B). Additionally, rmTBI animals spent less time in the quadrant containing the platform compared to sham controls when tested 24 hours after completing the initial trials (P = 0.0099, Figure 2.10 C). Interestingly, sensitive (n = 8) and resilient (n = 5) animals did not significantly differ in cognitive performance in this task, as measured by the latency to locate the platform (P = 0.0684;

Figure 2.10 D) or the percentage of time spent in the quadrant containing the platform (P = 0.0932; Figure 2.10 E).

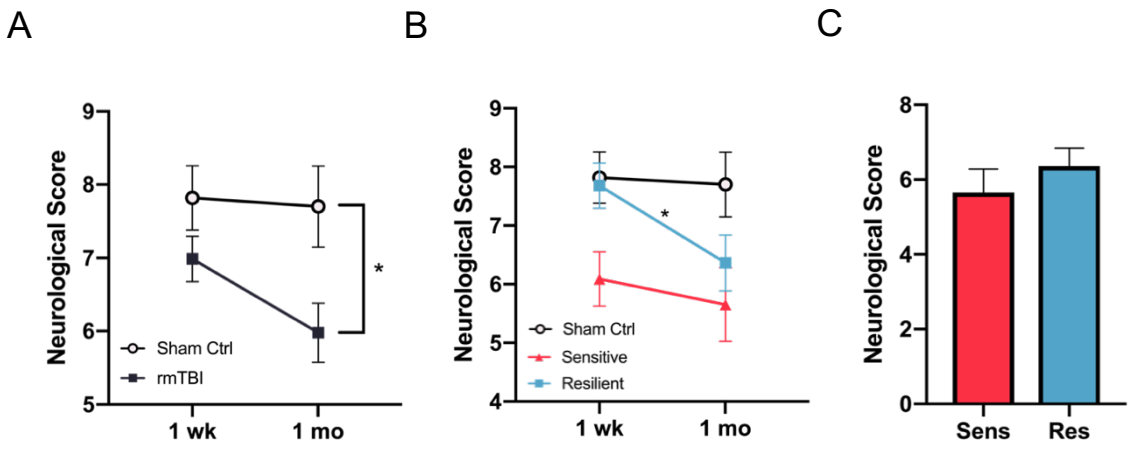

Figure 2.9: Sensitive and resilient rmTBI animals deteriorate neurologically one month post-impact. (A) Neurological scores of rmTBI (n = 48) or sham control (n = 20) animals are shown at one week and one month post-impact. Compared to sham controls, rmTBI animals had a lower neurological score one month post-impact (P = 0.0123). **(B)** Analysis of the change in neurological score between one week and one month post-impact revealed that resilient animals deteriorate significantly (P = 0.0435) between these time points. In contrast, neurological scores of sensitive and sham control animals did not differ at one month post-impact compared to their scores at one week post-impact. **(C)** Sensitive and resilient animals did not differ in neurological score when tested one month after exposure to rmTBI (P = 0.3863). Mean ± SEM are shown.

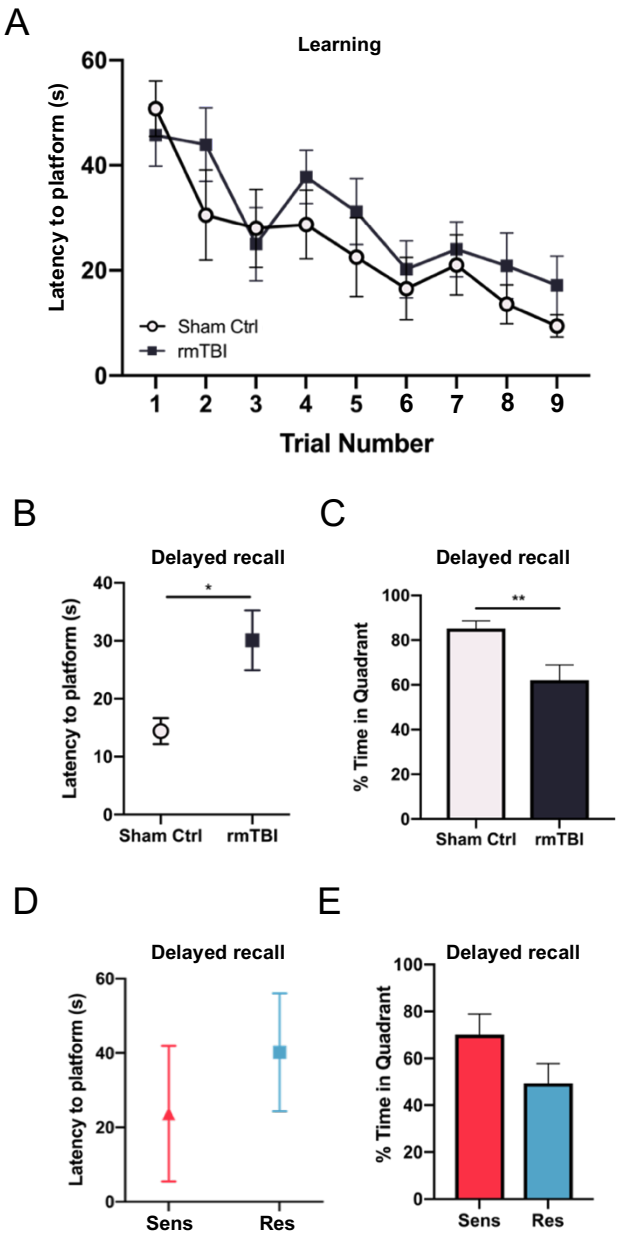

Figure 2.10: Sensitive and resilient rmTBI animals are impaired in MWM delayed recall one month post-impact. (A) One month post-impact, the latency to reach the escape platform did not differ between rmTBI and sham control animals across the initial nine learning trials. **(B and C)** Animals exposed to rmTBI had a longer latency to reach the escape platform (P = 0.0411) **(B)** and spent significantly less time in the quadrant containing the platform (P = 0.0099) **(C)** than sham controls when tested 24 hours after the initial learning was acquired. **(D and E)** Delayed recall of platform location did not differ between sensitive and resilient animals, as measured by the latency to locate the platform (P = 0.0684) **(D)** or the percentage of time spent in the quadrant containing the platform (P = 0.0932) **(E)**. Mean ± SEM are shown.

2.4. DISCUSSION

2.4.1 Summary

The goal of this chapter was to characterize a model of repetitive mild traumatic brain injury for use in adolescent rats. This model incorporates substantial rotational motion and involves the administration of up to five repetitive impacts. We showed that a single impact using this model produces transient changes in neurological status and an absence of gross anatomical lesions. These features are consistent with a mild brain injury in which concussion-like symptoms are present acutely but are minimally persistent. Importantly, exposure to repetitive impacts led to a progressive and significant deterioration in health in a subset of animals. Retrospective analysis of neurological scores revealed marked differences in responses within the population of animals exposed to rmTBI. A subgroup of animals "sensitive" to rmTBI was identified and these animals were shown to be distinct in neurological and physical response from other rmTBI-exposed animals that appeared "resilient" to the acute effects of rmTBI.

In particular, sensitive animals were classified based on acute mortality, significant morbidity, and lower neurological scores following exposure to rmTBI which often led to the inability of these animals to receive all five impacts. Classification of rmTBI-exposed animals into sensitive and resilient groups allowed for specific questions to be addressed regarding the differences that exist between these animals. Importantly, differences in impact pressure and mechanics were unable to explain the differential acute injury outcomes that were observed between sensitive and resilient animals, suggesting that these differences are instead mediated by the animals' response to the injuries themselves.

In the immediate seconds following impact, some rmTBI animals exhibited convulsions. While these events were seen in both sensitive and resilient animals, the duration of these events increased significantly in sensitive (but not resilient) animals upon repetitive injury. Further, sensitive animals had a longer latency to regain the righting reflex and to resume locomotor activity post-impact than resilient or sham controls.

Finally, we found that rmTBI animals have persistent neurological and cognitive impairments when tested one month post-impact. Interestingly, differences in neurological status that characterized sensitive and resilient animals acutely in this model did not persist to this delayed time point.

2.4.2 Characterization of a Single Mild TBI

A modified Marmarou closed-head weight-drop approach to model sports-related TBI in adolescent rodents was used. This model incorporated substantial acceleration and rotation of the head, which is an essential characteristic of concussive impacts sustained by humans (Meaney and Smith, 2011). A series of behavioural tasks were utilized to assess the acute effects of a single impact and performance on each of these tasks was assessed using a standardized scoring system (Table 2.1). A combined neurological score was formed from the individual scores of these tasks, which was designed to capture changes in neurological status (such as those relating to locomotor and balance abilities) following injury (Tagge et al., 2018).

In establishing the model, an impact mass of 500 g travelling a vertical distance of 85 cm was selected as the input parameters for this weight-drop model. Other models using the modified-Marmarou approach have varied in input parameters to model mild injury, partially owing to the use of different animal strains (mouse versus rat) and animal

ages. Kane et al. (2012) used a 95-gram mass from a distance of 1 meter in adult mice to produce a mild injury with the absence of skull fracture, intracranial hemorrhage, and low rates of mortality. Mychasiuk et al. (2014), used 150 grams and a fall distance of 0.5 meters in 4-week old juvenile rats while Goddeyne and colleagues (2015) used a 92-gram weight at 0.86 meters on juvenile (3 week-old) rats to produce a mild injury with similar outcomes. The parameters that we selected varied from those previously described in the literature, as we sought to model TBI in adolescent rats. Additionally, the impact parameters were evaluated on their ability to reliably generate neurological features consistent with a mild brain injury following a single impact. In particular, three criteria were identified based on the 2018 Berlin Consensus statement from the CISG on the definition of sports-related concussion (McCrory et al., 2017b) to define a mild injury:

***Criterion 1**: A single impact produces an acute decline in neurological status*

When tested ten minutes after a single mild injury, TBI animals showed a significant decrease in combined neurological score. This decline persisted when animals were tested two hours post-impact. These results suggest an acute impairment in neurological status occurs following a single mild TBI using this model. The ten-minute time point was selected as it was the earliest time in which all animals had regained the righting reflex and the ability to locomote, allowing for animals to adequately engage with the behavioural tests. The two-hour time point was selected to determine if changes were persistent beyond the immediate post-impact window, and to assess animals after the immediate effects of isoflurane anesthesia had dissipated. Our findings are similar to observations made by Tagge et al. (2018), in which they report a reduction in neurological scoring (using the same three behavioural tasks) when mice were assessed two minutes

after exposure to a mild impact. Together, the results from this criterion suggest that the impact parameters for this weight-drop model were well-suited to produce a significant decrease in neurological score in the first minutes to hours following a single mild injury.

***Criterion 2**: The acute neurological decline following impact is transient in nature*

Despite significant decline in neurological status in the moments to hours post-impact, behavioural scores of animals exposed to a mild impact returned to baseline when tested 24 hours later. This suggests that the acute decline in neurological status of animals following mild TBI was not permanent or even persistent overnight. Instead, a single injury with this model produced acute deficits that resolved 24 hours later, indicating a transient impairment in neurological status. This is consistent with the current definition of concussion generated by the 2017 Concussion in Sport Group consensus report, which states that "sports-related concussion typically results in the rapid onset of short-lived impairment of neurological function that resolves spontaneously" (McCrory et al., 2017b).

***Criterion 3**: No gross anatomical changes were observable following impact*

Twenty-four hours after a single mild injury, a subset of TBI animals and sham controls were sacrificed and their brains were harvested for gross tissue analysis. None of these animals showed evidence of brain contusions or skull fracture, although sub-cutaneous hematoma above the skull was common. Additionally, no signs of intracranial lesion were apparent on T2-weighted MR images acquired 24 hours post-impact. These findings are consistent with the 2017 Concussion in Sport Group consensus report's description of concussion as largely a "functional injury" in which "no abnormality is seen on standard structural neuroimaging studies" (McCrory et al., 2017b). Additionally, the

lack of gross structural injury is consistent with reports from other experiments involving the modified Marmarou approach, in which minimal or no skull fracture or intracranial bleeding were observed (Kane et al., 2012; Mychasiuk et al., 2014; Goddeyne et al., 2015).

Taken together, these results indicate that a single impact using our model recapitulates relevant aspects of the currently supported definition and understanding of sports-related concussion and mild traumatic brain injury.

2.4.3 Repetitive Mild TBI

Upon validation of the model to produce a mild injury following a single impact, we next exposed animals to repetitive injuries. Specifically, animals were given one impact per day for up to five consecutive days, for a maximum of five administered impacts. This injury timeline is consistent with previous models of rmTBI, in which adult mice (Kane et al., 2012) and juvenile rats (Goddeyne et al., 2015) were exposed to one impact per day for five consecutive days. However, in contrast to these models which described minimal injuries, our animals showed a progressive worsening of neurological signs following repetitive injuries. In particular, a subset of animals sensitive to rmTBI was identified due to their significant deterioration in health compared to other rmTBI-exposed animals that appeared resilient to the effects of repetitive injury. Our observation of the substantial variation in acute injury outcomes and behavioural responses between individual animals has previously been noted by others (Mychasiuk et al., 2014; Tagge et al., 2018), although was not further addressed by these groups. Given the clinical relevance due to the vast heterogeneity of responses to TBI (Saatman et al., 2008; Rosenbaum and Lipton, 2012) we sought to further explore these differences. As such, animals were retrospectively classified as “sensitive” to rmTBI if they: (1) Died acutely following an impact, (2) were unable to

receive 5 impacts (due to significant morbidity), or (3) had a combined neurological score of less than 6 after four consecutive impacts. All rmTBI animals that did not meet these three parameters were considered resilient. The ratios of sensitive to resilient animals were relatively consistent across multiple cohorts, although some variation in this frequency was observed (Appendix C).

In some cases, animals experienced immediate death following impact, although consistent with similar models of mild injury using the modified Marmarou approach (Kane et al., 2012; Mychasiuk et al., 2014; Goddeyne et al., 2015), no death was observed after a single impact. However, the mortality rate increased to 13% as consecutive impacts were administered, which is similar to the 10% mortality rate reported by Kane et al. (2012) after administration of five impacts to adult mice. In addition to increased mortality and lower neurological scores, sensitive animals also lost weight in response to repetitive injury, indicating that the deterioration of sensitive animals is not a test-specific phenomenon. The reason for weight loss in rmTBI-exposed animals may be related to changes in appetite following injury, as has been described in human patients with concussion (McCrory and Johnston, 2002).

2.4.4 Comparison of Impact Mechanics

A notable criticism of closed-head weight drop models of TBI is that it can be difficult to reliably produce a consistent injury as variability between impacts and the administered force can be high (Xiong et al., 2013). As such, we used pressure sensitive film and recorded high speed video footage of the impacts in order to address the possibility that differences in the administered impact pressure or impact mechanics were associated with the observed differential response to injury between sensitive and resilient animals.

We did not find any differences between sensitive and resilient animals in the mean pressure administered on each impact or in the overall pressure across all impacts. Importantly, the pressure film approach was sensitive enough to quantify differences in administered pressure between our model's inputs to produce a mild injury (500 g, 85 cm) compared to inputs of 450 g and a fall distance of 110 cm to produce a moderate injury (Appendix D). Additionally, the mean velocity, acceleration, angular velocity, and angular acceleration experienced by the head of each animal did not differ between sensitive and resilient animals. Given that variations in impact biomechanics did not account for the observed outcome differences between sensitive and resilient animals, these differences may instead be due to different responses to the trauma itself. A notable limitation of these findings is the relatively low frame rate that was used, and future studies would benefit from increasing the frame rate for assessment of impact biomechanics. Nevertheless, our findings are consistent with the notion that individual variability in outcome following mild injury can arise even when impact biomechanics are highly consistent, as has been suggested by others (Tagge et al., 2018).

2.4.5 Immediate Events Following Impact: Convulsions and Acute Recovery

In the immediate seconds following impact, convulsions were observed in nearly half (48%) of rmTBI-exposed animals, with approximately 15% of animals experiencing these movements after a single mild impact. This finding is in contrast to similar models of mild TBI in which convulsive movements are very rare or do not occur at all (Kane et al., 2012; Goddeyne et al., 2015). However, a convulsion rate of 33% following a single mild injury was reported in a model of closed-head mild TBI (Blaha et al., 2010), although the model did not involve the free-fall component and associated rotational motion used in

this study. Interestingly, both sensitive and resilient animals displayed post-impact convulsions and the majority (70%) of animals that had one convulsive event went on to have another following a subsequent injury. These results suggest that the presence alone of these post-impact convulsions is not necessarily associated with a more severe acute neurological outcome (i.e. sensitivity or resiliency to repetitive impacts). However, upon repetitive impacts sensitive animals did have an increasingly long duration of these movements, whereas resilient animals did not.

Due to the rapid onset and relatively brief duration of these convulsive movements following impact, it is likely that the convulsive events we observed in rmTBI-exposed animals are concussive convulsions. Unlike "post-traumatic seizures", concussive convulsions are characterized by myoclonic or tonic-clonic movements that occur in the immediate *seconds* following impact. Our animals often experienced an early phase of tonic stiffening immediately before the onset of myoclonic jerking, which is typical for concussive convulsions (McCrory and Berkovic, 1998). Further, the myoclonic movements were often associated with the hind limbs of the animals, in which they experienced kicking motions that were often bilateral and asymmetrical, as in the case of concussive convulsions (McCrory and Berkovic, 1998). In our study, these movements were characterized by a mean X-amplitude of 5.88 cm, a mean Y-amplitude of 6.38 cm, and a mean frequency of 1.1 Hz. To our knowledge, we are the first to characterize the amplitude and frequency of these movements in rodents following mild injury. However, one retrospective study in humans assessed video footage of impacts sustained during various sporting events leading to concussive convulsions and reported the frequency of

clonus ranging from 1 – 5 Hz following impact, indicating a similar frequency to our observations (Tényi et al., 2016).

Convulsions following sports-related TBI are estimated to have an incidence of 1 in 70 concussions, and so are relatively rare events (Perron et al., 2001). However, McCrory et al. report that more subtle motor manifestations, such as tonic posturing and clonic movements, are common events following concussion (McCrory and Berkovic, 2000). It is possible that our rodent model of TBI generates these events much more frequently due to the relative consistency of impact location and mechanics of our injuries, in comparison to the wide variability of injuries experienced by athletes in the sporting context.

The precise etiology of concussive convulsions is unknown, but it has been suggested that impact to the brain can lead to a transient loss in cortical inhibition of the brainstem, resulting in activation of brainstem reflexes and the rapid occurrence of convulsions (McCrory et al., 1997; McCrory and Berkovic, 1998). The outcome of concussive convulsions in athletes is generally regarded as good and these events have not been associated with any structural brain injury or epileptiform activity detected by follow-up electroencephalogram (EEG) (McCrory et al., 1997; McCrory and Berkovic, 1998; Ellis and Wennberg, 2016), although whether or not these events are completely benign remains unknown. Concussive convulsions have not been associated with an increased risk of post-traumatic epilepsy and are not thought to be epileptic in nature, and as such, anti-epileptic medications are not currently indicated (McCrory et al., 1997; McCrory and Berkovic, 1998; Ellis and Wennberg, 2016). In our model, both sensitive and resilient animals displayed post-impact convulsions and the duration of the convulsions became

progressively longer in sensitive animals following repetitive injury. Additionally, these events were more common in both groups of animals upon repetitive injury, possibly due to increasing vulnerability of the brain with exposure to repetitive trauma (Guskiewicz et al., 2003; Slobounov et al., 2007). Future experiments involving direct recording using electrocorticography are required to further elucidate the mechanistic details underlying these events, as well as how they relate to injury outcomes (see Chapter 5 for further discussion).

The latency to regain the righting reflex and latency to resume locomotion following impact were assessed. Compared to both resilient and sham controls, sensitive animals took longer to regain responsiveness following repetitive impacts using these two parameters. The latency to regain the righting reflex observed in our animals after a single mild impact is comparable to the results described by others using similar injury models (Kane et al., 2012; Mychasiuk et al., 2014; Goddeyne et al., 2015), as they observed righting latencies ranging from 120 – 200 seconds post-injury. However, when repetitive injuries (Kane et al., 2012; Goddeyne et al., 2015) were administered no change in righting latency was observed. This is in contrast to our observation that sensitive animals had a progressive increase in the latency to right after repetitive impacts. It is important to note that had we not classified animals as "sensitive" and "resilient" we would not have observed this differential effect. Similarly, it is possible that Kane et. al. (2012) and Goddeyne et al. (2015), observed variability in the time to right post-impact but considered all rmTBI animals as a single cohort.

2.4.6 Delayed Behavioural Outcomes of rmTBI

To assess the delayed outcomes of exposure to rmTBI, animals underwent neurological testing one month post-impact. rmTBI animals had a significantly lower combined neurological score than sham controls at this time point, indicating that this model of rmTBI produces lasting neurological deficits. Interestingly, there were no differences in neurological score between sensitive and resilient animals one month post-impact, suggesting that acute neurological signs may not predictive of delayed outcome. This is consistent with findings from Grubenhoff et al. in which the acute symptom severity of patients presenting to the emergency department within six hours of a mild TBI was not predictive of delayed symptom resolution one month later (Grubenhoff et al., 2014). Additionally, results from a mouse model in which CTE-like tauopathy was observed following two mild TBIs indicate that the acute neurobehavioural response to injury is not predictive of CTE-like pathology (Tagge et al., 2018). Further, clinical and post-mortem examination of former athletes has shown evidence of CTE pathology even in the absence of a prior history of concussion symptoms (McKee et al., 2009; Baugh et al., 2012).

The MWM was used to assess spatial learning and memory as indicators of cognitive performance (Morris, 1984; Vorhees and Williams, 2006). Animals exposed to rmTBI did not differ from sham controls in their ability to learn the location of the escape platform. This is consistent with previous reports in which rats exposed to a single mild TBI did not display any impairment in learning the location of the platform in the MWM task (Mychasiuk et al., 2014). However, rmTBI-exposed animals in our study displayed impaired recall of the escape platform location, suggesting that rmTBI animals may have reduced abilities in long-term memory (Vorhees and Williams, 2006). This is consistent

with impairment of delayed recall (as tested by the SCAT) in athletes who have previously experienced a concussion, compared to those who have not (Shehata et al., 2009).

Interestingly, no differences between sensitive and resilient animals were found in cognitive performance one-month post-impact in the MWM task. These findings accord with those of the combined neurological scoring in which sensitive and resilient animals did not differ at this delayed time point. Together, these findings indicate that acute neurological signs are not predictive of the delayed outcome of rmTBI in this model. This is consistent with the notion that symptoms of concussion following acute injury may be poor indicators of long-term outcome, as has been suggested by others both in clinical (McKee et al., 2009) and experimental (Tagge et al., 2018) contexts of rmTBI.

2.5. CONCLUSION

This chapter characterized a model of repetitive mild traumatic brain injury in adolescent rats in which acute injury outcomes differ markedly between injured animals. We proposed classification criteria to group animals into sensitive and resilient cohorts based on these responses, allowing us to investigate differences between sensitive and resilient animals throughout the acute and delayed time points investigated in this work. We found that sensitive animals deteriorate acutely in response to repetitive impacts, experience a longer duration of post-impact convulsions with repeated injury, and take longer to recover immediately post-impact than resilient or sham control animals. Impact analysis using pressure sensitive film and high-speed video footage revealed that sensitive and resilient animals do not experience differences in injury mechanics, suggesting that the differential acute neurological outcomes that emerge in this model of rmTBI may instead be mediated by the differential response of individual animals to these injuries.

Additionally, we found that acute neurological outcomes in this model were poor predictors of delayed outcome of repetitive mild TBI, which is consistent with previous reports in animal studies and in human patients.

CHAPTER 3:
MECHANISMS ASSOCIATED WITH SENSITIVITY TO REPETITIVE MILD TRAUMATIC BRAIN INJURY

3.1 INTRODUCTION

Accumulating evidence indicates that the BBB is compromised following TBI (Shlosberg et al., 2010). Of particular relevance to the work contained in this thesis, BBBD has been shown to occur in American football players (Weissberg et al., 2014), as well as in animal models of rmTBI (Laurer et al., 2001; Tagge et al., 2018). Disruption of the BBB can result in impaired regulation of the molecules and ions that would otherwise be sequestered from the brain tissue. Our research group has previously identified that serum albumin (the most abundant protein in the blood) can undergo extravasation under conditions of BBBD, leading to increased signalling of astrocytic TGFβ receptors. Binding of serum albumin with TGFβ receptors can lead to a transformation in the astrocytic transcriptional profile, inducing the expression of pro-inflammatory cytokines, as well as alterations in the extracellular matrix, altered potassium and glutamate buffering capacity, and synaptogenesis (Ivens et al., 2006; Cacheaux et al., 2009; Bar-Klein et al., 2014).

While these pathological changes have been described in detail in experimental models of BBBD and epilepsy, the role of TGFβ signalling in the context of rmTBI had yet to be examined. The present chapter aims to investigate the role of BBBD, TGFβ signalling, gliosis, and neuroinflammation following rmTBI. We hypothesized that increased BBBD, TGFβ signalling, and neuroinflammation would be associated with a more severe clinical outcome (i.e. sensitivity, in our model) following repetitive injuries.

3.2 METHODS

3.2.1 Dynamic Contrast-Enhanced MRI

DCE-MRI was performed as described elsewhere (Bar-Klein et al., 2017) 24 hours, one week, and one month following the first TBI using a 3 Tesla Agilent system under isoflurane anesthesia (1–2%) with a constant oxygen flow (99%, 1 L/h). Breathing was monitored continuously during imaging using a respiration monitor.

Scanning protocols included: (i) standard T2-weighted fast spin echo sequence (repetition time: 2500 ms; echo time: 64 ms; echo train length of 16, echo spacing 8ms; 46 averages; 128 x 128 data matrix, resulting in 0.297 mm in-plane resolution and a slice thickness of 1 mm; acquisition time: 15.3 min); acquired prior to Gadolinium injections (ii) two balanced steady state free precession 3D T1-weighted scans (repetition time: 8 ms; echo time: 4 ms; 4 frequencies, 10 s segment delay; 176x160x146 data matrix, resulting in 0.25 mm in-plane resolution, and 0.3 mm in the 2nd phase dimension; acquisition time: 13.1 min), one before and one approximately 25 minutes after the injection of the Gadolinium based tracer (Figure 3.1 A; multihance; gadobenate dimeglumine, intravenous (IV) administration, ~211.6mg/rat ; (iii) ten transverse T1-weighted gradient-echo classic scans (repetition time: 6.03 ms; echo time: 2.98 ms; flip angle: 20 degrees; 20 averages; 108 x 108 data matrix, resulting in 0.352 mm in-plane resolution and a slice thickness of 1.2 mm; acquisition time: 3 min) were performed, one immediately before and eight immediately following the injection of the multihance (Figure 3.1 B; gadobenate dimeglumine, IV, ~211.6 mg/rat). One final transverse T1-weighted scan was acquired approximately 40 minutes post-injection as a final time point.

Analysis was performed using in-house scripts (MATLAB® R2018a). Pre-processing included registration, extracting brain volume and creating brain mask objects. To visualize BBB integrity (represented as slope images; Figure 3.1 D), the linear dynamic method was used by fitting a linear curve to the dynamic scan intensities of the eight consecutive post-contrast T1 scans (14 slices). That is, a signal s(t) is fitted to a linear curve such that: $s(t) = A \times t + B$, where the slope (A) is the rate of wash-in or wash-out of the contrast agent from the brain (Figure 3.1 C). Additionally, for quantitative comparisons in BBB dysfunction, a "pathological" voxel threshold was set as any slope value exceeding the 90% percentile slope value of sham control animals (n = 15).

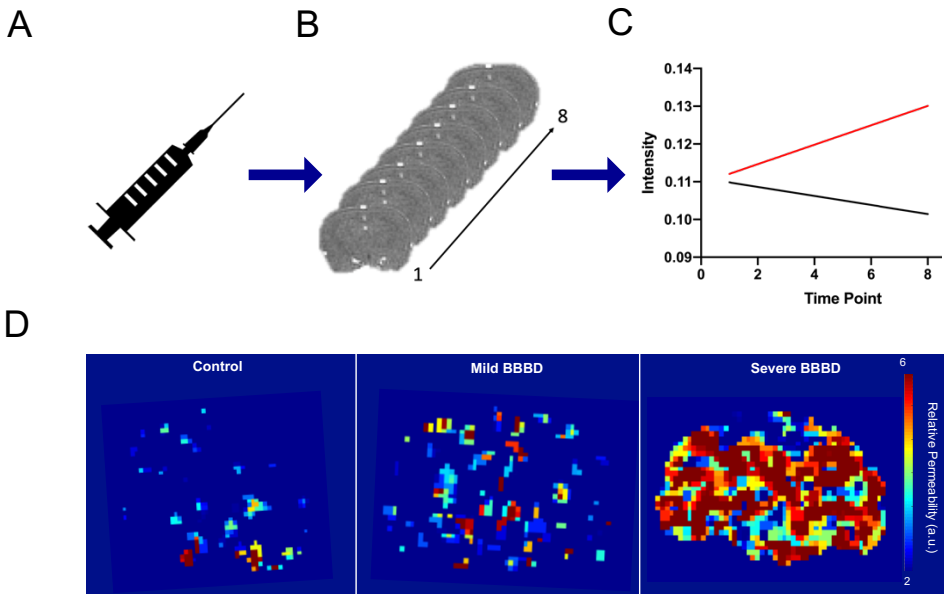

Figure 3.1: Schematic of DCE-MRI as a method for assessment of BBB integrity. (A) Injection of Gadolinium-based contrast agent immediately prior to the acquisition of eight consecutive T1 scans **(B)** permits dynamic changes in signal intensity to be assessed. **(C)** Slope values are calculated from changes in signal intensity within each brain voxel and can be visualized as slope images **(D)**.

3.2.2 Perfusion and Tissue Collection

Animals were deeply anaesthetized by IP injection of sodium pentobarbital (Euthanyl, Bimeda-MTC, Cambridge, ON) at a dose of 100 mg/kg and all were perfused transcardially with physiological saline (0.9% NaCl, pH 7.4).

For tissue designated for western blotting and real-time quantitative polymerase chain reaction (RT-qPCR), brain tissue was not fixed. Instead, following perfusion with physiological saline, brains were extracted, and sub-regions of interest were dissected on ice. Once isolated, sub-regions were placed in pre-labelled cryogenic tubes and flash-frozen in liquid nitrogen. The following sub-regions of interest were isolated: hippocampus, striatum, sensorimotor cortex (cortex directly below impact location), temporal cortex, and cerebellum. Dissection instruments were cleaned in 70% ethanol and rinsed with saline in between animals.

For tissue designated for immunofluorescent labelling, tissue was fixed during perfusion (immediately after saline clearance) with 4% paraformaldehyde (PFA) (Fisher Scientific #AC416785000) in 0.1 M sodium phosphate buffer (pH = 7.4). Brains were removed and stored in 4% PFA at 4°C before being cryoprotected in 30% sucrose in 0.1 M sodium phosphate buffer (pH = 7.4). Brains were then frozen with dry ice, embedded in Tissue-Tek O.C.T. compound (Sakura, Torrance, CA), and cut on a freezing microtome into 30 μm coronal sections. Sections were stored in Milloning's buffer (0.1 M sodium phosphate with 0.03% sodium azide, pH = 7.4) at 4°C until further processing.

3.2.3 Western Blotting

Brain tissue from sub-region of interest (hippocampus, sensorimotor cortex, temporal cortex, or striatum) was homogenized and protein lysates were extracted using Radioimmunoprecipitation assay buffer (RIPA) buffer (50 mM Tris-HCl, 150 mM NaCl, 1% NP-40, 0.5% Sodium deoxycholate, 0.1% SDS), containing a protease (Calbiochem #539134) and phosphatase inhibitor (Roche PhoStop Ref: 4906845001). Protein concentration (μg/mL) was determined using a spectrophotometer (NanoDrop 2000, Thermo Fisher Scientific). 20 μg of protein lysate was mixed with 4X Laemmli buffer (Bio-Rad #1610747), containing 5% 2-mercaptoethanol (Sigma M6250). After heating at 65°C for 10 mins, samples were loaded and separated by sodium dodecyl sulfate polyacrylamide gel electrophoresis (SDS-PAGE) using the Mini-PROTEAN Tetra System and pre-cast TGX™ Gels (Bio-Rad #456-1096) using a PowerPac (BioRad) set at 35 V for 15 mins, followed by 105 V for 1.5 hours. 10 μL of Spectra Multicolor Broad Range Protein Ladder (ThermoSci, #26634) was loaded on each gel and was used to indicate molecular weight of proteins of interest. Following separation, samples were transferred to a nitrocellulose membrane (0.45 μm, Bio-Rad #1620115) by using a PowerPac (BioRad) set at 105 V for 75 minutes.

Membranes were blocked to minimize non-specific antibody binding for 1 hour at room temperature with 5% non-fat dry milk (Apex #20-241) in TBST (10 mM Tris, 150 mM NaCl, 0.5% Tween 20, pH 8.0). Membranes were incubated overnight at 4°C with primary antibody in blocking buffer (see Table 3.2). The next day, membranes were washed 3x10 minutes with TBST and incubated with secondary (horseradish peroxidase-conjugated; HRP) antibodies for 1 hour at room temperature (see Table 3.2). Membranes were washed with TBST 3x10 minutes and visualized using

chemiluminescence SuperSignal West Dura Extended Substrate (ThermoFisher Scientific #34075), and Bio-Rad Chemidoc system with Bio-Rad Image Lab software (version 4.0.1). Densitometry analysis was done using Image J (National Institutes of Health; NIH).

Antibody Target	Predicted MW	Host	Dilution	Source
GAPDH	37 kDa	Rabbit	1:2000	Cell Signaling (#2118)
pSmad2	58 kDa	Rabbit	1:1000	Millipore (AB3849)
Smad2	60 kDa	Rabbit	1:1000	Cell Signaling (#5339)
TGFβ1	24 kDa	Mouse	1:750	Millipore (MABF346)
HMGB1	25 kDa	Rabbit	1:1000	Abcam (AB18256)
Anti-Rabbit HRP	N/A	Goat	1:2000	Cell Signaling (#7074)
Anti-Mouse HRP	N/A	Horse	1:2000	Cell Signaling (#7076)

Table 3.1. Antibodies used for western blotting

3.2.4 Immunofluorescence and Microscopy

Six free-floating sections (30 µm thick) were selected in the region of the hippocampus from each animal. Sections were incubated in phosphate buffered saline with 0.1% triton-X (Sigma #X-100) for 3x10 minute washes. Sections were blocked in 5% normal donkey serum in triton-X for one hour at room temperature before being incubated in primary antibody for one hour at room temperature and then overnight at 4°C (see Table 3.1). Following primary antibody incubation, sections were washed 3x10 minutes in PBS and then were incubated with the appropriate secondary antibody at room temperature on a shaker for 2 hours (see Table 3.1). Sections were removed from secondary antibody, washed 3 x 10 minutes in PBS and were mounted on Superfrost slides (Fisher Scientific).

After drying overnight, slides were cover-slipped using Fluoromount G with DAPI (Electron Microscopy Sciences) mounting media.

Images were acquired using a Zeiss Axiocam 503 monofluorescent microscope with Zen 2.3 Lite software. Immunoreactivity for each stain was quantified using ImageJ software (NIH) to determine the mean pixel intensity in the hippocampus. Images used for quantification were taken directly adjacent to the midline at the rostral hippocampus (dentate gyrus) at 10X magnification. All images were taken with the same exposure settings. No-primary and no-secondary controls were used for each stain to provide background staining values that were subtracted for quantification purposes.

Antibody Target	Host	Dilution	Source
GFAP-CY3 (555)	Mouse	1:2000	Sigma-Aldridge (#C9205)
Iba-1	Rabbit	1:2000	Wako (#019-19741)
Anti-Rabbit Alexa Fluor 488	Donkey	1:500	Invitrogen (#A21206)

Table 3.2. Antibodies used for immunofluorescence

3.2.5 Real-Time Quantitative Polymerase Chain Reaction

Total RNA was extracted from flash-frozen rat hippocampal and sensorimotor cortex tissue using TRIzol reagent (ThermoFisher Scientific #15596026) and chloroform (Fisher Scientific #C298-500). A microtube homogenizer with disposable plastic pestles was used to aid in tissue breakdown, cell lysis, and homogenization. Following homogenization, samples were centrifuged at 12,000 rpm for 30 minutes at 4°C to separate and remove genomic DNA. Isopropyl alcohol was added to assist with RNA precipitation and 1µL of Glycoblue (Invitrogen #AM9515) was added to assist with RNA pellet

visualization. Following incubation for 1 hour, samples were centrifuged at 12,000 rpm for 10 minutes at 4°C. The RNA pellets were isolated and washed with 75% ethanol and then allowed to dry before being dissolved in 20 μL of RNase-DNase free water. 2 μL of 10x DNase I Buffer (New England Biolabs, #m0303s), 1 μL of rDNase I (ThermoFisher Scientific, AM2235), and DNase Inactivation Reagent (ThermoFisher Scientific, AM1907) were added to each RNA sample for purification. Samples were centrifuged at 10,000 rpm for 1.5 minutes and RNA concentration was determined using a spectrophotometer (NanoDrop 2000, Thermo Fisher Scientific). Only samples with an RNA purity A_{260}/A_{280} ratio between 1.8 and 2.1 were used for RT-qPCR.

First-strand cDNA synthesis was performed from 1 μg isolated RNA template using iScript RT supermix (Bio-Rad #1708841). Incubation was performed using a thermal cycler (Bio-Rad C1000 Touch Thermal Cycler) under the following protocol: 25°C for 5 mins (anneal), 42°C for 30 mins (synthesis), 85°C for 5 mins (terminate), 12°C for ∞ (hold).

A reaction mixture containing SsoAdvanced Universal SYBR Green Supermix (Bio-Rad #172-5271), forward and reverse gene primers, and milli-Q H_2O was prepared and added to cDNA for amplification. PCR products were amplified using a CFX96 Real-Time PCR System (Bio-Rad), and threshold cycles were detected using SsoAdvanced Universal SYBR Green Supermix (Bio-Rad #172-5271). Mean threshold cycles were normalized to 18s internal control, and relative gene expression levels were quantified using the 2-ΔΔCT method (Livak and Schmittgen, 2001). Primer sequences were designed using ApE (A Plasmid Editor) software (University of Utah, M. Wayne Davis) and the NCBI/NIH RefSeq Database.

Gene Target	Fwd/Rev	Sequence (5' to 3')
18S	Fwd	GGG AGG TAG TGA CGA AAA ATA AC
18S	Rev	TTG CCC TCC AAT GGA TCC T
GFAP	Fwd	GCG GAG ACG TAT CAC CTC TG
GFAP	Rev	GTC TCT TTG AAG CCG GCA TTG
Vimentin	Fwd	CAA CAC CGA GTT CAA GAA CAC
Vimentin	Rev	CAT CTC CTC CTC GTA GAG GT
Iba-1	Fwd	GAG CCA GAG CAA GGA TTT GC
Iba-1	Rev	GTA CTT CGT CTT GAA GGC CTC
IL-1α	Fwd	GGC CAA AGT TCC TGA CTT G
IL-1α	Rev	CCT TGA AGG TGA AGG TGG AC
IL-1β	Fwd	CTG TTC TTT GAG GCT GAC AG
IL-1β	Rev	GCT TCT CCA CAG CCA CAA TG
IL-6	Fwd	CAA AGC CAG AGT CAT TCA GAG C
IL-6	Rev	GGA GAG CAT TGG AAG TTG GG
TNFα	Fwd	CCA AAT GGG CTC CCT CTC ATC
TNFα	Rev	GTT GTC TTT GAG ATC CAT GCC
TLR4	Fwd	TGC TCA GAC ATG GCA GTT TC
TLR4	Rev	TCA AGG CTT TTC CAT CCA AC
COX2	Fwd	TGT ATG CTA CCA TCT GGC TTC GG
COX2	Rev	GTT TGG AAC AGT CGC TCG TCA TC
RAGE	Fwd	CTG AGG TAG GGC ATG AGG ATG
RAGE	Rev	GCC TGC AGC TTG TCC TTC AT

Table 3.3. Primers used for RT-qPCR

3.2.6 Statistical Analyses

Statistical analyses were performed using GraphPad Prism version 8.0 for Macintosh (GraphPad Software, La Jolla California USA). Where appropriate, group means with standard error of the mean and sample size were reported. Differences between groups for all tests were reported as exact p-values, and differences were considered

statically significant at an alpha level of less than 0.05. When two groups were compared, Student's t-test and Mann Whitney-U test were used for calculating group differences for normally or non-normally distributed data, respectively. When repeated measures were performed, the Wilcoxon matched pairs signed rank test was used. When three or more groups were compared, a one-way ANOVA was performed. Post-hoc testing was performed using Tukey's post-hoc analysis.

3.3 RESULTS

3.3.1 Blood-Brain Barrier Dysfunction Increases Acutely Following rmTBI

DCE-MRI was used to assess BBB integrity in TBI and sham control animals. Animals were scanned at three different time points: 24 hours after a single mild TBI (n = 4), one week after rmTBI (n = 19) or sham procedure (n = 15), and one month after rmTBI (n = 8). Slope values were calculated for each brain voxel as described in Section 3.2.1, and a cumulative frequency histogram was constructed (Figure 3.2 A). One week after the first impact was administered, animals exposed to rmTBI showed a notable rightward shift of the cumulative frequency distribution of slope values compared to sham controls at this time point. Further, this rightward shift after one week was also apparent in comparison to the cumulative frequency curve of rmTBI animals scanned one month post-impact, or animals scanned 24 hours after a single mild injury. This finding suggested that animals exposed to rmTBI had a greater percentage of positive slope values than sham controls when scanned one week post-impact, or compared to TBI animals scanned after a single impact or one month following repetitive impacts. This provided an indication that one week after exposure to repetitive impact, TBI animals have increased BBB permeability.

To quantify the extent of BBB permeability, a threshold slope value (slope A = 0.00038) was selected based on the 90% percentile of the cumulative frequency distribution of sham control animals (Figure 3.2 A). Slope values greater than this threshold were deemed "pathological" to allow for comparison between rmTBI-exposed and sham control animals. This approach assumes that more positive slope values are indicative of increased retention of contrast agent in the brain due to impaired BBB integrity, whereas smaller slope values indicate more rapid clearance of the contrast agent, as would be expected under "healthy" BBB conditions.

When scanned 24 hours after a single impact, no differences in the number of pathological voxels were observed between TBI and sham control animals ($P = 0.4107$; data not shown). However, one week post impact, rmTBI animals had significantly more pathological voxels than sham controls ($P = 0.0138$; Figure 3.2 B). This difference was not maintained when animals were scanned one month later, as rmTBI animals at this time point did not differ significantly from sham controls ($P = 0.4331$; data not shown). A subset of rmTBI animals ($n = 17$) underwent neuroimaging at both one week and one month after injury and there was a significant decrease in BBB permeability between these time points ($P = 0.0004$; Figure 3.2 D). Subdivision of the rmTBI animals scanned one week post-impact into those that were acutely sensitive ($n = 12$) or resilient ($n = 7$) to repetitive injury revealed that sensitive animals have significantly more BBBD than sham controls ($P = 0.0087$; Figure 3.2 C). Sensitive animals also appeared to have more pathological voxels than resilient animals, although this trend was not significant ($P = 0.2614$; Figure 3.2 C). Resilient animals and sham controls did not significantly differ in the percentage of pathological voxels when scanned one week post-injury ($P = 0.2372$; Figure 3.2 C).

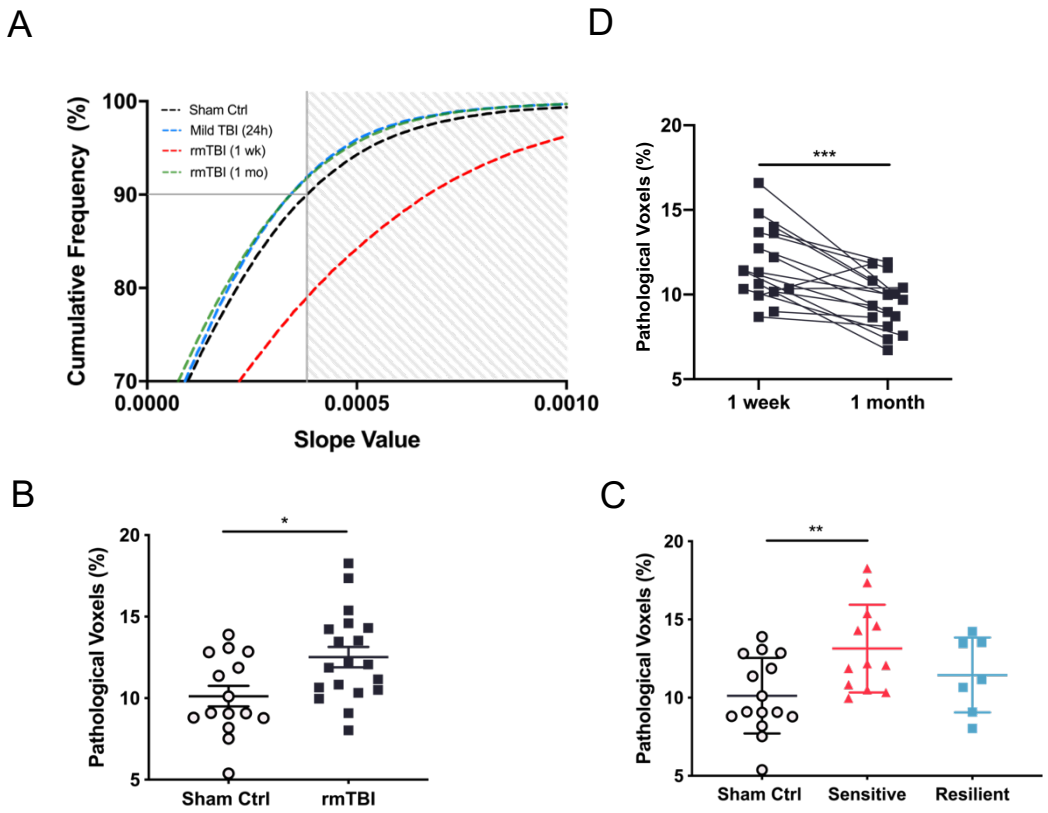

Figure 3.2: rmTBI animals have greater BBBD one week post-impact. (A) The cumulative frequency distribution of slope values from DCE-MRI showed a notable rightward shift of slope values from rmTBI animals scanned one week post-impact, indicating a greater amount of BBBD compared to sham controls or animals scanned 24 hours or one month post-injury. The shaded region indicates slope values greater than the cut-off value for pathological voxels (A = 0.00038) which was determined as the slope value corresponding to the 90th percentile value of sham controls. **(B)** rmTBI animals (n = 19) had a greater amount of pathological slope values compared to sham controls (n = 15) when scanned one week after repetitive impacts (P = 0.0138). **(C)** Retrospective grouping of animals as sensitive (n = 12) or resilient (n = 7) revealed that sensitive animals have more pathological voxels than sham controls one week post-impact (P = 0.0087). **(D)** Acute BBBD in rmTBI animals (n = 17) one week post-impact is resolved when assessed one month later. Mean ± SEM are shown for B and C.

3.3.2 Sensitive Animals Have More TGFβ Signalling

Previous work conducted by our research group has implicated astrocytic transforming growth factor beta signalling as an important signalling pathway that can become activated under conditions of BBBD (Ivens et al., 2006; Cacheaux et al., 2009; Bar-Klein et al., 2014). Based on our findings that rmTBI-exposed animals (specifically, sensitive animals) exhibited BBBD, we hypothesized that sensitive animals may also have more TGFβ signalling than resilient or sham control animals.

To test this hypothesis, a subset of rmTBI-exposed (n = 11 sensitive, n = 7 resilient) and sham control animals (n = 8) were sacrificed one week after the first impact, and their brains were harvested for protein analysis. The phosphorylated fraction of Smad2 was assessed by western blot in ipsilateral hippocampal tissue (right hemisphere), as Smad2 is a major downstream effector protein of TGFβ signalling. The hippocampus was selected as the primary brain region of interest due to its described susceptibility to injury following trauma (Tang et al., 1997; Geddes et al., 2003; Aungst et al., 2014), and its role in memory and cognitive function (Montagne et al., 2015).

Analysis of phosphorylated Smad2 protein levels by western blot revealed the presence of two isoforms of pSmad2: a full-length isoform at 53kDa, and a 48kDa isoform, presumably produced from the Smad2 splice variant lacking exon 3 (pSmad2Δexon3) (Figure 3.3 A). For sensitive, resilient, and sham control animals each of these isoforms and the combination of both together (total pSmad2) was compared between groups (Figure 3.3 B). Each of these combinations was also divided by the total amount of Smad2 (unphosphorylated) to provide a readout of TGFβ signalling (Figure 3.3 B), as has been reported elsewhere (Cho et al., 2016; Denis et al., 2016).

Analysis of each independent pSmad2 isoform was performed to assess if differences in the respective splice variants were present (Figure 3.3 B). Resilient animals showed significantly less hippocampal pSmad2 (53kDa) than sham control ($P = 0.0244$) or sensitive ($P = 0.0053$) animals. Sensitive animals did not differ in pSmad2 (53kDa) protein expression compared to sham controls ($P = 0.9742$). Sensitive animals had significantly more hippocampal pSmad2 (48kDa) expression than resilient ($P < 0.0001$) or sham control animals ($P = 0.0121$), while sham controls and resilient animals did not significantly differ ($P = 0.1599$). When both isoforms of pSmad2 were analyzed together, resilient animals exhibited significantly less pSmad2 (total) protein expression than sham control ($P = 0.0267$) and sensitive animals ($P =0.0003$). Sensitive animals did show slightly more pSmad2 (total) than sham controls, all though this increase was not significant ($P = 0.3579$).

Assessment of unphosphorylated Smad2 protein levels (Figure 3.3 B) showed that resilient animals had significantly less Smad2 protein expression than sham controls ($P = 0.0242$), although this effect was not significant when compared to sensitive animals ($P = 0.1634$), which did not differ from sham controls ($P = 0.4007$).

Next, TGFβ signalling activity was quantified by determining the ratio of phosphorylated Smad2 to unphosphorylated Smad2 (Figure 3.3 B). Sensitive animals had a higher phosphorylated fraction of hippocampal total Smad2 (total pSmad2/Smad2) than resilient ($P = 0.0016$) or sham control ($P = 0.0462$) animals. Subsequent analysis of each splice variant of pSmad2 revealed that sensitive animals had higher amounts of pSmad2Δexon3/Smad2 (48kDa only) than resilient ($P < 0.0001$) or sham control animals ($P = 0.0007$), while resilient and sham controls did not differ significantly ($P = 0.6652$). In

contrast, pSmad2/Smad2 (53kDa only) levels did not differ between sensitive, resilient, and sham control animals ($P = 0.0707$).

To determine if the observed changes in TGFβ signalling conferred by the phosphorylated fraction of 48kDa Smad2 were region-specific, the phosphorylated fraction of this isoform was also assessed in the sensorimotor cortex (approximately below the location of the impact), the temporal cortex, and the striatum (Figure 3.3 C). There were no observed differences between sensitive, resilient, and sham controls in the phosphorylated fraction of 48kDa Smad2 in the temporal cortex ($P = 0.3530$) or the striatum ($P = 0.8592$). However, in the sensorimotor cortex the phosphorylated fraction of 48kDa Smad2 was significantly higher in both sensitive ($P = 0.0065$) and resilient ($P = 0.0337$) animals compared to sham controls. Sensitive and resilient animals did not differ in expression levels of pSmad2(48kDa)/Smad2 in the sensorimotor cortex ($P = 0.7641$).

A

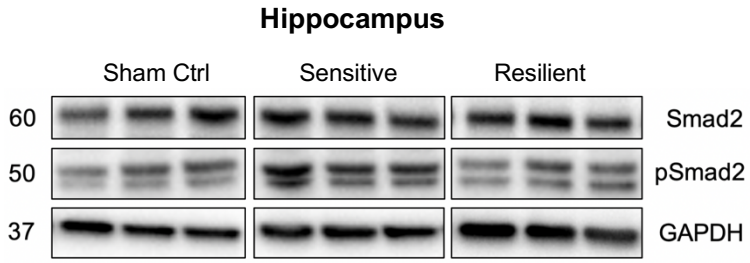
Hippocampus
Sham Ctrl
Sensitive
Resilient
60
50
37
Smad2
pSmad2
GAPDH

B

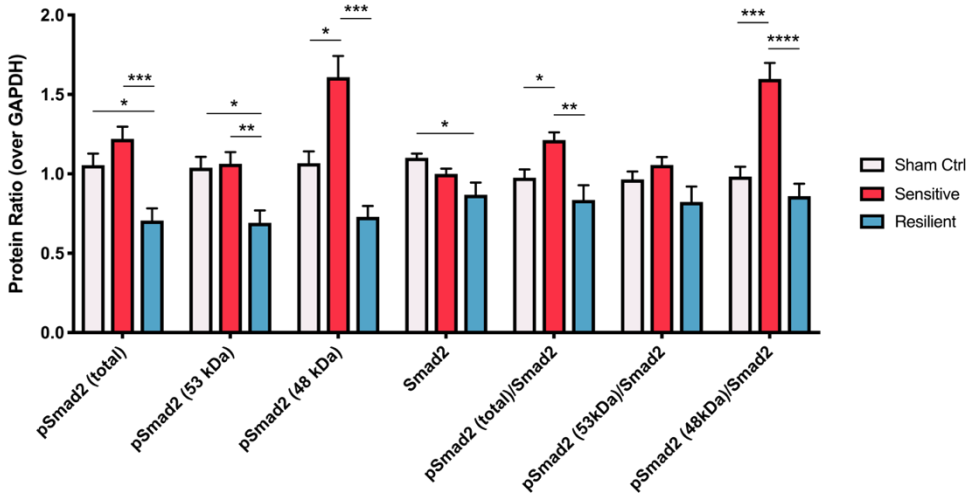
Protein Ratio (over GAPDH)
2.0
1.5
1.0
0.5
0.0
pSmad2 (total)
pSmad2 (53 kDa)
pSmad2 (48 kDa)
Smad2
pSmad2 (total)/Smad2
pSmad2 (53kDa)/Smad2
pSmad2 (48kDa)/Smad2
Sham Ctrl
Sensitive
Resilient

C

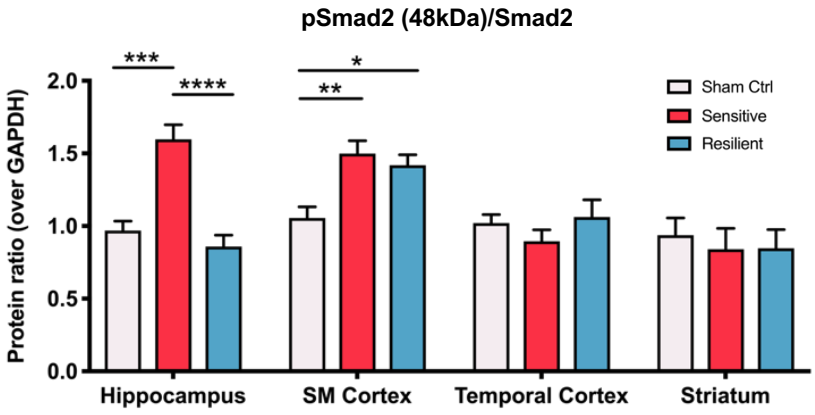
pSmad2 (48kDa)/Smad2
Protein ratio (over GAPDH)
2.0
1.5
1.0
0.5
0.0
Hippocampus
SM Cortex
Temporal Cortex
Striatum
Sham Ctrl
Sensitive
Resilient

Figure 3.3: Sensitive animals have higher hippocampal TGFβ signalling than resilient or sham control animals. (A) Representative images of western blot against hippocampal Smad2, pSmad2, and GAPDH (housekeeping). **(B)** TGFβ signalling was assessed in sensitive (n = 11), resilient (n = 7), and sham controls (n = 8) by western blot against Smad2 and pSmad2. Compared to sham controls, sensitive animals showed significantly more pSmad2Δexon3 (P = 0.0121), pSmad2(total)/Smad2 (P = 0.0462), and pSmad2Δexon3/Smad2 (P = 0.0007). Compared to resilient animals, sensitive animals had significantly more total pSmad2 (P = 0.0003), pSmad2 (53kDa) (P = 0.0053), pSmad2Δexon3 (P < 0.0001), pSmad2(total)/Smad2 (P = 0.0016), and pSmad2Δexon3/Smad2 (P < 0.0001). Thus, hippocampal TGFβ signalling was increased in sensitive animals compared to resilient or sham control animals one week post-impact. Resilient animals showed less Smad2 expression than sham control animals (0.0242). **(C)** Assessment of TGFβ signalling by quantifying pSmad2Δexon3/Smad2 levels revealed significant differences between sensitive, resilient, and sham controls in the hippocampus (as shown in **B**), and in the sensorimotor (SM) cortex where both sensitive (P = 0.0065) and resilient (P = 0.0337) animals showed significantly more TGFβ signalling than sham controls. In contrast, no differences in TGFβ signalling were found between sensitive, resilient, and sham controls in the temporal cortex (P = 0.3530) or the striatum (P = 0.8592).

To determine if changes in TGFβ signalling were accompanied by increased levels of TGFβ1 protein levels, we probed for the TGFβ1 cytokine (Figure 3.4 A-C). We focused specifically on the hippocampus and sensorimotor cortex, as these were the two brain regions in which we observed altered levels of TGFβ signalling following impact. No changes in TGFβ1 protein levels were found between sensitive, resilient, and sham control animals in the hippocampus (P = 0.2289; Figure 3.4 A and C). In contrast, resilient animals showed significantly lower levels of TGFβ1 compared to sensitive animals in the sensorimotor cortex (P = 0.0305; Figure 3.4 B and C) and did not differ from sham controls (P = 0.2342; Figure 3.4 B and C). Sensitive animals also did not differ from sham controls in TGFβ1 levels in the sensorimotor cortex (P = 0.7391; Figure 3.4 B and C).

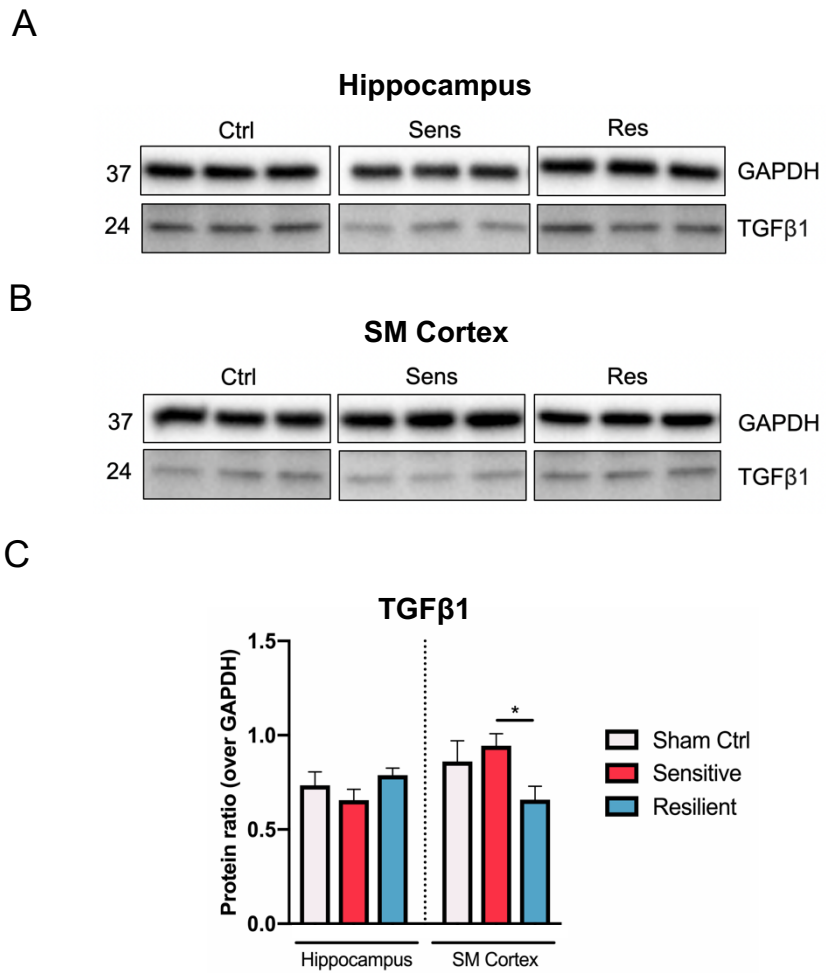

Figure 3.4: Assessment of TGFβ1 cytokine expression (A and B) Representative images of hippocampal **(A)** and sensorimotor cortex **(B)** western blots against TGFβ1 and GAPDH (housekeeping). **(C)** Western blot quantification of TGFβ1 cytokine expression in the hippocampus showed no differences between sensitive (n = 11), resilient (n = 7), and sham control (n = 8) animals (P = 0.2289). In the sensorimotor cortex, resilient animals showed less TGFβ1 expression than sensitive animals (P = 0.0305) but did not differ significantly from sham controls (P = 0.2342).

3.3.3 Sensitive Animals Have Greater Acute Gliosis Following rmTBI

Previous work by our group has shown that BBBD leads to the leakage of serum albumin into the brain, where it signals through astrocytic TGFβ receptors to trigger astrocytic activation (Cacheaux et al., 2009; David et al., 2009; Levy et al., 2015).

Additionally, perivascular microgliosis has been described following mild TBI and rapid migration of microglia has been described following BBBD (Nimmerjahn et al., 2005; Burda and Sofroniew, 2014; Tagge et al., 2018). As such, we hypothesized that the increase in BBBD and TGFβ signalling observed in the hippocampus of sensitive animals would be associated with increased hippocampal gliosis.

To address this hypothesis, we quantified transcript and protein levels for markers of gliosis. Specifically, brains were collected from rmTBI and sham control animals one week post-impact and RT-qPCR was performed on hippocampal tissue (left hemisphere) to assess transcript levels of two astrocytic proteins, glial fibrillary acidic protein (GFAP) and vimentin, and the microglia protein, ionized calcium binding adaptor molecule 1 (Iba-1). Additionally, immunofluorescence for GFAP and Iba-1 was performed on tissue collected one week and one month post-impact.

Sensitive animals had increased hippocampal GFAP ($P = 0.0307$; Figure 3.5 A) and vimentin mRNA expression ($P = 0.0241$; Figure 3.5 A) compared to resilient animals, although this effect was not significant compared to sham controls (GFAP: $P = 0.0782$; vimentin: $P = 0.0898$). Resilient animals did not differ from sham controls in GFAP ($P = 0.9798$) or vimentin ($P = 0.9302$) mRNA expression. No differences were found between sensitive, resilient, and sham control animals in Iba-1 mRNA expression ($P = 0.1769$; Figure 3.5 B).

Next, we asked if sensitive ($n = 6$), resilient ($n = 5$), and sham control ($n = 6$) animals differed in relative protein expression levels of GFAP and Iba-1. Immunofluorescent staining against GFAP in the hippocampus (dentate gyrus) revealed increased GFAP fluorescent intensity in sensitive animals compared to resilient ($P =$

0.0038; Figure 3.5 C and D) or sham control animals (P = 0.0024; Figure 3.5 C and D). GFAP hippocampal fluorescence did not differ between resilient and sham control animals (P = 0.9731; Figure 3.5 C and D). Similarly, sensitive animals showed more hippocampal Iba-1 fluorescent intensity compared to resilient (P = 0.0138; Figure 3.5 E and F) or sham control animals (P = 0.0367; Figure 3.5 E and F). Resilient and sham control animals did not differ in hippocampal Iba-1 fluorescent intensity (P = 0.8736; Figure 3.5 E and F).

To investigate the temporal relationship between BBBD and gliosis, a subset of rmTBI and sham control animals were sacrificed one month post-impact. Immunofluorescent staining was performed against GFAP and Iba-1 as before on coronal brain sections from sensitive (n = 3), resilient (n = 5), and sham control (n = 4) animals. No significant differences were found in hippocampal GFAP immunoreactivity (total fluorescent intensity) between sensitive, resilient, and sham controls (P = 0.2324; Figure 3.5 C and D) at this time point. Similarly, hippocampal Iba-1 immunoreactivity (total fluorescent intensity) did not differ between sensitive, resilient, and sham control animals (P = 0.6445; Figure 3.5 E and F) one month post-impact.

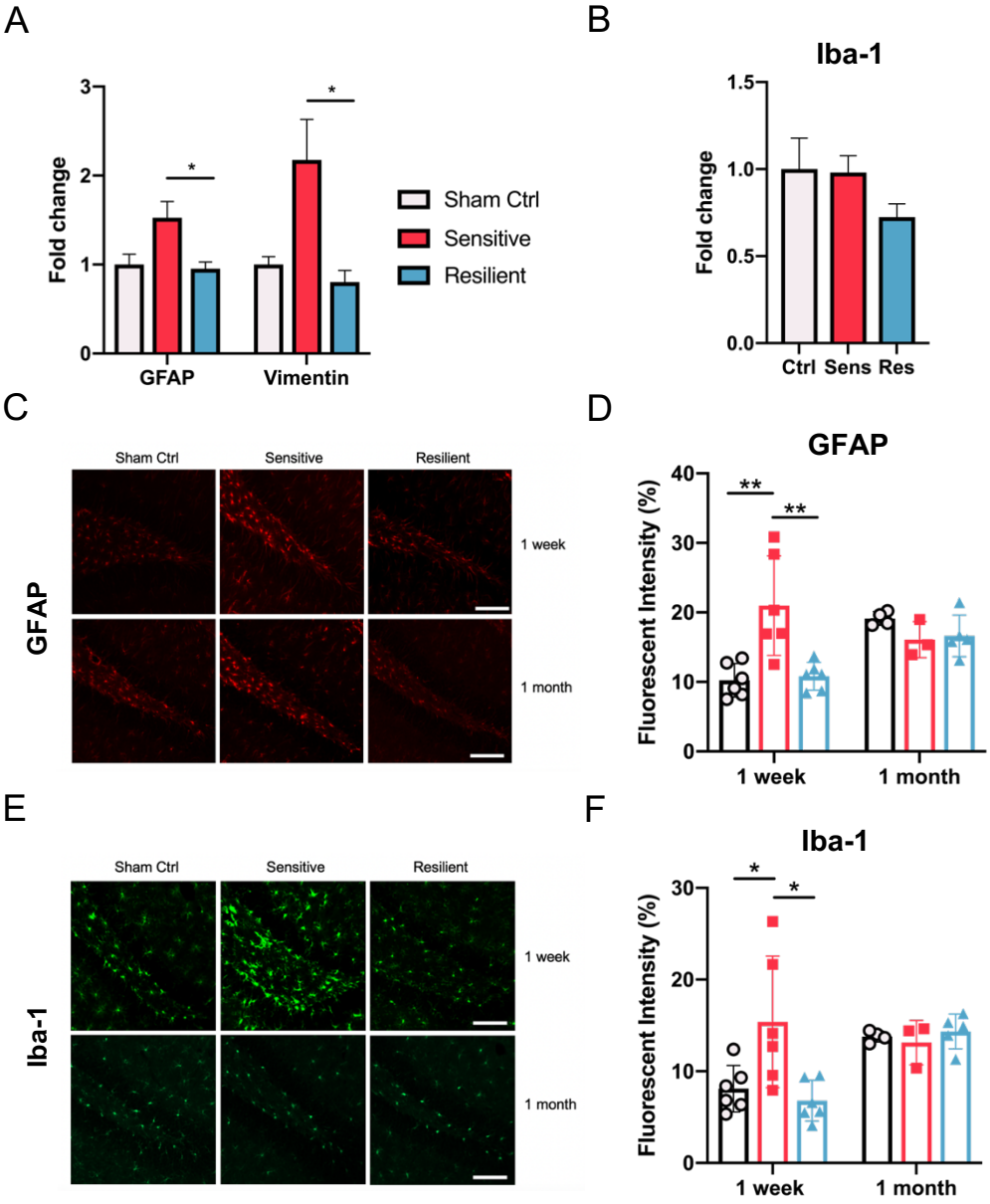
A
Fold change
3
2
1
0
*
*
GFAP
Vimentin
Sham Ctrl
Sensitive
Resilient
B
Iba-1
Fold change
1.5
1.0
0.5
0.0
Ctrl Sens Res
C
Sham Ctrl
Sensitive
Resilient
GFAP
1 week
1 month
D
GFAP
Fluorescent Intensity (%)
40
30
20
10
0
**
**
1 week
1 month
E
Sham Ctrl
Sensitive
Resilient
Iba-1
1 week
1 month
F
Iba-1
Fluorescent Intensity (%)
30
20
10
0
*
*
1 week
1 month

Figure 3.5: Sensitive animals have greater hippocampal gliosis. (A) Sensitive (n = 11) animals had increased expression of GFAP and vimentin mRNA compared to resilient (n = 7) animals (GFAP: P = 0.0307, vimentin: P = 0.0241), but not sham control (n = 8) animals (GFAP: P = 0.0782, vimentin: P = 0.0898). **(B)** No differences in Iba-1 mRNA transcript levels were detected between sensitive, resilient, and sham control animals (P = 0.1769). **(C and E)** Representative images of the dentate gyrus are shown from immunofluorescence against GFAP **(C**) and Iba-1 **(E)** for sensitive, resilient, and sham control animals at one week and one month post-impact. Scale bar = 100 μm. **(D)** Quantification of total fluorescent intensity of GFAP at one week post-impact revealed more hippocampal GFAP immunoreactivity in sensitive animals (n = 6) compared to resilient (n = 5) (P = 0.0038) and sham control animals (n = 6) (P = 0.0024). No differences in hippocampal GFAP immunoreactivity were found between sensitive (n = 3), resilient (n = 4), and sham control (n = 4) animals one month post-impact (P = 0.2324). **(E)** Quantification of total fluorescent intensity of Iba-1 at one week post-impact revealed more hippocampal Iba-1 immunoreactivity in sensitive animals (n = 6) compared to resilient (n = 5) (P = 0.0138) and sham control animals (n = 6) (P = 0.0367). No differences in hippocampal Iba-1 immunoreactivity were found between sensitive (n = 3), resilient (n = 4), and sham control (n = 4) animals one month post-impact (P = 0.6445).

3.3.4 Sensitive Animals Have Higher HMGB1 and IL-6 Expression

To determine if an increase in astroglial and microglial activation was accompanied by increased neuroinflammation, the damage-associated molecular pattern, high-mobility group box protein 1 (HMGB1) was quantified by western blot on tissue from the hippocampus (Figure 3.6 B), sensorimotor cortex, temporal cortex, and striatum of sensitive (n = 11), resilient (n = 7), and sham control (n = 8) animals. Sensitive animals showed more hippocampal HMGB1 expression than sham controls (P = 0.0086; Figure 3.6 A), while HMGB1 levels between sensitive and resilient animals did not differ (P = 0.2206; Figure 3.6 A). Resilient and sham control animals did not differ in hippocampal HMGB1 protein expression (P = 0.2161; Figure 3.6 A). No differences in HMGB1 expression between sensitive, resilient, and sham control animals were found in the sensorimotor

cortex (P = 0.3765; Figure 3.6 A), temporal cortex (P = 0.6168; Figure 3.6 A), or the striatum (P = 0.3168; Figure 3.6 A).

Next, a series of pro-inflammatory gene transcripts were assessed by using RT-qPCR on RNA extracted from whole hippocampus (left hemisphere). A panel of seven genes was selected for this purpose: IL-1α, IL-1β, IL-6, tumor necrosis factor alpha (TNFα), toll-like receptor (TLR) 4, cyclooxygenase 2 (COX2), and receptor for advanced glycation end products (RAGE), based on previous literature describing their role in post-injury neuroinflammation (Woodroofe et al., 1991; Shohami et al., 1997; Strauss et al., 2000; Scaffidi et al., 2002; Park et al., 2004; Levy et al., 2015). A general trend indicating increased levels of pro-inflammatory genes was observed in sensitive animals (n = 9) compared to resilient (n = 7) and sham control (n = 5) animals. However, these differences were not significant across any of the pro-inflammatory genes selected, with the exception of IL-6. Notably, sensitive animals had higher levels of IL-6 mRNA transcript compared to resilient animals (P = 0.0397; Figure 3.6 C) and sham controls (P = 0.0222).

A

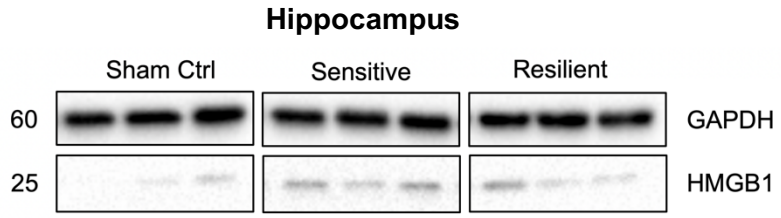
Hippocampus
Sham Ctrl
Sensitive
Resilient
60
25
GAPDH
HMGB1

B

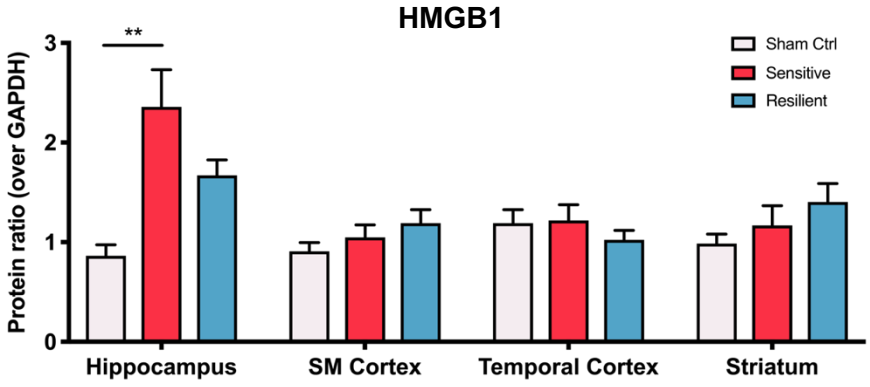
HMGB1
Protein ratio (over GAPDH)
**
Sham Ctrl
Sensitive
Resilient
Hippocampus
SM Cortex
Temporal Cortex
Striatum

C

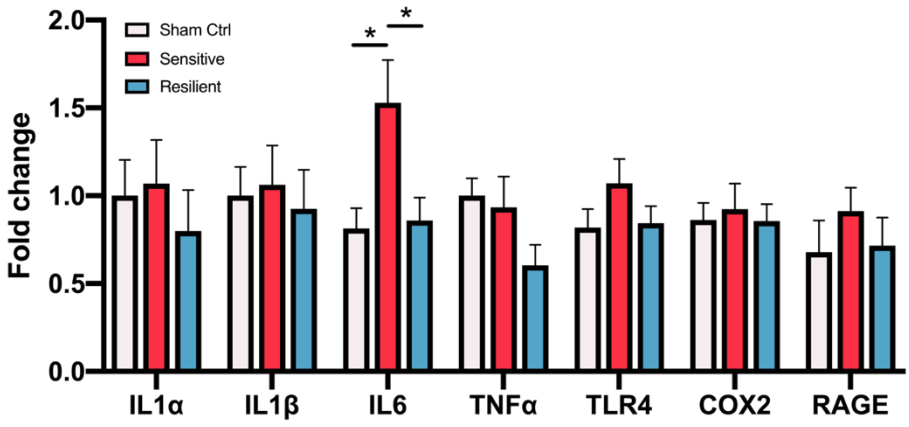
Fold change
Sham Ctrl
Sensitive
Resilient
*
*
IL1α
IL1β
IL6
TNFα
TLR4
COX2
RAGE

Figure 3.6: Sensitive animals have more hippocampal HMGB1 and IL-6 expression. (A) Hippocampal HMGB1 protein expression was increased in sensitive (n = 11) animals compared to sham controls (n = 8) (P = 0.0086) but did not differ from resilient (n = 7) animals (P = 0.2206) one week post-impact. No differences in HMGB1 expression were found between sensitive, resilient, and sham controls in the sensorimotor cortex (P = 0.3765), the temporal cortex (P = 0.6168), or the striatum (P = 0.3168). **(B)** Representative images of western blot against hippocampal HMGB1 and GAPDH (housekeeping). **(C)** Hippocampal transcript levels of a panel of proinflammatory genes are shown. No significant differences were found between sensitive (n = 9), resilient (n = 7), and sham controls (n = 5) between any of the genes of interest, with the exception of IL-6. Sensitive animals had significantly higher levels of hippocampal IL-6 mRNA than resilient (P = 0.0397) or sham control animals (P = 0.0222).

3.4 DISCUSSION

3.4.1 Summary

The goal of this chapter was to evaluate the presence and extent of BBBD, TGFβ signalling, and neuroinflammation as potential mechanisms associated with brain response and clinical outcome to rmTBI. Using DCE-MRI, we showed that BBBD is common following rmTBI and is more pronounced in sensitive animals, which experience worse acute outcomes following injury. We also found that TGFβ signalling is higher following rmTBI in sensitive animals compared to resilient animals and sham controls. We further showed that increased BBBD and TGFβ signalling in this model was associated with reactive gliosis and neuroinflammation in the hippocampus of sensitive animals. The observed changes in gliosis coincided with the time course of acute BBB opening following repetitive injury, with BBB integrity and reactive gliosis returning to normal levels when assessed one month post-injury.

3.4.2 Blood-Brain Barrier Dysfunction Following rmTBI

Our DCE-MRI findings indicate that rmTBI animals have significantly more BBBD than sham control animals. In particular, we found that one week after repetitive impacts (but not 24 hours after a single impact, or one month after repetitive impacts), TBI animals have significantly more pathological voxels compared to sham control animals. As such, we show that BBB permeability is increased following exposure to rmTBI. This is consistent with previous reports describing impaired BBB integrity in animals (Tagge et al., 2018) and in human football players (Weissberg et al., 2014) after exposure to repetitive mild injury.

In particular, sensitive animals had significantly more BBBD than sham controls, although they did not significantly differ from resilient animals. It is possible that this study was underpowered or not sensitive enough to detect more subtle differences in BBB permeability that may exist between sensitive and resilient animals, as a trend showing increased BBB permeability in sensitive animals was observed. Nevertheless, that sensitive animals showed increased BBBD compared to sham controls indicates that BBBD is associated with a more severe clinical outcome in this model. This is consistent with previous work that has shown increased BBB permeability in patients with post-concussion syndrome (Korn et al., 2005; Yoo et al., 2019), although these studies were conducted at a later time point (median: 4 to 17 months post-injury) than our study. Interestingly, our findings indicate that BBB integrity was restored one month post-impact. This is in contrast with human studies that indicate long-lasting impairment in BBB integrity following mild TBI (Korn et al., 2005; Tomkins et al., 2008). However, the nature of the injuries described in these studies may be more severe as several patients were reported to have intracranial

hemorrhage, and prolonged loss of consciousness (on the order of days). Additionally, these human studies were conducted in adult patients (approximately 30 years of age), while the animals in our studies are equivalent to adolescent ages. Thus, it is possible that there is increased ability of the BBB to be repaired following injury at a young age, although further experiments are required to assess this possibility. Species-related differences in BBB repair following injury may also be relevant.

In our model, changes in BBB integrity were not detectable 24 hours after a single mild impact, although this finding is limited by a small sample size. Previous work in animals has suggested that opening of the BBB may peak as early as 4 hours after a single impact (Shapira et al., 1993; Başkaya et al., 1997; Stahel et al., 2000), although this assessment was performed using Evans Blue staining, which may have a different sensitivity to detecting BBBD than our *in vivo* method using DCE-MRI (Saunders et al., 2015). Additionally, these observations were made in a CCI model of TBI (Başkaya et al., 1997) and in a weight drop model with no rotational motion and with significantly higher mortality than our studies (Shapira et al., 1993), suggesting that these approaches produced injuries that are likely more severe than ours. Alternatively, it is possible that there was rapid opening of the BBB, consistent with the occurrence of primary BBB damage (Shlosberg et al., 2010), which was no longer detectable when the animals were scanned 24 hours later. Evidence from other experimental models of mild TBI (blast and FPI) with low mortality rates support this possibility, as they observed increased BBBD within hours post-injury but significant resolution of BBBD 24 hours later (Tanno et al., 1992; Hue et al., 2016). Limitations to our DCE-MRI experiments include manual masking and lack of

regional analysis of BBBD, which may yield important information regarding differences between sensitive and resilient animals.

3.4.3 Transforming Growth Factor Beta Signalling

Given our finding that sensitive animals have more BBBD following repetitive injury, we hypothesized that sensitive animals would exhibit more TGFβ signalling than resilient or control animals. Protein quantification of hippocampal tissue using western blot revealed the expression of two isoforms of pSmad2 – the full-length protein (53kDa) and a splice variant lacking exon 3 (48kDa). The expression of these two isoforms appeared to be differentially regulated across rmTBI and sham control animals, with sensitive animals showing significantly more hippocampal pSmad2Δexon3 expression compared to resilient and sham control animals. TGFβ receptor activity was assessed by comparing the fraction of phosphorylated Smad2 to unphosphorylated Smad2, which revealed that sensitive animals have significantly more hippocampal TGFβ signalling than resilient or sham controls. This is due to an increased 48kDa pSmad2Δexon3/Smad2 ratio in sensitive animals.

The Smad2 gene contains 11 exons, and exon 3 of Smad2 is not found in any other Smad protein. Alternative splicing of Smad2 can result in the expression of a Smad2 isoform which does not contain exon 3 (Smad2Δexon3). The amount of Smad2Δexon3 transcript is estimated to be one-tenth of that of full-length Smad2 but it may be more active in mediating transcription following TGFβ signalling. This increase in potency is due to the removal of exon 3, which allows for direct DNA-binding ability by Smad2Δexon3 (Yagi et al., 1999).

Our study provides evidence, for the first time, that alternative splicing of Smad2 may be differentially regulated under conditions of head trauma. While additional work is required to further characterize the mechanisms underlying differential regulation of pSmad2 isoforms, it is interesting to briefly consider the potential implications of increased expression of pSmad2Δexon3 in animals sensitive to rmTBI. The increased potency of pSmad2Δexon3 in mediating downstream transcriptional changes following activation by the TGFβ receptor may be highly relevant to the neuroinflammatory response observed in sensitive animals, in particular, the upregulation of IL-6.

Increased TGFβ signalling was selectively observed in the hippocampus of sensitive animals. However, TGFβ signalling in the sensorimotor cortex was significantly increased in both sensitive *and* resilient animals. It is possible that increased TGFβ signalling in the sensorimotor cortex of resilient animals is the result of increased BBBD in this brain region, as this area is approximately located directly below the site of impact. However, regional analysis of DCE-MRI to evaluate whether there is focal disruption of BBBD in this region is required to address this possibility. No changes in TGFβ signalling were detected in the temporal cortex or the striatum. These findings indicate that increased TGFβ signalling following rmTBI is region-specific and may be selectively elevated in brain regions associated with increased susceptibility to injury (Tang et al., 1997; Geddes et al., 2003; Aungst et al., 2014). Whether or not the observed regional differences in TGFβ signalling are also accompanied with regional differences in BBB permeability is of interest, and future studies should be directed at addressing this possibility.

Across all isoforms, resilient animals had lower expression of hippocampal pSmad2 as well as Smad2 (unphosphorylated) than sensitive or sham controls. The details

underlying why resilient animals have significantly lower levels of Smad2 and pSmad2 are not clear, however, a number of mechanisms relating to the regulation of the TGFβ-Smad pathway may be implicated. One such mechanism is by the degradation of Smad proteins (both phosphorylated and unphosphorylated) via the ubiquitin-proteosome pathway (Lo and Massagué, 1999; Miyazono, 2000; Wrana, 2000). It is possible that the intracellular pool of Smad2 is downregulated in resilient animals as a result of increased Smad2 degradation via enhanced ubiquitin-proteosome activity. Additionally, alterations in epigenetic remodelling, RNA splicing, microRNA expression, and mRNA methylation may also be involved in the differential regulation of Smad2 levels (Derynck and Budi, 2019). It is unlikely that mechanisms to control the activation (i.e. phosphorylation) of Smad2, such as the role of inhibitory Smad proteins (e.g. Smad6 and Smad7), are exclusively involved in the reduction in TGFβ signalling that we observed, as the amount of non-activated hippocampal Smad2 was also significantly reduced in resilient animals (Derynck and Budi, 2019).

Finally, TGFβ1 cytokine levels were assessed in the hippocampus and sensorimotor cortex as these were the two brain regions in which increased TGFβ signalling was observed. No differences in hippocampal TGFβ1 levels were detected between sensitive, resilient, and sham controls, indicating that the increase in hippocampal TGFβ signalling that we observed in sensitive animals is not the result of increased TGFβ1 cytokine expression. This finding is consistent with our overall hypothesis for this chapter, as differences in TGFβ signalling in the context of rmTBI may largely be mediated by the binding of serum albumin to TGFβ receptors following impairment of the BBB, rather than through the direct action of TGFβ1.

In the sensorimotor cortex, resilient animals showed significantly less TGFβ1 expression than sensitive animals, although this difference was not significant compared to sham controls. Interestingly, this is the brain region in which TGFβ signalling activity (pSmad2/Smad2) was greatest in resilient animals. This observation lends additional evidence to the notion that TGFβ signalling under conditions of BBBD may largely be mediated through the action of albumin signalling through TGFβRs, rather than through the direct action of the TGFβ1 cytokine on these receptors.

3.4.4 Acute and Delayed Reactive Gliosis

Sensitive animals had significantly higher GFAP and Iba-1 immunoreactivity than resilient or sham controls one week post-injury, consistent with the occurrence of reactive gliosis. This finding is in line with our hypothesis and previous work indicating that BBBD can directly lead to the activation of astrocytes (Ding et al., 2000; Tomkins et al., 2007; Cacheaux et al., 2009; Burda and Sofroniew, 2014; Bar-Klein et al., 2017) and that mild TBI can induce perivascular microgliosis (Tagge et al., 2018).

No differences in GFAP or Iba-1 expression were found between sensitive, resilient, and sham controls one month post-injury. Importantly, the time course of reactive gliosis observed in sensitive animals coincides with the time course of BBBD, which suggests that these two aspects of the injury response to rmTBI are closely linked, as has been suggested before (Tagge et al., 2018). Indeed, reactive glia are known to effect changes that can influence the integrity of the BBB, for example through the upregulation of MMP-9 in astrocytes. MMP-9 upregulation can alter the properties of endothelial cell tight junctions, thereby compromising the integrity of the BBB (Shigemori et al., 2006; Burda and Sofroniew, 2014). A leaky BBB can also lead to infiltration of immune cells

and the initiation of reactive gliosis (Ding et al., 2000; Tomkins et al., 2007; Burda and Sofroniew, 2014; Bar-Klein et al., 2017). While the precise cause-and-effect relationship between BBBD and reactive gliosis in the context of rmTBI cannot be determined from our studies, it is likely that each influences the other during the cascade of events following repetitive injury.

Surprisingly, we observed slightly different extents of reactive gliosis depending on the method used. Our mRNA findings suggest a notably modest increase in gliosis than what we observed using immunofluorescence to assess GFAP and Iba-1 immunoreactivity. This discrepancy may be due to the use of whole hippocampus for RT-qPCR, whereas the immunofluorescence approach was specific to quantifying differences in GFAP and Iba-1 immunoreactivity in the dentate gyrus of the hippocampus. Indeed, it is likely that sub-regions of the hippocampus are particularly sensitive to the effects of BBBD, as has been described by others (Montagne et al., 2015).

3.4.5 Neuroinflammation

Given that reactive gliosis was observed in animals sensitive to rmTBI, we tested whether neuroinflammation was also increased in these animals. We quantified the expression of the prototypical damage-associated molecular pattern, HMGB1, in sensitive, resilient, and sham control animals by western blot. HMGB1 is an important mediator of inflammation and can signal through TLR2, TLR4, and RAGE to trigger a robust inflammatory response (Scaffidi et al., 2002; Park et al., 2004; Bianchi and Manfredi, 2009) . HMGB1 can also regulate the transcription of proinflammatory cytokines and is released under conditions of injury (Bianchi and Manfredi, 2009). Following TBI in children, elevated HMGB1 levels have been associated with a worse outcome and CSF

levels of HMGB1 have been shown to be upregulated in patients following severe TBI (Csuka et al., 1999; Morganti-Kossmann et al., 1999; Au et al., 2012; Laird et al., 2014).

We found that sensitive animals had more hippocampal HMGB1 expression than sham controls, while no differences were found in the sensorimotor cortex, temporal cortex, or striatum. These findings suggest that rmTBI animals have elevated injury signalling in the hippocampus following repetitive impacts, with the extent of this signalling greater in sensitive animals compared to sham controls. While our findings cannot discern the origin of the DAMP signal in rmTBI animals, it would be interesting to determine which cell type these signals originate from and whether or not they are indicative of neuronal injury or are secreted by glial cells, as has been proposed in other models of brain injury (Maroso et al., 2010). As before, the differential hippocampal regulation of HMGB1 (but not in the other brain areas) may be due to the selective susceptibility of the hippocampus to injury (Tang et al., 1997; Geddes et al., 2003; Aungst et al., 2014).

We next used RT-qPCR to analyze mRNA transcript levels for a variety of pro-inflammatory genes which can be altered under injury conditions. Across the selected panel of genes, sensitive animals had more hippocampal IL-6 mRNA transcript levels than resilient or sham controls. Given that sensitive animals had increased BBBD, hippocampal TGFβ signalling, and reactive gliosis, this finding is not entirely surprising and comports with prior work showing IL-6 as the first cytokine to be upregulated and secreted by astrocytes under conditions of BBBD due to TGFβ signalling (Levy et al., 2015). Further, increased IL-6 levels have been detected in the CSF of patients with TBI, and serum levels of IL-6 have been shown to correlate with injury severity in animals exposed to mild TBI (Kossmann et al., 1995; Yang et al., 2013). Together, these findings are consistent with the

notion that animals that are acutely sensitive to rmTBI experience early BBBD, greater astrocytic TGFβ signalling, reactive gliosis, neuroinflammation, and selective upregulation of IL-6.

3.5 CONCLUSION

We used a clinically-relevant, minimally-invasive neuroimaging approach (DCE-MRI) to quantify changes in BBB integrity following rmTBI. We showed that exposure to rmTBI produces a transient opening of the BBB in the acute phase of injury, with resolution at a later time course. Additionally, we found increased TGFβ, reactive gliosis, and neuroinflammation that coincides with the time course of BBB opening in this model. To our knowledge, this study is the first to characterize changes in TGFβ signalling following repetitive mild TBI. Additionally, we showed that changes in BBB integrity, TGFβ signalling, reactive gliosis, and neuroinflammation are associated with a more severe acute clinical outcome following repetitive injury. These findings open the possibility for therapeutic intervention by targeting TGFβ signalling, which may be ideally situated to influence the cascade of events involving BBBD following rmTBI. Importantly, previous work showing that pharmacological inhibition of TGFβ signalling can successfully prevent albumin-induced epileptogenesis (Bar-Klein et al., 2014) provides added support for the use of this approach as a therapeutic intervention in our model. Thus, the next chapter of this thesis will test the effects of two TGFβ signalling antagonists as a novel treatment strategy for the acute and delayed complications of rmTBI.

CHAPTER 4:
TGFβ ANTAGONISM AS A TREATMENT STRATEGY FOR REPETITIVE MILD TRAUMATIC BRAIN INJURY

4.1 INTRODUCTION

Given our findings indicating increased pathological TGFβ signalling following repetitive injury, we sought to test the effects of blocking TGFβ signalling on the acute and delayed injury outcomes of rmTBI. We selected two candidate TGFβ antagonists for this purpose: IPW-5371 (IPW) and losartan.

IPW is a pre-clinical small molecule transforming growth factor beta receptor 1 kinase antagonist with the ability to cross the BBB. IPW has a favorable clinical profile as it can be taken orally and has stability that allows for once per day dosing. Its use as a TGFβ blocker has previously been shown in a model of irradiation to block abhorrent TGFβ signalling and reduce cardiac and pulmonary fibrosis (Rabender et al., 2016). Additionally, and highly relevant to our proposed application, IPW was shown by our group to be beneficial in preventing TGFβ signalling, dysfunctional network activity, seizure vulnerability, and cognitive decline under conditions of BBBD in aged animals and using an albumin infusion model (Senatorov et al., 2019).

Currently, there are no FDA-approved TGFβ signalling antagonists available. However, losartan is an approved and clinically available antihypertensive drug (angiotensin II receptor type 1 antagonist) that has been shown to act as a TGFβ antagonist. It was first identified for use as a peripheral TGFβ inhibitor to treat chronic renal allograft rejection (Lavoie et al., 2005). More recently, losartan was shown by our group to prevent delayed spontaneous seizures under conditions of BBB through the inhibition of TGFβ signalling in the brain (Bar-Klein et al., 2014).

Testing these two therapeutic interventions in our model allowed us to balance the specificity of the mechanism of action of IPW with the clinical translatability of losartan.

Our goal was to conduct a pre-clinical drug study in our rodent model of rmTBI to inform future pre-clinical and clinical trials.

4.2 METHODS

4.2.1 Experimental Design

Animals were randomly assigned to one of the following treatment conditions: IPW-5371 (IPW; n = 19), losartan (LOS; n = 19), vehicle (VEH; n = 22), or sham control (SHAM; n = 10). Sample size (n=19 per treatment group, including additional 20% for mortality) was calculated using a power analysis with $\alpha = 0.05$, a power of 0.8, and an effect size of 1 (based on an improvement in neurological score from 5 to 8 with SD = 3 following treatment). An improvement in neurological score in this range would indicate the prevention or amelioration of animals from being classified as sensitive to resilient following treatment. Dosing of IPW (20 mg/kg; per Senatorov et al., 2019), LOS (60 mg/kg; per Bar-Klein et al., 2017), or VEH (0.9% saline) was delivered by IP injection once per day for nine consecutive days. An injection volume of 1 mL/kg was used, and abdomen injection sites were alternated from left to right each day. The first dose was given ten minutes after the first TBI or sham anesthesia exposure and each dose was administered 24 hours later (and always ten minutes after any subsequent impacts).

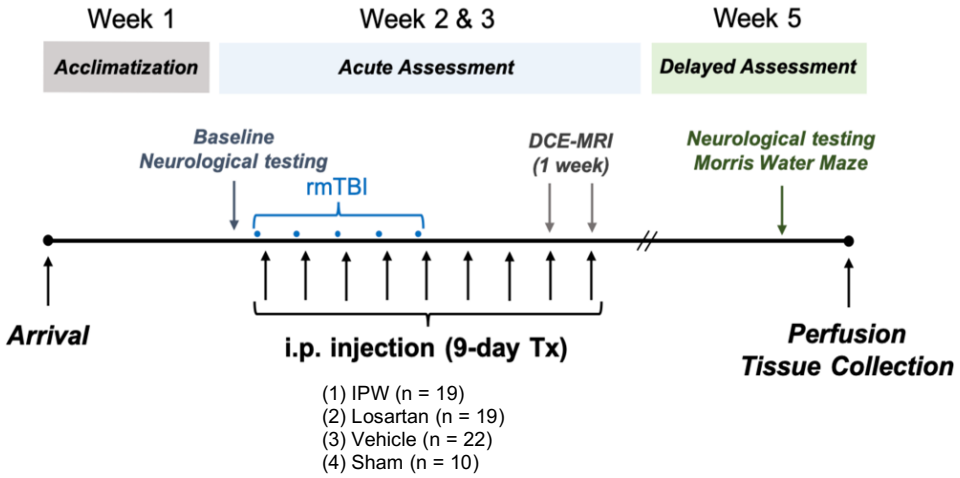

Figure 4.1. Experimental timeline for TGFβ antagonist study. (A) Experimental timeline for pre-clinical randomized blind drug study for use of TGFβ signalling antagonists as therapeutic intervention in rmTBI.

4.2.2 Preparation of IPW-5371

A 20 mg/mL solution of IPW (developed and provided by Innovation Pathways, Paolo Alto, CA) was prepared by adding IPW to 0.5% methyl cellulose in 0.9% NaCl (saline) + Tween 80. Briefly, a ratio of 1 mg IPW to 1 uL of Tween 80 was used to wet the IPW powder and a 20 mg/mL solution was prepared in (gravity filtered) 0.5% methyl cellulose. IPW was suspended in solution by constant stirring at 4°C overnight and was kept at 4°C for up to one week.

4.2.3 Preparation of Losartan

A 60 mg/mL stock solution of losartan potassium was prepared in 0.9% saline by vortexing for 1 minute or until fully dissolved. Samples were split into 1 mL aliquots which were stored at -20°C and thawed for use each day.

4.2.4 Additional Methods Described in Previous Chapters

This chapter employed a variety of methods whose details have been described in previous chapters. Any modifications specific to the present chapter are listed below and are indicated with an asterisk. Specifically: Animals were cared for as described in section 2.2.1, the rmTBI protocol was employed as per section 2.2.2 and 2.2.3. Immediate post-impact recovery was analyzed as described in section 2.2.6*. Combined neurological assessment was performed as per sections 2.2.7, 2.2.8, 2.2.9, 2.2.10. DCE-MRI was performed as described in section 3.2.1*. The MWM was performed as per section 2.2.12. Perfusion and tissue collection were performed as described in section 2.2.2 and western blotting was performed as described in section 3.2.3.

The specific modifications to the above-mentioned methods are as follows:

DCE-MRI

DCE-MRI was performed on drug-treated (IPW: n = 9, LOS: n = 8), and vehicle control (n = 12) animals one week after the first impact (when changes in BBBD were noted; see section 3.3.1).

Immediate Post-Impact Recovery Analysis

The amplitude and frequency of post-impact convulsions were not assessed.

4.2.5 Statistical Analyses

Statistical analyses were performed using GraphPad Prism version 8.0 for Macintosh (GraphPad Software, La Jolla California USA). Where appropriate, group means with standard error of the mean and sample size were reported. Differences between

groups for all tests were reported as exact p-values, and differences were considered statically significant at an alpha level of less than 0.05. When two groups were compared, Student's t-test and the Mann Whitney-U test were used for calculating group differences for normally or non-normally distributed data, respectively. The log-rank (Mantel-Cox) test was used to compare survival curves. Categorical data were compared using the chi-square test.

4.3 RESULTS

4.3.1 IPW and Losartan are Effective in Antagonizing TGFβ Signalling

One month post-impact, a subset of sham control (n = 4), vehicle control (n = 3), IPW-treated (n = 6), and losartan-treated (n = 6) animals were sacrificed and brains harvested for protein analysis by western blot. TGFβ signalling in the hippocampus and sensorimotor cortex was assessed by determining the ratio of pSmad2/Smad2, as described in Chapter 3 (Figure 4.2). We tested the effect of IPW and losartan on TGFβ signalling in the sensorimotor cortex, as this was significantly increased in vehicle-treated rmTBI animals ($P < 0.0001$; Figure 4.2 A and B) compared to sham controls one month post-injury. Both IPW ($P = 0.0007$) and losartan ($P = 0.0105$) reduced the amount of TGFβ signalling in the sensorimotor cortex compared to vehicle controls (Figure 4.2 A and B). Hippocampal TGFβ signalling in vehicle controls did not differ from sham controls ($P = 0.6286$; Figure 4.2 C).

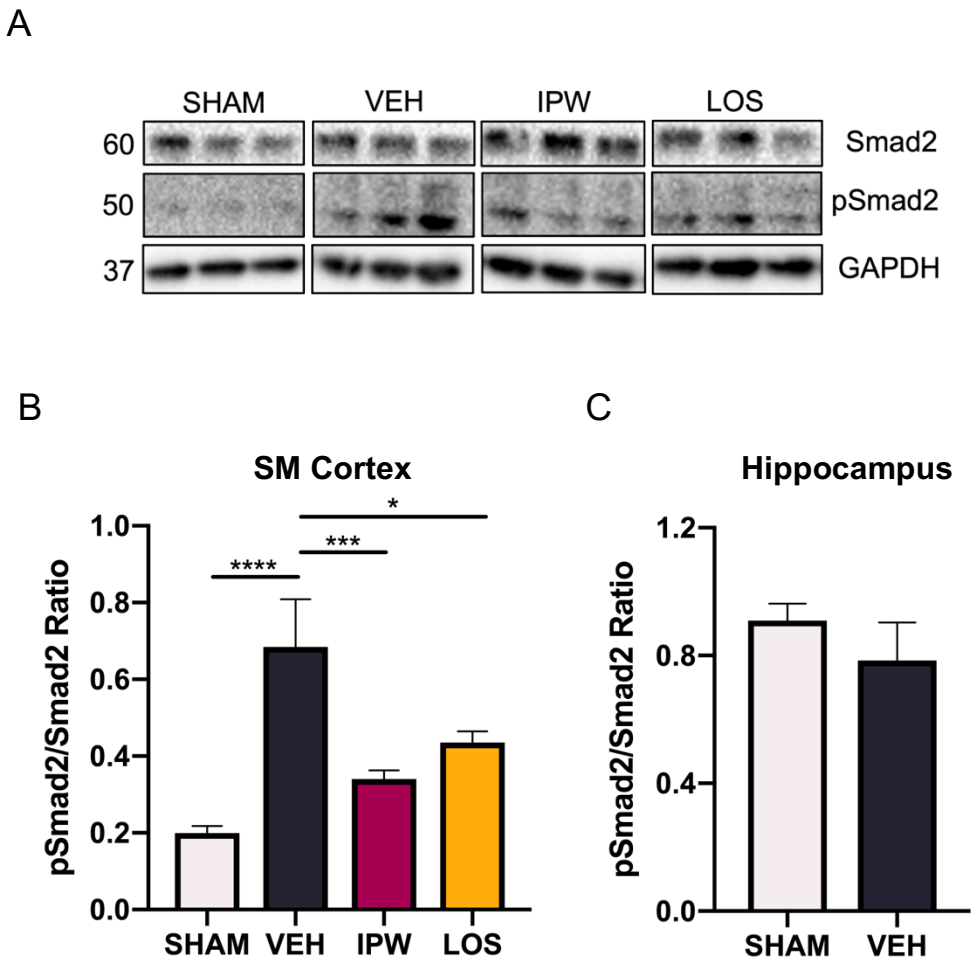

Figure 4.2: Early treatment with IPW and losartan reduces TGFβ signalling one month post-impact. (A) Representative images of western blot against Smad2 and pSmad2 in the sensorimotor cortex of sham, vehicle, IPW, and losartan-treated animals. **(B)** TGFβ signalling in the SM cortex was increased in vehicle-treated rmTBI animals (n = 3) compared to sham controls (n = 4) one month post-impact ($P < 0.0001$). Early treatment with IPW (n = 6) and losartan (n = 6) was effective in antagonism of elevated TGFβ signalling in the SM cortex compared to vehicle controls (IPW: $P = 0.0007$, LOS: $P = 0.0105$). **(C)** Hippocampal TGFβ signalling was not increased in vehicle-treated rmTBI animals (n = 3) compared to sham controls (n = 4) one month post-impact ($P = 0.6286$).

4.3.2 Acute Neurological Outcomes of rmTBI are Not Altered by Treatment

Throughout the rmTBI protocol, acute neurological assessment was performed to determine if IPW and losartan were able to alter acute neurological outcomes resulting from repetitive injury. As before, vehicle-treated animals deteriorated significantly

compared to sham controls after repetitive injury. In particular, vehicle-treated animals had lower combined neurological scores than sham controls after 3 impacts (P = 0.0200), 4 impacts (P = 0.0105), and 5 impacts (P = 0.0187). However, across all time points assessed, IPW and losartan-treated animals did not differ significantly from vehicle controls (Figure 4.3 A).

Next, we compared the percentage of acutely sensitive animals between our treatment and vehicle control groups. Sensitivity to rmTBI was assessed as before (see Chapter 2). While a trend indicating a reduction in sensitivity was present among IPW-treated animals (63% sensitive), it did not reach significance compared to vehicle controls (73% sensitive animals) (P = 0.5114; Figure 4.3 B). Losartan-treated animals (84% sensitive) did not differ from vehicle controls (P = 0.3757; Figure 4.3 B). Weight change over the acute course of injuries was similar between the vehicle and treated groups (Figure 4.3 C).

Finally, a survival curve was constructed to determine if IPW or losartan treatment resulted in changes in acute mortality following repetitive impacts. No differences in survival curves were observed between IPW, losartan, and vehicle-treated animals (P = 0.8998; Figure 4.3 D).

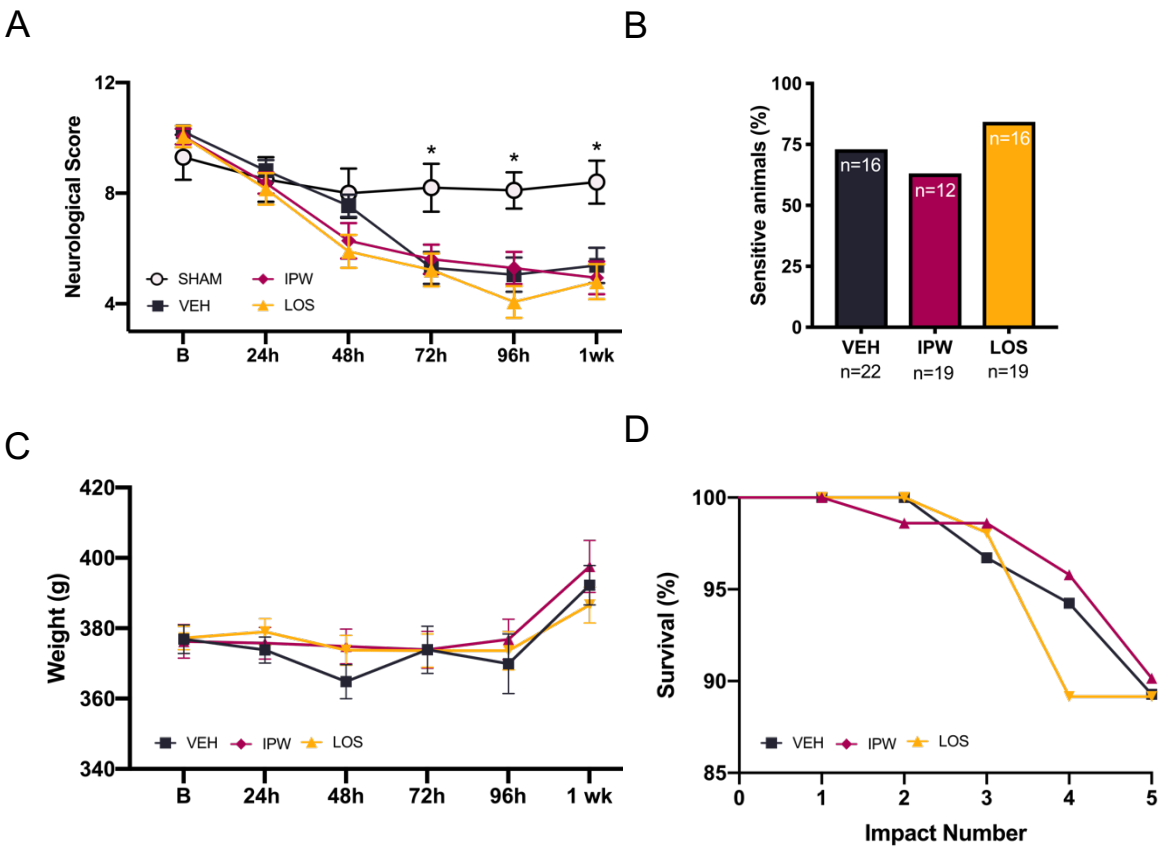

Figure 4.3: Acute neurological outcomes are not altered by treatment with TGFβ antagonists. (A) Vehicle-treated rmTBI animals (n = 22) deteriorated in combined neurological scoring compared to sham controls (n = 10) animals after three impacts (72h: P = 0.0200), four impacts (96h: P = 0.0105), and five impacts (1 wk: P = 0.0187). Animals treated with IPW and losartan did not differ in neurological score from vehicle-treated animals across any of the acute time points. **(B)** Compared to vehicle controls, treatment with IPW and losartan did not alter the percentage of sensitive animals upon exposure to rmTBI (IPW: P = 0.5114, LOS: P = 0.3757). **(C)** IPW and losartan did not alter body weight compared to vehicle-treated animals upon exposure to rmTBI across any of the acute time points. **(D)** Survival curves for vehicle, IPW, and losartan treatments did not differ (P = 0.8998).

4.3.3 IPW Reduces Occurrence and Duration of Post-Impact Convulsions

As described in section 2.3.5, some animals exposed to rmTBI exhibit immediate post-impact convulsions which are typically characterized by the rapid onset of a tonic phase followed by tonic-clonic movement of the hind limbs. A subset of post-impact

recovery videos were assessed in vehicle- (n = 8), IPW (n = 14), and losartan- (n = 14) treated animals for the occurrence and duration of post-impact convulsions.

After the second impact (and following the first dose of drug) IPW-treated animals had significantly fewer convulsions compared to vehicle controls (P = 0.0154; Figure 4.4 A), and the duration of the convulsions was shorter (P = 0.0405; Figure 4.4 B). IPW-treated animals also had shorter convulsions after three impacts (P = 0.0326; Figure 4.4 B) but did not differ significantly from vehicle control animals in the occurrence of post-impact convulsions (Occurrence: P = 0.0557; Figure 4.4 A). IPW-treated animals did not differ from vehicle controls after four (Occurrence: P = 0.7353; Duration: P = 0.6318; Figure 4.4 A and B), or five (Occurrence: P = 0.6733; Duration: P = 0.8214; Figure 4.4 A and B) impacts.

Losartan-treated animals did not have fewer post-impact convulsions than vehicle controls after two impacts, although the duration of convulsions was shorter (Occurrence: P = 0.0946; Duration: P = 0.0473; Figure 4.4 A and B). Losartan-treated animals did not differ in convulsion occurrence or duration after three (Occurrence: P = 0.3624; Duration: P = 0.8987; Figure 4.4 A and B), four (Occurrence: P > 0.9999; Duration: P = 0.8810; Figure 4.4 A and B), or five (Occurrence: P = 0.7094; Duration: P > 0.9999; Figure 4.4 A and B) impacts, compared to controls.

4.3.4 IPW Accelerates Acute Post-Impact Recovery

The latency to regain the righting reflex was assessed following the first three impacts that were administered, as these impacts are experienced by the majority of animals (as opposed to impacts four and five, which are largely experienced by resilient

animals). No significant differences were found between IPW or losartan-treated animals compared to vehicle controls after the second impact and following the first drug administration (IPW: P = 0.0986; LOS: P = 0.5951; Figure 4.4 C). However, after the third impact, IPW-treated animals regained the righting reflex faster than vehicle controls (P = 0.0071; Figure 4.4 C), while losartan-treated animals did not differ from controls (P = 0.5535; Figure 4.4 C). After two impacts (and following the first dose of drug), IPW-treated animals resumed locomotion faster than vehicle controls (P = 0.0247; Figure 4.4 D), while losartan-treated animals did not differ from controls after two impacts (P = 0.3729; Figure 4.4 D). After three impacts, IPW-treated animals had a significantly shorter latency to right compared to vehicle controls (P = 0.0107; Figure 4.4 D), while losartan-treated animals did not differ from vehicle controls (P = 0.2804; Figure 4.4 D).

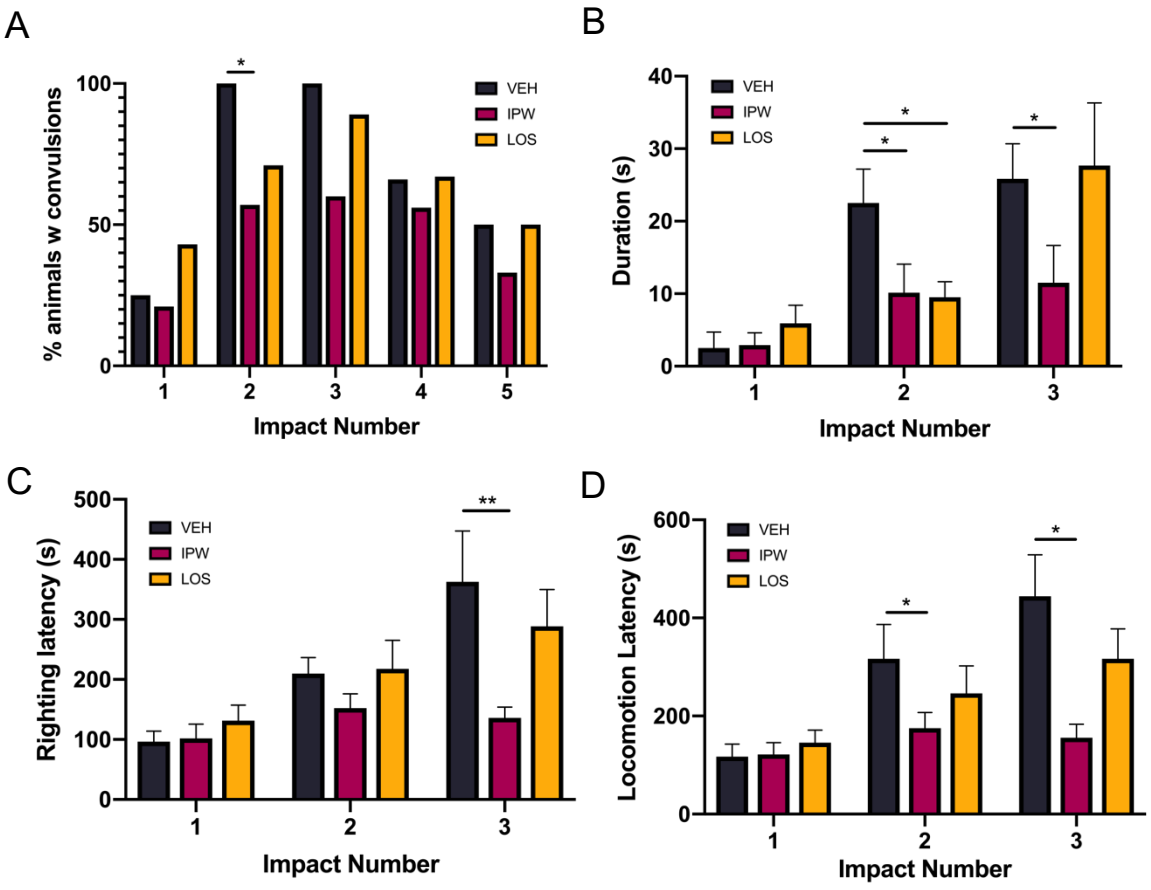

Figure 4.4: IPW reduces post-impact convulsions and accelerates acute recovery following rmTBI. (A) The occurrence of post-impact convulsions between vehicle- (n = 8), IPW- (n = 14), and losartan- (n = 14) treated animals is shown. IPW-treated animals had significantly fewer convulsions than vehicle controls after the second impact (P = 0.0154). Losartan-treated animals did not differ from vehicle controls in the occurrence of convulsions across all time points. **(B)** IPW-treated animals had significantly shorter convulsions than vehicle controls after two (P = 0.0405) and three (P = 0.0326) impacts. Losartan-treated animals had shorter convulsions after two (P = 0.0473) impacts, but this effect did not persist after the third impact was given (P = 0.8987). **(C)** Treatment with IPW reduced the latency to regain the righting reflex compared to vehicle controls after three impacts were administered (P = 0.0071). No differences in latency to right were observed between losartan-treated animals and vehicle controls. **(D)** IPW-treated animals resumed locomotor activity faster than vehicle controls after two (P = 0.0247) and three (P = 0.0107) impacts. Losartan-treated animals did not differ from vehicle controls across any of the impacts.

4.3.5 IPW Protects BBB Integrity Following rmTBI

Using DCE-MRI, we assessed the integrity of the BBB one week post-impact in IPW (n = 9), losartan (n = 8), vehicle (n = 12), and sham control (n = 6) animals. Notably, IPW-treated animals were similar to sham controls while losartan or vehicle-treated animals showed a rightward shift in the cumulative frequency distribution of slope values (Figure 4.5 A), indicating increased BBBD. IPW-treated animals had fewer pathological voxels (see section 3.2.1 for methods) than vehicle controls (P = 0.0339; Figure 4.5 B), indicating that IPW prevented rmTBI-induced BBBD. In contrast, losartan-treated animals did not differ in the percentage of pathological voxels compared to vehicle controls (P = 0.1153; Figure 4.5 B).

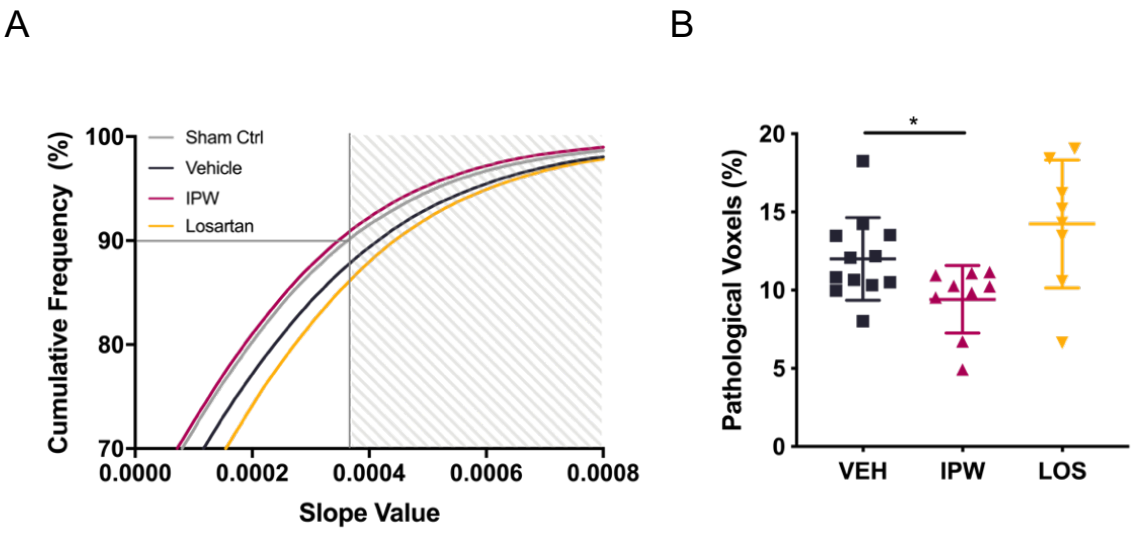

Figure 4.5: IPW protects BBB integrity following rmTBI. (A) One week post-impact, the cumulative frequency distribution of slope values from DCE-MRI showed a notable rightward shift of slope values from vehicle- (n = 12) and losartan- (n = 8) treated animals, compared to animals treated with IPW (n = 9) or sham (n = 6) controls. The shaded region indicates slope values greater than the cut off value for pathological voxels, which corresponds to the 90th percentile slope value for sham controls. **(B)** IPW-treated animals had significantly fewer (P = 0.0339; Mann-Whitney) pathological voxels than vehicle-treated animals, indicating that IPW protected against rmTBI-induced BBBD. Losartan-treated animals did not differ in the quantity of pathological voxels compared to vehicle controls (P = 0.1153; Mann-Whitney).

4.3.6 Losartan Prevents Delayed Complications of rmTBI

Finally, the delayed complications that were previously observed in rmTBI animals were assessed (see section 2.3.5). First, the combined neurological score of sham controls (n = 10), vehicle controls (n = 18), IPW (n = 15), and losartan-treated (n = 14) animals was assessed. As found previously, the combined neurological score of vehicle control animals was significantly lower than that of sham controls one month post-impact (P = 0.0057; Figure 4.6 A). Both IPW and losartan-treated animals had higher combined neurological scores compared to vehicle controls at this time point, although this difference was only significant in losartan-treated animals (IPW: P = 0.1645, LOS: P = 0.0322; Figure 4.6 A).

Morris water maze performance was assessed as a measure of spatial learning and memory. There were no significant differences in the learning phase of the water maze task between IPW, losartan and vehicle-treated animals (Figure 4.6 B). However, when tested 24 hours later in the delayed recall portion of the task, losartan-treated animals had a shorter latency to locate the platform ($P = 0.0041$; Figure 4.6 C) and spent more time in the quadrant containing the platform ($P = 0.0061$; Figure 4.6 D) than vehicle controls. IPW-treated animals did not differ significantly from vehicle-treated animals in the latency to the platform ($P = 0.1817$; Figure 4.6 C) or the percentage of time spent in the quadrant containing the platform ($P = 0.0908$; Figure 4.6 D).

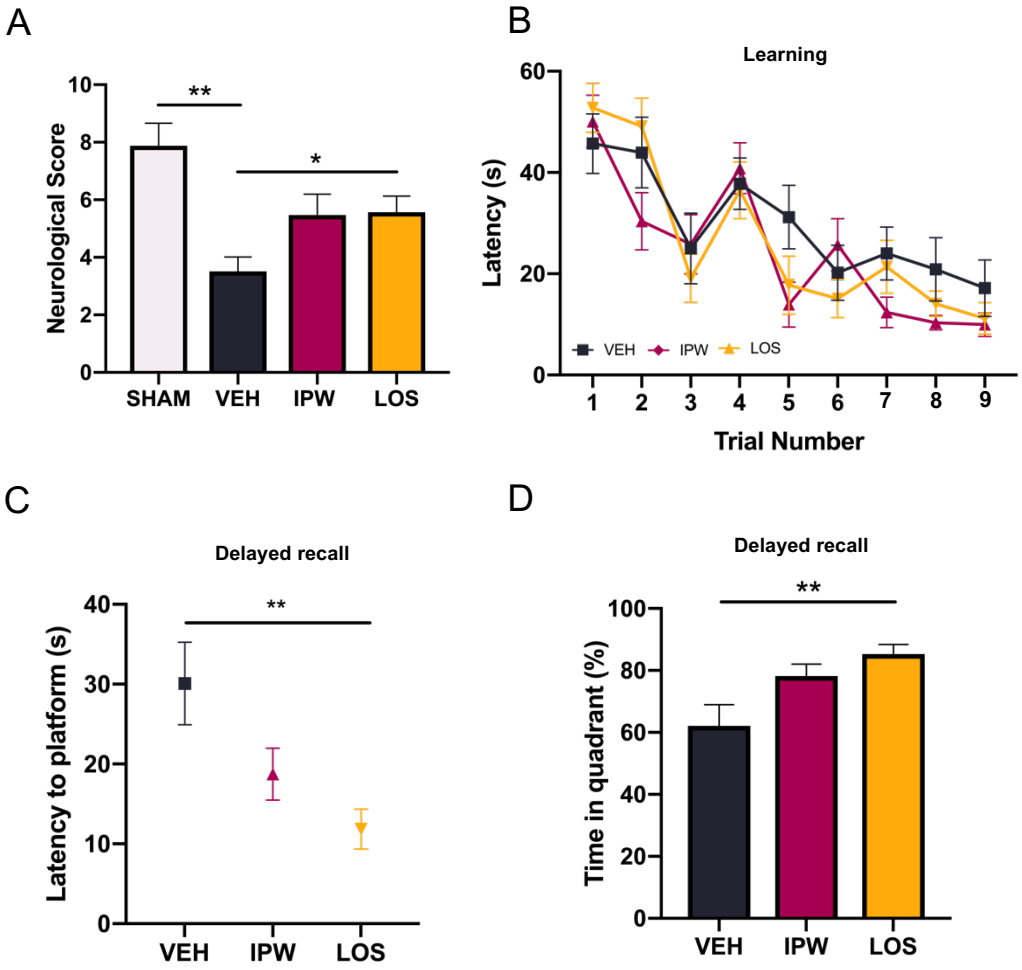

Figure 4.6: Early losartan treatment prevents delayed rmTBI complications. **(A)** The neurological scores of vehicle (VEH: n = 18), IPW (n = 15), losartan (LOS: n = 14) and sham control (SHAM: n = 10) animals were assessed one month-post impact. Vehicle-treated animals had a lower score one month post-impact than sham controls (P = 0.0057). Early treatment with losartan prevented delayed deterioration in neurological score compared to vehicle controls (P = 0.0322). IPW-treated animals did not differ significantly from vehicle controls (P = 0.1645). **(B - D)** MWM performance was assessed in vehicle (VEH: n = 13), IPW- (n = 13), and losartan-treated animals (LOS: n = 13). **(B)** IPW and losartan treatment did not alter the learning portion of task compared to vehicle controls. **(C)** 24h after initial learning, losartan-treated animals had a shorter latency to locate the escape platform than vehicle-treated animals (P = 0.0041) and **(D)** spent more time in the maze quadrant containing the escape platform (P = 0.0061). IPW-treated animals did not differ from vehicle controls in delayed recall, as assessed by the latency to the platform **(C)** (P = 0.1817) or **(D)** the amount of time spent in the quadrant containing the platform (P = 0.0908).

4.4 DISCUSSION

4.4.1 Summary

In this chapter, we sought to evaluate the potential of TGFβ antagonism as a novel treatment strategy for acute and delayed complications of rmTBI. To do so, we tested the effects of two different TGFβ antagonists, IPW and losartan, in our rodent model of rmTBI.

Treatment with IPW reduced the occurrence and duration of acute post-impact convulsions. Further, IPW accelerated the ability to regain righting posture and locomotor function immediately post-impact and protected the integrity of the BBB following repetitive injury. Losartan did not significantly improve the acute events following injury and was not BBB-protective. However, losartan-treated animals performed significantly better in delayed neurological and cognitive testing one month post-impact, indicating that early treatment with losartan was able to prevent these long-term complications of rmTBI. We did not find any differences in acute neurological performance or mortality using these two interventions. Together, our results indicate that some early and delayed complications of rmTBI may be prevented by early inhibition of TGFβ signalling.

4.4.2 Antagonism of TGFβ Signalling by Losartan and IPW

Our findings described in Chapter 3 indicate that changes in TGFβ signalling occur in the hippocampus and sensorimotor cortex within one week following exposure to rmTBI. Thus, we assessed TGFβ signalling in these two brain areas in treated and control animals. One month post-impact, vehicle controls (which were exposed to rmTBI) had significantly more TGFβ signalling in the sensorimotor cortex than sham controls, although these two groups of animals did not differ in hippocampal TGFβ signalling

Our results from Chapter 3 indicated that acute hippocampal TGFβ signalling was specifically increased in sensitive animals, while remaining comparable to sham controls in resilient animals. Of the three vehicle controls that were sacrificed for protein analysis from the drug study, two met the criteria for acute sensitivity while one was retrospectively classified as resilient. As such, if the pattern of TGFβ signalling one week post-impact is representative of the changes at one month post-impact, the differential amounts of hippocampal TGFβ signalling between sensitive and resilient animals may mask the appearance of increased TGFβ signalling in this brain area. In contrast, TGFβ signalling in the sensorimotor cortex of both sensitive and resilient animals was shown to be significantly higher than sham controls one week post-impact, thus this effect would not be relevant. Alternatively, it is possible that the early increase in TGFβ signalling in the hippocampus is not persistent to one month post-impact, whereas the changes in TGFβ signalling in the sensorimotor cortex remain elevated at this delayed time point.

Both IPW and losartan reduced the increase in TGFβ signalling in the sensorimotor cortex that was observed in vehicle-treated animals, indicating that both interventions were able to sufficiently engage with their intended targets. Future studies are required to assess the complete time course of TGFβ antagonism in this model.

4.4.3 Acute Events Following Injury

As described in Chapter 2, we observed immediate post-impact convulsions in a subset of animals exposed to rmTBI. Within the first three impacts, a progressive increase in the number of animals experiencing convulsions was observed, however, by impact four and five, there was a decline in the percentage of animals that experienced these convulsive events. This is likely due to the decrease in animals that are exposed to impacts 4 and 5, as

most sensitive animals have already been removed from being subjected to additional impacts upon significant deterioration. As such, impacts 4 and 5 are often preferentially administered to resilient animals that are able to tolerate the higher number of repetitive injuries. Therefore, we focused the remainder of our analysis to the post-impact events following the first three impacts, as these time points represent the most accurate depiction of the entire population of animals exposed to rmTBI.

The duration of post-impact convulsions following rmTBI was decreased by treatment with IPW. In particular, after two and three impacts, IPW-treated animals had significantly shorter convulsions. Additionally, losartan-treated animals had shorter convulsions after the second impact, but this effect was not maintained following the third impact. These findings suggest that early antagonism of TGFβ reduces the duration of post-impact convulsions. It is unclear why losartan was able to reduce the duration of post-impact convulsions after two but not three impacts. It is possible that upon repetitive injuries, the early benefit of losartan is unable to continue to minimize the extent of these convulsive events due to a less substantial antagonism of TGFβ (compared to IPW) at this time point.

What is the underlying pathophysiology of the post-impact convulsions observed in this model and how might TGFβ antagonism be related? As discussed in Chapter 2, it is likely that the convulsive events are related to the phenomenon of concussive convulsions which have primarily been clinically described in the context of sport (McCrory and Berkovic, 1998). While the mechanistic details underlying these events remains poorly understood, it has been suggested that concussive convulsions may be the result of rapid cortical inhibition following impact that results in the activation of brainstem reflexes

which ultimately lead to the occurrence of convulsions. However, a key question remains regarding what causes this rapid cortical inhibition following impact. One interesting possibility is that cortical inhibition arises due to the occurrence of spreading depolarizations (SDs) that manifest in the immediate seconds following impact.

SDs are electrophysiological waves that depolarize neurons and astrocytes, suppressing spontaneous cortical activity and leading to electrical silence (Dreier, 2011). SDs have been described previously in patients experiencing severe TBI (Hartings et al., 2009; Hartings et al., 2011). However, recent results from animal experiments conducted by our group (Abo Ghazleh, unpublished data) and others (Bouley et al., 2018) suggest that SDs can also occur following mild TBI. Further experiments are required to elucidate the relationship between concussive convulsions and SDs, as well as how TGFβ signalling may be involved. It is possible that TGFβ antagonism or other effects of the two therapeutic interventions tested in this study may act to directly or indirectly affect the initiation and/or propagation of SDs. This possibility requires further investigation (see Chapter 5 for additional discussion).

In addition to differences in post-impact convulsions, we observed that IPW-treated, but not losartan-treated, animals regained the righting reflex and resumed locomotion faster than vehicle-treated animals upon repetitive impacts. It is likely that the improvement in acute recovery following impact is related to the occurrence of post-impact convulsions, as animals that experienced post-impact convulsions may take longer to regain the righting reflex and locomotor abilities following impact. This may be due to impaired consciousness resulting from the convulsions and/or the occurrence of SDs, although direct assessment of consciousness is not possible in an animal model. In any

case, that IPW-treated animals had fewer and shorter convulsions than vehicle controls, whereas losartan-treated animals did not, likely explains the improved ability of IPW-treated animals to resume functioning post-impact.

4.4.4 Acute Neurological Outcomes and Mortality

As discussed in Chapter 2, the combined neurological score is derived from three behavioural tests (open field, beam walk, and inverted wire mesh) which are sensitive to changes in animal locomotion, balance, and weakness. These tests may also be sensitive to alterations in animal motivation, attention, or curiosity, for example in the case of an animal that does not traverse the beam post-impact but otherwise appears to be able to locomote normally. Given that neither IPW nor losartan were able to alter acute neurological scoring in rmTBI-exposed animals or significantly affect the percentage of sensitive animals compared to vehicle controls, it is likely that the underlying neurobehavioural deficits observed in our model are not directly caused by changes to BBB integrity or TGFβ signalling *per se*. It has previously been suggested that acute symptoms of concussion may result from rapid changes in shear stress which occur due to mechanical loading in the cortex due to physical impact (Tagge et al., 2018). This may be caused by direct membrane deformation during force loading, which can lead to rapid depolarization of neurons through the opening of stretch-sensitive channels (Hemphill et al., 2015). Our findings are consistent with this notion and suggest that abhorrent TGFβ signalling does not appear to directly contribute to acute neurobehavioual deficits in this model, although we cannot completely confirm that TGFβ signalling was attenuated during the early phase of the injuries.

In addition to acute neurological outcomes, IPW and losartan did not significantly alter animal body weight compared to vehicle controls. The decrease in body weight that we observed following repetitive injury (and characterized further in Chapter 2) could be attributed to several possibilities, including dehydration or loss of appetite. Indeed, changes in appetite have been previously described in patients following mild TBI (McCrory and Johnston, 2002; Paniak et al., 2002; Kashluba et al., 2004). These features may be closely related to changes in hypothalamic function ensuing from repetitive impacts, and our findings indicate that these events appear to occur independently of changes in TGFβ signalling.

Finally, acute mortality resulting from exposure to rmTBI was not prevented by treatment with IPW or losartan. The mechanisms underlying acute post-impact mortality following repetitive impacts, sometimes referred to as "second impact syndrome" (SIS), remain poorly understood. SIS is thought to occur when an individual sustains an initial head trauma and then receives a subsequent TBI before the resolution of the initial injury occurs (Cantu, 1998; Ling et al., 2015). Exposure to repetitive impacts in close succession can, in rare cases, lead to catastrophic outcomes and even death (McLendon et al., 2016). Several mechanisms have been proposed to underlie second impact syndrome, including diffuse edema leading to compression of the brain's parenchyma and vasculature, or the inability of the brain's vasculature to autoregulate leading to increased intracranial pressure upon repetitive injury (Cantu, 1998; Bey and Ostick, 2009). These events are often accompanied by brain hyperemia which can lead to fatal herniation, although the pathophysiological mechanisms underlying these events remain poorly understood

(Weinstein et al., 2013). Unfortunately, the two treatments used in this study were unable to prevent these catastrophic outcomes following repetitive impacts.

4.4.5 Effect on BBB Integrity

DCE-MRI was used to assess the ability of IPW and losartan to protect the integrity of the BBB, which we have previously shown to be disrupted following rmTBI. We found that IPW, but not losartan, protected the integrity of the BBB following exposure to rmTBI. Consistent with the overall hypothesis of this thesis, this may be the result of the specific mechanism of action of IPW, in which the TGFβR1 kinase is potently inhibited. As described previously, increased astrocytic TGFβ signalling under conditions of BBBD can result in a cascade of events involving neuroinflammation and neural dysfunction. It is possible that the early inhibition of this pathway resulted in a protective effect on BBB integrity by limiting the action of neuroinflammatory mediators that may exacerbate BBBD. Together, that inhibition of TGFβ signalling was able to prevent BBBD in this model of rmTBI indicates that this pharmacological approach may hold therapeutic promise as a BBB protective agent, as has been suggested previously (Bar-Klein et al., 2017).

4.4.6 Delayed Outcomes

Finally, delayed neurological and cognitive performance in rmTBI-exposed animals was assessed one month post-impact. Both IPW and losartan-treated animals performed better than vehicle controls in these two domains, although this improvement was only significant in losartan-treated animals. This is an interesting finding, given that losartan appeared to have little effect during the acute course of injuries. As mentioned in

Chapter 2, the acute symptomatology and underlying mechanisms of concussion may not be linked to delayed outcomes (Tagge et al., 2018). Indeed, it appears that early treatment with losartan conferred long-term neuroprotective benefits despite minimally altering the acute outcomes of repetitive injury. This lends further support to the uncoupling of acute and delayed complications of rmTBI.

It is also possible that in addition to its ability to block TGFβ signalling, losartan may act on other targets which may have been responsible for the improved delayed neurological and cognitive outcomes that we observed. Indeed, losartan has been shown to be neuroprotective in various animal models of disease, including AD (Ongali et al., 2014), stroke (Smeda and McGuire, 2007; Smeda and Daneshtalab, 2011; Zhang et al., 2012), and epilepsy (Pechlivanova et al., 2011; Bar-Klein et al., 2014). Additionally, losartan's effects as an angiotensin receptor antagonist cannot be excluded as a possible alternative mechanism underlying the beneficial delayed effects that we observed. Angiotensin II has been shown to signal through astrocytic angiotensin II type 1 receptors to regulate the infiltration of peripheral leukocytes (Füchtbauer et al., 2011). Future work is required to elucidate the mechanistic details underlying the beneficial effects of IPW and losartan in the context of rmTBI. Moreover, a pharmacokinetic study is required to assess the concentration of IPW and losartan reaching the brain following IP administration, as well as how the concentration of each drug varies in regions with normal or compromised vascular permeability. Future studies should also employ a combination of pharmacokinetic and pharmacodynamic approaches to optimize dose selection for these drugs.

4.5 CONCLUSION

Together, the results of this pre-clinical drug study suggest that early treatment with TGFβ antagonists may be beneficial in preventing acute and delayed complications of rmTBI. Importantly, both TGFβ antagonists used in this study were able to engage with their pharmacological targets to prevent increased TGFβ signalling one month post-injury. With respect to rmTBI-related complications, we observed differential benefits of our two therapeutic interventions, although both were unable to alter acute neurological function or overall mortality. The pre-clinical small molecule specific TGFβ signalling antagonist, IPW, was able to reduce the occurrence and duration of post-impact convulsions and reduced the delay in acute recovery post-impact. Additionally, IPW protected the integrity of the BBB following repetitive injury. In contrast, losartan did not appear to affect the acute events of repetitive injury, however, it was successful in improving delayed neurological and cognitive deficits following repetitive injury. Our findings suggest that acute sensitivity to impact and long-term complications following rmTBI may be mediated by independent processes and suggest that early TGFβ antagonism may be beneficial in preventing some acute and delayed neurological and cognitive complications of rmTBI.

Chapter 5:
General Discussion

5.1 Summary of Central Findings

This thesis sought to investigate the role of pro-inflammatory TGFβ signalling in rmTBI and to assess its viability as a therapeutic target for rmTBI. To do so, we first established impact parameters in a modified weight-drop model of mild TBI that produce acute signs of transient concussion-like outcomes in rodents following a single injury. We then characterized a model of rmTBI that recapitulates the clinical spectrum of outcomes that are commonly observed following repetitive injury (Chapter 2). Importantly, the concussion-like outcomes that we observed during the early phases of repetitive injury were not predictive of delayed complications, consistent with the notion that chronic sequelae of repetitive head trauma can be induced in the absence of acute concussion symptoms.

In Chapter 3, we showed that pathological BBBD, TGFβ signalling, reactive gliosis, and neuroinflammation are associated with a more severe acute clinical outcome following repetitive injury. Our identification of TGFβ signalling as an early and critical step of rmTBI-associated deterioration highlighted the potential of this pathway as a candidate for therapeutic intervention in rmTBI. Thus, we tested the effects of two TGFβ antagonists (IPW and losartan) on the acute and delayed complications of rmTBI (Chapter 4). We showed that early treatment with IPW was successful in improving acute post-impact recovery and protected the integrity of the BBB, whereas treatment with losartan prevented delayed neurological and cognitive complications of repetitive injury. Together, our results indicate that antagonism of TGFβ signalling can be beneficial in improving acute and delayed outcomes of rmTBI, although the mechanistic details underlying these effects warrant further investigation.

5.2 General Limitations

There are several general limitations relating to the use of our animal model of rmTBI. We used isoflurane to anesthetize our animals prior to the administration of each impact. Although sham controls (anesthesia only) were used, we cannot account for the influence that exposure to isoflurane may have on injury outcomes following rmTBI. Indeed, previous work has shown that isoflurane can be neuroprotective and may prevent BBBD and neuroinflammation (Statler et al., 2006; Luh et al., 2011; Bar-Klein et al., 2017). Thus, our findings regarding deterioration of rmTBI animals may actually be conservative, although it is also possible that the interaction between isoflurane and rmTBI is inherently different between sensitive and resilient animals.

We elected to use adolescent male rats in our model due to the high numbers of young male athletes involved in contact-sports (Daneshvar et al., 2011). However, the generalizability of our findings is limited by a lack of rigorous testing on female animals or animals of various ages. Interestingly, preliminary evidence from a pilot study that we conducted suggests that female animals and younger animals may be more susceptible to acute complications of rmTBI than the adolescent male animals that we assessed (data not shown). These preliminary findings warrant more investigation into sex and age differences in our model and are consistent with current clinical evidence suggesting that females and youth may report greater concussion symptoms and longer recovery times (Field et al., 2003; Broshek et al., 2005; Berz et al., 2013; Noble and Hesdorffer, 2013; Miller et al., 2016).

5.3 Future Experimental Considerations

A number of questions have been raised by the findings described in this thesis. In particular, a few central questions remain: What makes one animal acutely sensitive to repetitive impacts over another? Additionally, what is the relationship between acute and delayed complications of rmTBI? Can we predict which individuals will develop complications following rmTBI? The answers to these questions are currently an active area of investigation in the Friedman laboratory and some possibilities will be discussed below.

5.3.1 Cortical Network Dysfunction

Investigation into cortical network dysfunction, including the occurrence and features of SDs and epileptiform activity, as it relates to BBBD is ongoing. These functional network abnormalities may provide an explanation for the differences in outcome between animals. In particular, SDs may play a role in the generation of post-impact convulsions. Recent evidence from our group and others suggests that SDs are common events following mild TBI (Bouley et al., 2018; Abo Ghazleh, unpublished data). The development or characteristics of SDs or seizures following impact may differ between sensitive and resilient animals. For example, slight variations between individuals in tissue landscape, genetics, and brain response to trauma may alter the propensity of SDs or seizures to arise or propagate. Based on the findings in this thesis and the current understanding of the events following concussive injury, we propose the following mechanistic framework (Figure 5.1) for the observations reported in this thesis:

Impact to the head induces mechanical deformation of cortical tissue and cellular membranes, resulting in rapid membrane depolarization and the release of glutamate

(Katayama et al., 1990). Increased glutamate release contributes to ion channel opening and a large flux of cations (Giza and Hovda, 2014; Hemphill et al., 2015). These changes can lead to cortical dysfunction and may trigger the initiation of SDs (cortical inhibition) or epileptic seizures (cortical excitation). It has been hypothesized that concussive convulsions may arise from rapid cortical inhibition following impact and the activation of subcortical (e.g. brainstem or spinal) reflexes leading to convulsion (McCrory and Berkovic, 1998, 2000). Indeed, SDs cause rapid inhibition of neuronal firing (Dreier, 2011) and may be responsible for cortical inhibition leading to the generation of post-impact convulsions. While concussive convulsions are not thought to be epileptic (that is, involving cortical excitation) in nature, the precise mechanisms underlying concussive convulsions remain unknown. Future investigations using electrocorticographical recordings obtained immediately following impact are essential to elucidate the mechanisms underlying concussive convulsions (that is, if cortical inhibition or excitation is involved), and their relationship to acute neurological outcomes in this model.

Both SDs and epileptic seizures can lead to dysfunction of the BBB (Gursoy-Ozdemir et al., 2004; Li et al., 2013; Rüber et al., 2018; Prager et al., 2019). Moreover, pro-inflammatory TGFβ signalling can be triggered by and contribute to BBBD, leading to long-term complications (Ivens et al., 2006; Cacheaux et al., 2009; Bar-Klein et al., 2014; Weissberg et al., 2015). Under conditions of repetitive impacts, inflammation, TGFβ signalling, and BBBD arising from prior injury may alter the propensity of cortical networks to be excited. Additionally, there is some evidence to suggest that BBBD may alter the threshold for SD generation (Tomkins et al., 2007). It is possible that antagonism

of TGFβ signalling reduced the occurrence and duration of post-impact convulsions in rmTBI animals in our study through these mechanisms.

Alternative mechanisms involved in mediating long-term complications of rmTBI include axonal injury and hyperphosphorylation of tau. These mechanisms may be triggered by the same common event (i.e. head impact) as acute concussion symptoms but may differ mechanistically and in their time course (Tagge et al., 2018). The extent to which axonal injury and tau phosphorylation are related to BBBD and pro-inflammatory TGFβ signalling is not known. However, it is possible that these mechanisms may contribute to or act independently from BBBD and TGFβ signalling following rmTBI. These mechanisms may be responsible for the delayed (but not acute) deterioration of resilient animals in our studies.

Based on the results presented in this thesis we hypothesize that sensitive animals experience more SDs (or longer SDs) than resilient animals, leading to longer post-impact convulsions, a slower rate of post-impact recovery, and more severe acute neurological outcomes. The occurrence of SDs can initiate BBBD, which can, in turn, lead to pro-inflammatory TGFβ signalling, which was increased in the brains of sensitive animals following injury. Additionally, primary BBBD and inflammation following mild TBI may be initiated independently from SD generation. Network alterations and increased vulnerability following injury may predispose the brain to increased damage following repetitive impacts, further potentiating the pathological process that was initiated following the first impact. These events may lead to increased acute symptoms of concussion, including concussive convulsions. While these early pathological events can contribute to delayed complications of rmTBI, alternative mechanisms (such as axonal injury,

hyperphosphorylation of tau, and neuroinflammation) may also lead to delayed complications of rmTBI, even in the absence of early symptoms of concussion.

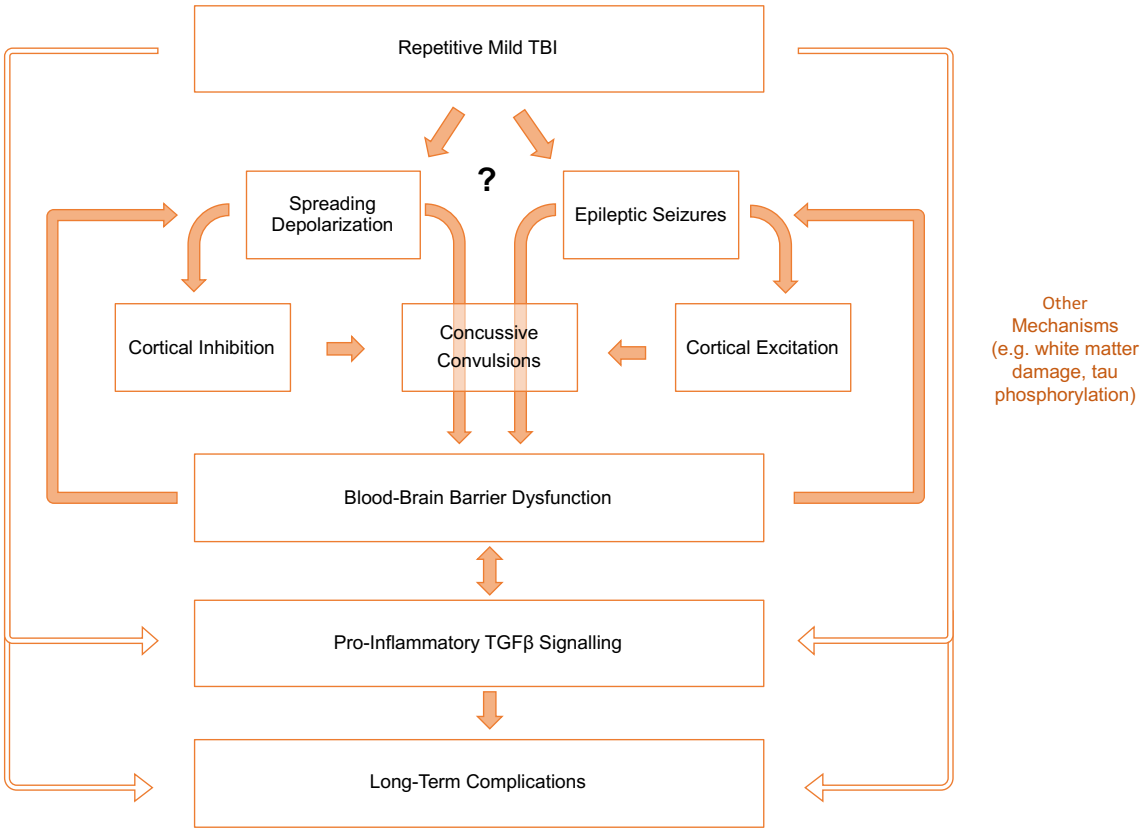

Figure 5.1. Schematic of possible mechanisms leading to acute and delayed complications following rmTBI.

Future experiments are required to test the hypotheses raised in this theoretical framework. In particular, direct recording using electrocorticography following repetitive impacts is required to assess the occurrence of cortical inhibition versus excitation following mild TBI, as well as how these relate to acute injury outcomes, including concussive convulsions. This approach may yield valuable insight into the pathophysiology of concussion and the relationship between acute and delayed complications of rmTBI.

5.3.2 Sensitivity to rmTBI: Other Mechanisms

It is likely that more than one mechanism is responsible for the development of complications of rmTBI. Another possibility is that differential stress responses between sensitive and resilient animals underlie their susceptibility to injury. In a preliminary study, serum from rmTBI animals was collected and a radioimmunoassay was performed to quantify corticosterone levels over the course of the injuries. Interestingly, we found that resilient animals had an increase in serum corticosterone following a single mild impact, whereas corticosterone levels in sensitive animals did not differ after a single mild TBI (Appendix E). It is possible that differences in corticosterone regulation and animal stress response play significant roles in the sensitivity to acute TBI. Acute activation of the stress response and the hypothalamic-pituitary-adrenal axis is essential for stress adaptation and maintenance of energy homeostasis following exposure to a stressor (De Kloet et al., 2005; Johnson and Renn, 2006). Interestingly, recent clinical evidence from a study in young hockey players (11-13 years old) suggests that players with abnormally low cortisol levels are more likely to have worse symptoms and a longer period of recovery following mild TBI (Ritchie et al., 2018). Moreover, evidence from animal models has indicated that impaired secretion of corticosterone following an acute stressor may influence the susceptibility to developing characteristics similar to post-traumatic stress disorder (Cohen et al., 2006). Future work is warranted to assess whether early differences in the stress response to injury are involved in mediating sensitivity to rmTBI.

It is also possible that genetic differences may be involved in the differential response to injury that we observed in our model. Sprague Dawley rats are an outbred rodent strain. Outbred strains are defined as “a closed population of genetically variable

animals bred to maintain maximum heterozygosity" (Festing, 1993; Chia et al., 2005). Thus, there is genetic heterogeneity among the animals used in our study. Several genes have been associated with poor outcome following mild TBI, including apolipoprotein E (Kutner et al., 2000), dopamine D2 receptor (McAllister et al., 2005), and IL genes (Jordan, 2007). However, these associations were largely in the context of delayed injury outcomes and cognitive performance, rather than acute symptoms of concussion. Alternatively, it is possible that genetic differences relating to the susceptibility of SD generation and propagation may be relevant in our model.

Finally, we presented pressure and impact tracking data that suggests that differences in acute outcomes between sensitive and resilient animals are not explained by differences in impact biomechanics. However, it is possible that more subtle differences in biomechanics following impact are present and that these may be relevant to mediating or contributing to the differential sensitivities that we observed to repetitive trauma. Distinctive injury mechanics may also give rise to differences in SD generation and propagation. Future investigations into the role that injury biomechanics may play in this model are ongoing by our research group.

5.3.3 BBBD as a Biomarker for rmTBI

The work in this thesis implicates early BBBD as a key event following rmTBI, consistent with reports in humans (Weissberg et al., 2014) and in animals (Tagge et al., 2018). We found that sensitivity to rmTBI was associated with increased BBBD one week after impact, leading us to ask if BBBD was elevated earlier in the time course of injury development. We assessed BBB integrity 24 hours after a single mild TBI in four animals

and did not find evidence of elevated BBBD at this time point. However, this finding is limited by a small sample size and future studies should be directed at evaluating if early changes in BBBD (perhaps, 24 or 48 hours after initial injury) are detectable prior to the onset of acute neurological deterioration in this model. The results of these investigations may yield critical information regarding the predictive ability of BBBD to act as a clinically-relevant biomarker for complications of rmTBI, as well as for the development of future therapies (i.e. as a pharmacodynamic biomarker).

5.3.4 Antagonism of TGFβ in rmTBI

In a model of BBBD-induced epilepsy, our group has previously shown that losartan can reduce the development of seizures (Bar-Klein et al., 2014). Thus, early treatment with TGFβ antagonists may also prove to be effective in preventing the development of post-traumatic epilepsy following repetitive head trauma. Investigations are currently underway by our group to assess the effect of TGFβ antagonism with IPW and losartan on the development of abnormal brain activity and post-traumatic epilepsy in this model of rmTBI.

Given that we observed different beneficial effects on the acute and delayed outcomes following injury using IPW and losartan, it would also be interesting to test the effect of combination therapy using both of these drugs together. This approach may prove beneficial in improving both the acute and delayed outcomes of repetitive injuries. In addition, further characterization of the precise mechanisms underlying the favourable effects of treatment with IPW and losartan are required to discern if antagonism of TGFβ

signalling or another target (such as angiotensin II receptor I inhibition, in the case of losartan) is responsible for the benefit of these treatments.

5.4 Concluding Remarks

The work detailed in this thesis identifies TGFβ signalling as a key mediator of rmTBI-related complications. We provide evidence that increased BBBD, TGFβ signalling, and neuroinflammation are associated with more severe neurological outcomes during the acute phases of repetitive injury. Moreover, we show that early pharmacological inhibition of TGFβ signalling can protect the integrity of the BBB, improve early recovery following impact, and prevent delayed complications of rmTBI. Together, our findings highlight the potential of TGFβ signalling antagonism as a future therapeutic strategy for rmTBI, but also identify the need for further studies to elucidate the detailed effects of these treatments as they relate to acute and delayed outcomes of rmTBI.

References

Abbott NJ, Rönnbäck L, Hansson E (2006) Astrocyte–endothelial interactions at the blood–brain barrier. Nature Reviews Neuroscience 7:41.

Abbott NJ, Patabendige AA, Dolman DE, Yusof SR, Begley DJ (2010) Structure and function of the blood–brain barrier. Neurobiology of Disease 37:13-25.

Adams JH, Graham D, Murray LS, Scott G (1982) Diffuse axonal injury due to nonmissile head injury in humans: an analysis of 45 cases. Annals of Neurology 12:557-563.

Adams JH, Doyle D, Ford I, Gennarelli T, Graham D, McLellan D (1989) Diffuse axonal injury in head injury: definition, diagnosis and grading. Histopathology 15:49-59.

Andreone BJ, Chow BW, Tata A, Lacoste B, Ben-Zvi A, Bullock K, Deik AA, Ginty DD, Clish CB, Gu C (2017) Blood-brain barrier permeability is regulated by lipid transport-dependent suppression of caveolae-mediated transcytosis. Neuron 94:581-594.

Andriessen TM, Jacobs B, Vos PE (2010) Clinical characteristics and pathophysiological mechanisms of focal and diffuse traumatic brain injury. Journal of Cellular and Molecular Medicine 14:2381-2392.

Attwell D, Buchan AM, Charpak S, Lauritzen M, MacVicar BA, Newman EA (2010) Glial and neuronal control of brain blood flow. Nature 468:232.

Au AK, Aneja RK, Bell MJ, Bayir H, Feldman K, Adelson PD, Fink EL, Kochanek PM, Clark RS (2012) Cerebrospinal fluid levels of high-mobility group box 1 and cytochrome C predict outcome after pediatric traumatic brain injury. Journal of Neurotrauma 29:2013-2021.

Aubry M, Cantu R, Dvorak J, Graf-Baumann T, Johnston K, Kelly J, Lovell M, McCrory P, Meeuwisse W, Schamasch P (2002) Summary and agreement statement of the first International Conference on Concussion in Sport, Vienna 2001. The Physician and Sportsmedicine 30:57-63.

Aungst SL, Kabadi SV, Thompson SM, Stoica BA, Faden AI (2014) Repeated mild traumatic brain injury causes chronic neuroinflammation, changes in hippocampal synaptic plasticity, and associated cognitive deficits. Journal Of Cerebral Blood Flow & Metabolism 34:1223-1232.

Bar-Klein G, Lublinsky S, Kamintsky L, Noyman I, Veksler R, Dalipaj H, Senatorov VV, Swissa E, Rosenbach D, Elazary N (2017) Imaging blood–brain barrier dysfunction as a biomarker for epileptogenesis. Brain 140:1692-1705.

Bar-Klein G, Cacheaux LP, Kamintsky L, Prager O, Weissberg I, Schoknecht K, Cheng P, Kim SY, Wood L, Heinemann U, Kaufer D, Friedman A (2014) Losartan prevents acquired epilepsy via TGF-beta signaling suppression. Annals of Neurology 75:864-875.

Başkaya MK, Rao AM, Doğan A, Donaldson D, Dempsey RJ (1997) The biphasic opening of the blood–brain barrier in the cortex and hippocampus after traumatic brain injury in rats. Neuroscience Letters 226:33-36.

Baugh CM, Stamm JM, Riley DO, Gavett BE, Shenton ME, Lin A, Nowinski CJ, Cantu RC, McKee AC, Stern RA (2012) Chronic traumatic encephalopathy: neurodegeneration following repetitive concussive and subconcussive brain trauma. Brain Imaging and Behavior 6:244-254.

Behzadian MA, Wang X-L, Windsor LJ, Ghaly N, Caldwell RB (2001) TGF-β increases retinal endothelial cell permeability by increasing MMP-9: possible role of glial cells in endothelial barrier function. Investigative Ophthalmology & Visual Science 42:853-859.

Ben-Shlomo Y (1997) The epidemiology of Parkinson's disease. Baillieres Clinical Neurology 6:55-68.

Berz K, Divine J, Foss KB, Heyl R, Ford KR, Myer GD (2013) Sex-specific differences in the severity of symptoms and recovery rate following sports-related concussion in young athletes. The Physician and Sportsmedicine 41:58-63.

Beschorner R, Nguyen TD, Gözalan F, Pedal I, Mattern R, Schluesener HJ, Meyermann R, Schwab JM (2002) CD14 expression by activated parenchymal microglia/macrophages and infiltrating monocytes following human traumatic brain injury. Acta Neuropathologica 103:541-549.

Bey T, Ostick B (2009) Second impact syndrome. Western Journal of Emergency Medicine 10:6.

Bianchi ME, Manfredi AA (2009) Immunology. Dangers in and out. Science 323:1683-1684.

Black KL, Hanks RA, Wood DL, Zafonte RD, Cullen N, Cifu DX, Englander J, Francisco GE (2002) Blunt versus penetrating violent traumatic brain injury: frequency and factors associated with secondary conditions and complications. The Journal of Head Trauma Rehabilitation 17:489-496.

Blaha M, Schwab J, Vajnerova O, Bednar M, Vajner L, Michal T (2010) Intracranial pressure and experimental model of diffuse brain injury in rats. Journal of Korean Neurosurgical Society 47:7.

Blennow K, Brody DL, Kochanek PM, Levin H, McKee A, Ribbers GM, Yaffe K, Zetterberg H (2016) Traumatic brain injuries. Nature Reviews Disease Primers 2:16084.

Bouley J, Chung DY, Ayata C, Brown Jr RH, Henninger N (2018) Cortical spreading depression denotes concussion injury. Journal of Neurotrauma 36:1008-1017.

Brionne TC, Tesseur I, Masliah E, Wyss-Coray T (2003) Loss of TGF-β1 leads to increased neuronal cell death and microgliosis in mouse brain. Neuron 40:1133-1145.

Brodbelt A, Stoodley M (2007) CSF pathways: a review. British Journal of Neurosurgery 21:510-520.

Brody DL, Mac Donald C, Kessens CC, Yuede C, Parsadanian M, Spinner M, Kim E, Schwetye KE, Holtzman DM, Bayly PV (2007) Electromagnetic controlled cortical impact device for precise, graded experimental traumatic brain injury. Journal of Neurotrauma 24:657-673.

Broshek DK, Kaushik T, Freeman JR, Erlanger D, Webbe F, Barth JT (2005) Sex differences in outcome following sports-related concussion. Journal of Neurosurgery 102:856-863.

Burda JE, Sofroniew MV (2014) Reactive gliosis and the multicellular response to CNS damage and disease. Neuron 81:229-248.

Cacheaux LP, Ivens S, David Y, Lakhter AJ, Bar-Klein G, Shapira M, Heinemann U, Friedman A, Kaufer D (2009) Transcriptome profiling reveals TGF-β signaling involvement in epileptogenesis. Journal of Neuroscience 29:8927-8935.

Cantu RC (1998) Second-impact syndrome. Clinics in Sports Medicine 17:37-44.

Caro DH (2011) Traumatic brain injury care systems: 2020 transformational challenges. 10.5539.

Carroll L, Cassidy JD, Peloso P, Borg J, Von Holst H, Holm L, Paniak C, Pépin M (2004) Prognosis for mild traumatic brain injury: results of the WHO Collaborating Centre Task Force on Mild Traumatic Brain Injury. Journal of Rehabilitation Medicine 36:84-105.

Cassidy JD, Carroll L, Peloso P, Borg J, von Holst H, Holm L, Kraus J, Coronado V (2004) Incidence, risk factors and prevention of mild traumatic brain injury: results of the WHO collaborating centre task force on mild traumatic brain injury. Journal of Rehabilitation Medicine 36:28-60.

CDC Traumatic Brain Injury | Concussion | Traumatic Brain Injury | CDC Injury Center.

Cernak I (2005) Animal models of head trauma. NeuroRX 2:410-422.

Chancellor SE, Franz ES, Minaeva OV, Goldstein LE (2019) Pathophysiology of Concussion. In: Seminars In Pediatric Neurology: Elsevier.

Chen H, Richard M, Sandler DP, Umbach DM, Kamel F (2007) Head injury and amyotrophic lateral sclerosis. American Journal of Epidemiology 166:810-816.

Chen Y, Constantini S, Trembovler V, Weinstock M, Shohami E (1996) An experimental model of closed head injury in mice: pathophysiology, histopathology, and cognitive deficits. Journal of Neurotrauma 13:557-568.

Chia R, Achilli F, Festing MF, Fisher EM (2005) The origins and uses of mouse outbred stocks. Nature Genetics 37:1181.

Cho J-H, Ryu H-M, Oh E-J, Yook J-M, Ahn J-S, Jung H-Y, Choi J-Y, Park S-H, Kim Y-L, Kwak IS (2016) Alpha1-Antitrypsin Attenuates Renal Fibrosis by Inhibiting TGF-β1-Induced Epithelial Mesenchymal Transition. Plos One 11:e0162186.

Chu CT, Ji J, Dagda RK, Jiang JF, Tyurina YY, Kapralov AA, Tyurin VA, Yanamala N, Shrivastava IH, Mohammadyani D (2013) Cardiolipin externalization to the outer mitochondrial membrane acts as an elimination signal for mitophagy in neuronal cells. Nature Cell Biology 15:1197.

Cohen H, Zohar J, Gidron Y, Matar MA, Belkind D, Loewenthal U, Kozlovsky N, Kaplan Z (2006) Blunted HPA axis response to stress influences susceptibility to posttraumatic stress response in rats. Biological Psychiatry 59:1208-1218.

Coronado VG, Haileyesus T, Cheng TA, Bell JM, Haarbauer-Krupa J, Lionbarger MR, Flores-Herrera J, McGuire LC, Gilchrist J (2015) Trends in Sports- and Recreation-Related Traumatic Brain Injuries Treated in US Emergency Departments: The National Electronic Injury Surveillance System-All Injury Program (NEISS-AIP) 2001-2012. Journal of Head Trauma Rehabilitation 30:185-197.

Corps KN, Roth TL, McGavern DB (2015) Inflammation and neuroprotection in traumatic brain injury. Journal of the American Medical Association Neurology 72:355-362.

Correale J, Villa A (2007) The blood–brain barrier in multiple sclerosis: functional roles and therapeutic targeting. Autoimmunity 40:148-160.

Csuka E, Morganti-Kossmann MC, Lenzlinger PM, Joller H, Trentz O, Kossmann T (1999) IL-10 levels in cerebrospinal fluid and serum of patients with severe traumatic brain injury: relationship to IL-6, TNF-α, TGF-β1 and blood–brain barrier function. Journal of Neuroimmunology 101:211-221.

Daneshvar DH, Nowinski CJ, McKee AC, Cantu RC (2011) The epidemiology of sport-related concussion. Clinics in Sports Medicine 30:1-17.

David Y, Cacheaux LP, Ivens S, Lapilover E, Heinemann U, Kaufer D, Friedman A (2009) Astrocytic dysfunction in epileptogenesis: consequence of altered potassium and glutamate homeostasis? Journal of Neuroscience 29:10588-10599.

Davis AE (2000) Mechanisms of traumatic brain injury: biomechanical, structural and cellular considerations. Critical Care Nursing Quarterly 23:1-13.

Davis GA, Purcell L, Schneider KJ, Yeates KO, Gioia GA, Anderson V, Ellenbogen RG, Echemendia RJ, Makdissi M, Sills A (2017) The child sport concussion assessment tool 5th edition (child scat 5): background and rationale. Br J Sports Med 51:859-861.

De Kloet ER, Joëls M, Holsboer F (2005) Stress and the brain: from adaptation to disease. Nature Reviews Neuroscience 6:463.

Denis J-F, Sader F, Gatien S, Villiard É, Philip A, Roy S (2016) Activation of Smad2 but not Smad3 is required to mediate TGF-β signaling during axolotl limb regeneration. Development 143:3481-3490.

Derynck R, Zhang YE (2003) Smad-dependent and Smad-independent pathways in TGF-β family signalling. Nature 425:577.

Derynck R, Budi EH (2019) Specificity, versatility, and control of TGF-β family signaling. Sci Signal 12:570.

Ding M, Haglid KG, Hamberger A (2000) Quantitative immunochemistry on neuronal loss, reactive gliosis and BBB damage in cortex/striatum and hippocampus/amygdala after systemic kainic acid administration. Neurochemistry International 36:313-318.

Dixon CE, Clifton GL, Lighthall JW, Yaghmai AA, Hayes RL (1991) A controlled cortical impact model of traumatic brain injury in the rat. Journal of Neuroscience Methods 39:253-262.

Doherty CP, O'Keefe E, Wallace E, Loftus T, Keaney J, Kealy J, Humphries MM, Molloy MG, Meaney JF, Farrell M (2016) Blood–brain barrier dysfunction as a hallmark pathology in chronic traumatic encephalopathy. Journal of Neuropathology & Experimental Neurology 75:656-662.

Dreier JP (2011) The role of spreading depression, spreading depolarization and spreading ischemia in neurological disease. Nature Medicine 17:439.

Echemendia RJ, Meeuwisse W, McCrory P, Davis GA, Putukian M, Leddy J, Makdissi M, Sullivan SJ, Broglio SP, Raftery M (2017a) The concussion recognition tool 5th edition (CRT5): background and rationale. Br J Sports Med 51:870-871.

Echemendia RJ, Meeuwisse W, McCrory P, Davis GA, Putukian M, Leddy J, Makdissi M, Sullivan SJ, Broglio SP, Raftery M (2017b) The sport concussion assessment tool 5th edition (SCAT5): background and rationale. Br J Sports Med 51:848-850.

El Sayed T, Mota A, Fraternali F, Ortiz M (2008) Biomechanics of traumatic brain injury. Computer Methods in Applied Mechanics and Engineering 197:4692-4701.

Ellis MJ, Wennberg R (2016) Convulsions in a 17-year-old boy after a head injury sustained while playing hockey. CMAJ 188:443-445.

Engel S, Schluesener H, Mittelbronn M, Seid K, Adjodah D, Wehner H-D, Meyermann R (2000) Dynamics of microglial activation after human traumatic brain injury are revealed by delayed expression of macrophage-related proteins MRP8 and MRP14. Acta Neuropathologica 100:313-322.

Feeney DM, Boyeson MG, Linn RT, Murray HM, Dail WG (1981) Responses to cortical injury: I. Methodology and local effects of contusions in the rat. Brain Research 211:67-77.

Fenstermacher J, Gross P, Sposito N, Acuff V, Pettersen S, Gruber K (1988) Structural and Functional Variations in Capillary Systems within the Brain. Annals of the New York Academy of Sciences 529:21-30.

Festing M (1993) Genetic variation in outbred rats and mice and its implications for toxicological screening. Journal of Experimental Animal Science 35:210-220.

Field M, Collins MW, Lovell MR, Maroon J (2003) Does age play a role in recovery from sports-related concussion? A comparison of high school and collegiate athletes. The Journal of Pediatrics 142:546-553.

Friedman A, Kaufer D, Heinemann U (2009) Blood–brain barrier breakdown-inducing astrocytic transformation: novel targets for the prevention of epilepsy. Epilepsy Research 85:142-149.

Füchtbauer L, Groth-Rasmussen M, Holm TH, Løbner M, Toft-Hansen H, Khorooshi R, Owens T (2011) Angiotensin II Type 1 receptor (AT1) signaling in astrocytes regulates synaptic degeneration-induced leukocyte entry to the central nervous system. Brain, Behavior, and Immunity 25:897-904.

Gavett BE, Stern RA, Cantu RC, Nowinski CJ, McKee AC (2010) Mild traumatic brain injury: a risk factor for neurodegeneration. Alzheimer's Research & Therapy 2:18.

Geddes DM, LaPlaca MC, Cargill II RS (2003) Susceptibility of hippocampal neurons to mechanically induced injury. Experimental Neurology 184:420-427.

Gennarelli TA, Thibault LE, Adams JH, Graham DI, Thompson CJ, Marcincin RP (1982) Diffuse axonal injury and traumatic coma in the primate. Annals of Neurology 12:564-574.

Gentleman S, Leclercq P, Moyes L, Graham D, Smith C, Griffin W, Nicoll J (2004) Long-term intracerebral inflammatory response after traumatic brain injury. Forensic Science International 146:97-104.

Giza CC, Hovda DA (2014) The new neurometabolic cascade of concussion. Neurosurgery 75:S24-S33.

Goddeyne C, Nichols J, Wu C, Anderson T (2015) Repetitive mild traumatic brain injury induces ventriculomegaly and cortical thinning in juvenile rats. Journal of Neurophysiology 113:3268-3280.

Goldberg PL, MacNaughton DE, Clements RT, Minnear FL, Vincent PA (2002) p38 MAPK activation by TGF-β1 increases MLC phosphorylation and endothelial monolayer permeability. American Journal of Physiology - Lung Cellular and Molecular Physiology 282:146-154.

Goldman SM, Tanner CM, Oakes D, Bhudhikanok GS, Gupta A, Langston JW (2006) Head injury and Parkinson's disease risk in twins. Annals of Neurology 60:65-72.

Goldstein LE, Fisher AM, Tagge CA, Zhang X-L, Velisek L, Sullivan JA, Upreti C, Kracht JM, Ericsson M, Wojnarowicz MW (2012) Chronic traumatic encephalopathy in blast-exposed military veterans and a blast neurotrauma mouse model. Science Translational Medicine 4:134ra160-134ra160.

Greve MW, Zink BJ (2009) Pathophysiology of traumatic brain injury. Mount Sinai Journal Of Medicine 76:97-104.

Grubenhoff JA, Deakyne SJ, Brou L, Bajaj L, Comstock RD, Kirkwood MW (2014) Acute concussion symptom severity and delayed symptom resolution. Pediatrics 134:54-62.

Gursoy-Ozdemir Y, Qiu J, Matsuoka N, Bolay H, Bermpohl D, Jin H, Wang X, Rosenberg GA, Lo EH, Moskowitz MA (2004) Cortical spreading depression activates and upregulates MMP-9. The Journal of Clinical Investigation 113:1447-1455.

Gursoy-Ozdemir Y, Yemisci M, Dalkara T (2012) Microvascular protection is essential for successful neuroprotection in stroke. Journal of Neurochemistry 123:2-11.

Guskiewicz KM, McCrea M, Marshall SW, Cantu RC, Randolph C, Barr W, Onate JA, Kelly JP (2003) Cumulative effects associated with recurrent concussion in collegiate football players: the NCAA Concussion Study. Journal of the American Medical Association 290:2549-2555.

Hartings JA, Strong AJ, Fabricius M, Manning A, Bhatia R, Dreier JP, Mazzeo AT, Tortella FC, Bullock MR (2009) Spreading depolarizations and late secondary insults after traumatic brain injury. Journal of Neurotrauma 26:1857-1866.

Hartings JA, Bullock MR, Okonkwo DO, Murray LS, Murray GD, Fabricius M, Maas AI, Woitzik J, Sakowitz O, Mathern B (2011) Spreading depolarisations and outcome after traumatic brain injury: a prospective observational study. The Lancet Neurology 10:1058-1064.

Heinemann U, Kaufer D, Friedman A (2012) Blood-brain barrier dysfunction, TGFβ signaling, and astrocyte dysfunction in epilepsy. Glia 60:1251-1257.

Hemphill MA, Dauth S, Yu CJ, Dabiri BE, Parker KK (2015) Traumatic brain injury and the neuronal microenvironment: a potential role for neuropathological mechanotransduction. Neuron 85:1177-1192.

Herculano-Houzel S (2009) The human brain in numbers: a linearly scaled-up primate brain. Frontiers in Human Neuroscience 3:31.

Hue CD, Cho FS, Cao S, Nicholls RE, Vogel III EW, Sibindi C, Arancio O, "Dale" Bass CR, Meaney DF, Morrison III B (2016) Time course and size of blood–brain barrier opening in a mouse model of blast-induced traumatic brain injury. Journal of Neurotrauma 33:1202-1211.

Hyder AA, Wunderlich CA, Puvanachandra P, Gururaj G, Kobusingye OC (2007) The impact of traumatic brain injuries: a global perspective. Neurorehabilitation 22:341-353.

Ivens S, Kaufer D, Flores LP, Bechmann I, Zumsteg D, Tomkins O, Seiffert E, Heinemann U, Friedman A (2006) TGF-β receptor-mediated albumin uptake into astrocytes is involved in neocortical epileptogenesis. Brain 130:535-547.

Janigro D (2012) Are you in or out? Leukocyte, ion, and neurotransmitter permeability across the epileptic blood–brain barrier. Epilepsia 53:26-34.

Jassam YN, Izzy S, Whalen M, McGavern DB, El Khoury J (2017) Neuroimmunology of traumatic brain injury: time for a paradigm shift. Neuron 95:1246-1265.

Jellinger KA, Paulus W, Wrocklage C, Litvan I (2001) Traumatic brain injury as a risk factor for Alzheimer disease. Comparison of two retrospective autopsy cohorts with evaluation of ApoE genotype. Bmc Neurology 1:3.

Johnson KL, Renn C (2006) The hypothalamic-pituitary-adrenal axis in critical illness. Aacn Advanced Critical Care 17:39-49.

Johnson VE, Stewart JE, Begbie FD, Trojanowski JQ, Smith DH, Stewart W (2013) Inflammation and white matter degeneration persist for years after a single traumatic brain injury. Brain 136:28-42.

Johnston KM, McCrory P, Mohtadi NG, Meeuwisse W (2001) Evidence-based review of sport-related concussion. Clinical Journal of Sport Medicine 11:150-159.

Jordan BD (2007) Genetic influences on outcome following traumatic brain injury. Neurochemical Research 32:905-915.

Jordan BD (2013) The clinical spectrum of sport-related traumatic brain injury. Nature Reviews Neurology 9:222.

Kane MJ, Angoa-Pérez M, Briggs DI, Viano DC, Kreipke CW, Kuhn DM (2012) A mouse model of human repetitive mild traumatic brain injury. Journal of Neuroscience Methods 203:41-49.

Kashluba S, Paniak C, Blake T, Reynolds S, Toller-Lobe G, Nagy J (2004) A longitudinal, controlled study of patient complaints following treated mild traumatic brain injury. Archives of Clinical Neuropsychology 19:805-816.

Katayama Y, Becker DP, Tamura T, Hovda DA (1990) Massive increases in extracellular potassium and the indiscriminate release of glutamate following concussive brain injury. Journal of Neurosurgery 73:889-900.

Kay T, Harrington D, Adams R, Anderson T, Berrol S, Cicerone K, Dahlberg C, Gerber D, Goka R, Harley P (1993) Mild traumatic brain injury committee of the head injury interdisciplinary special interest group of the American Congress of Rehabilitation Medicine. Definition of mild traumatic brain injury. Journal of Head Trauma Rehabilitation 8:86-87.

Kazim SF, Shamim MS, Tahir MZ, Enam SA, Waheed S (2011) Management of penetrating brain injury. Journal of Emergencies, Trauma and Shock 4:395.

Kniesel U, Wolburg H (2000) Tight junctions of the blood–brain barrier. Cellular and Molecular Neurobiology 20:57-76.

Knowland D, Arac A, Sekiguchi KJ, Hsu M, Lutz SE, Perrino J, Steinberg GK, Barres BA, Nimmerjahn A, Agalliu D (2014) Stepwise recruitment of transcellular and paracellular pathways underlies blood-brain barrier breakdown in stroke. Neuron 82:603-617.

Korn A, Golan H, Melamed I, Pascual-Marqui R, Friedman A (2005) Focal cortical dysfunction and blood–brain barrier disruption in patients with postconcussion syndrome. Journal of Clinical Neurophysiology 22:1-9.

Kossmann T, Hans V, Imhof H-G, Stocker R, Grob P, Trentz O, Morganti-Kossmann C (1995) Intrathecal and serum interleukin-6 and the acute-phase response in patients with severe traumatic brain injuries. Shock 4:311-317.

Kumar A, Loane DJ (2012) Neuroinflammation after traumatic brain injury: opportunities for therapeutic intervention. Brain, Behavior, and Immunity 26:1191-1201.

Kutner KC, Erlanger DM, Tsai J, Jordan B, Relkin NR (2000) Lower cognitive performance of older football players possessing apolipoprotein E ε4. Neurosurgery 47:651-658.

Lagraoui M, Latoche JR, Cartwright NG, Sukumar G, Dalgard CL, Schaefer BC (2012) Controlled cortical impact and craniotomy induce strikingly similar profiles of inflammatory gene expression, but with distinct kinetics. Frontiers in Neurology 3:155.

Laird MD, Shields JS, Sukumari-Ramesh S, Kimbler DE, Fessler RD, Shakir B, Youssef P, Yanasak N, Vender JR, Dhandapani KM (2014) High mobility group box protein-1 promotes cerebral edema after traumatic brain injury via activation of toll-like receptor 4. Glia 62:26-38.

Laurer HL, Bareyre FM, Lee VM, Trojanowski JQ, Longhi L, Hoover R, Saatman KE, Raghupathi R, Hoshino S, Grady MS (2001) Mild head injury increasing the brain's vulnerability to a second concussive impact. Journal of Neurosurgery 95:859-870.

Lavoie P, Robitaille G, Agharazii M, Ledbetter S, Lebel M, Larivière R (2005) Neutralization of transforming growth factor-β attenuates hypertension and prevents renal injury in uremic rats. Journal of Hypertension 23:1895-1903.

Levy N, Milikovsky DZ, Baranauskas G, Vinogradov E, David Y, Ketzef M, Abutbul S, Weissberg I, Kamintsky L, Fleidervish I (2015) Differential TGF-β Signaling in Glial Subsets Underlies IL-6–Mediated Epileptogenesis in Mice. The Journal of Immunology 195:1713-1722.

Li W, Watts L, Long J, Zhou W, Shen Q, Jiang Z, Li Y, Duong TQ (2016) Spatiotemporal changes in blood-brain barrier permeability, cerebral blood flow, T2 and diffusion following mild traumatic brain injury. Brain Research 1646:53-61.

Li Y-J, Wang Z-H, Zhang B, Zhe X, Wang M-J, Shi S-T, Bai J, Lin T, Guo C-J, Zhang S-J (2013) Disruption of the blood–brain barrier after generalized tonic-clonic seizures correlates with cerebrospinal fluid MMP-9 levels. Journal of Neuroinflammation 10:848.

Lieh-Lai MW, Theodorou AA, Sarnaik AP, Meert KL, Moylan PM, Canady AI (1992) Limitations of the Glasgow Coma Scale in predicting outcome in children with traumatic brain injury. The Journal of Pediatrics 120:195-199.

Lincoln AE, Caswell SV, Almquist JL, Dunn RE, Norris JB, Hinton RY (2011) Trends in concussion incidence in high school sports: a prospective 11-year study. The American Journal of Sports Medicine 39:958-963.

Ling H, Hardy J, Zetterberg H (2015) Neurological consequences of traumatic brain injuries in sports. Molecular and Cellular Neuroscience 66:114-122.

Livak KJ, Schmittgen TD (2001) Analysis of relative gene expression data using real-time quantitative PCR and the 2− ΔΔCT method. Methods 25:402-408.

Lo RS, Massagué J (1999) Ubiquitin-dependent degradation of TGF-β-activated Smad2. Nature Cell Biology 1:472.

Luh C, Gierth K, Timaru-Kast R, Engelhard K, Werner C, Thal SC (2011) Influence of a brief episode of anesthesia during the induction of experimental brain trauma on secondary brain damage and inflammation. Plos One 6:e19948.

Maas AI, Menon DK, Adelson PD, Andelic N, Bell MJ, Belli A, Bragge P, Brazinova A, Büki A, Chesnut RM (2017) Traumatic brain injury: integrated approaches to improve prevention, clinical care, and research. The Lancet Neurology 16:987-1048.

Marchi N, Angelov L, Masaryk T, Fazio V, Granata T, Hernandez N, Hallene K, Diglaw T, Franic L, Najm I (2007) Seizure-promoting effect of blood–brain barrier disruption. Epilepsia 48:732-742.

Marchi N, Bazarian JJ, Puvenna V, Janigro M, Ghosh C, Zhong J, Zhu T, Blackman E, Stewart D, Ellis J (2013) Consequences of repeated blood-brain barrier disruption in football players. Plos One 8:e56805.

Marklund N, Hillered L (2011) Animal modelling of traumatic brain injury in preclinical drug development: where do we go from here? British Journal of Pharmacology 164:1207-1229.

Marmarou A, Foda MAA-E, Van Den Brink W, Campbell J, Kita H, Demetriadou K (1994) A new model of diffuse brain injury in rats: Part I: Pathophysiology and biomechanics. Journal of Neurosurgery 80:291-300.

Maroso M, Balosso S, Ravizza T, Liu J, Aronica E, Iyer AM, Rossetti C, Molteni M, Casalgrandi M, Manfredi AA (2010) Toll-like receptor 4 and high-mobility group box-1 are involved in ictogenesis and can be targeted to reduce seizures. Nature Medicine 16:413.

Massagué J (2000) How cells read TGF-β signals. Nature Reviews Molecular Cell Biology 1:169.

McAllister TW (2011) Neurobiological consequences of traumatic brain injury. Dialogues in Clinical Neuroscience 13:287.

McAllister TW, Rhodes CH, Flashman LA, McDonald BC, Belloni D, Saykin AJ (2005) Effect of the dopamine D2 receptor T allele on response latency after mild traumatic brain injury. American Journal of Psychiatry 162:1749-1751.

McCrory P, Meeuwisse W, Johnston K, Dvorak J, Aubry M, Molloy M, Cantu R (2009) Consensus statement on Concussion in Sport–the 3rd International Conference on Concussion in Sport held in Zurich, November 2008. South African Journal of Sports Medicine 21.

McCrory P, Johnston K, Meeuwisse W, Aubry M, Cantu R, Dvorak J, Graf-Baumann T, Kelly J, Lovell M, Schamasch P (2005) Summary and agreement statement of the 2nd international conference on Concussion in Sport, Prague 2004. British Journal of Sports Medicine 39:196-204.

McCrory P, Meeuwisse WH, Aubry M, Cantu RC, Dvorak J, Echemendia RJ, Engebretsen L, Johnston KM, Kutcher JS, Raftery M (2013) Consensus statement on concussion in sport—the 4th international conference on Concussion in Sport held in Zurich, November 2012. Pm&R 5:255-279.

McCrory P, Meeuwisse W, Dvorak J, Aubry M, Bailes J, Broglio S, Cantu RC, Cassidy D, Echemendia RJ, Castellani RJ (2017a) Consensus statement on concussion in sport—the 5th international conference on concussion in sport held in Berlin, October 2016. Br J Sports Med 51:838-847.

McCrory P et al. (2017b) Consensus statement on concussion in sport - the 5th international conference on concussion in sport held in Berlin, October 2016. Br J Sports Med 51:838-847.

McCrory PR, Berkovic SF (1998) Concussive convulsions. Sports Medicine 25:131-136.

McCrory PR, Berkovic SF (2000) Video analysis of acute motor and convulsive manifestations in sport-related concussion. Neurology 54:1488-1491.

McCrory PR, Johnston KM (2002) Acute clinical symptoms of concussion: assessing prognostic significance. The Physician and Sportsmedicine 30:43-47.

McCrory PR, Bladin PF, Berkovic SF (1997) Retrospective study of concussive convulsions in elite Australian rules and rugby league footballers: phenomenology, aetiology, and outcome. BMJ 314:171.

McCutcheon JE, Marinelli M (2009) Age matters. European Journal of Neuroscience 29:997-1014.

McKee AC, Robinson ME (2014) Military-related traumatic brain injury and neurodegeneration. Alzheimer's & Dementia 10:S242-S253.

McKee AC, Stein TD, Kiernan PT, Alvarez VE (2015) The neuropathology of chronic traumatic encephalopathy. Brain Pathology 25:350-364.

McKee AC, Cantu RC, Nowinski CJ, Hedley-Whyte ET, Gavett BE, Budson AE, Santini VE, Lee H-S, Kubilus CA, Stern RA (2009) Chronic traumatic encephalopathy in athletes: progressive tauopathy after repetitive head injury. Journal of Neuropathology & Experimental Neurology 68:709-735.

McKee AC, Gavett BE, Stern RA, Nowinski CJ, Cantu RC, Kowall NW, Perl DP, Hedley-Whyte ET, Price B, Sullivan C (2010) TDP-43 proteinopathy and motor neuron disease in chronic traumatic encephalopathy. Journal of Neuropathology & Experimental Neurology 69:918-929.

McKee AC, Stein TD, Nowinski CJ, Stern RA, Daneshvar DH, Alvarez VE, Lee H-S, Hall G, Wojtowicz SM, Baugh CM (2013) The spectrum of disease in chronic traumatic encephalopathy. Brain 136:43-64.

McKee AC, Cairns NJ, Dickson DW, Folkerth RD, Keene CD, Litvan I, Perl DP, Stein TD, Vonsattel J-P, Stewart W (2016) The first NINDS/NIBIB consensus meeting to define neuropathological criteria for the diagnosis of chronic traumatic encephalopathy. Acta Neuropathologica 131:75-86.

McLendon LA, Kralik SF, Grayson PA, Golomb MR (2016) The controversial second impact syndrome: a review of the literature. Pediatric Neurology 62:9-17.

McMillin MA, Frampton GA, Seiwell AP, Patel NS, Jacobs AN, DeMorrow S (2015) TGFβ1 exacerbates blood–brain barrier permeability in a mouse model of hepatic encephalopathy via upregulation of MMP9 and downregulation of claudin-5. Laboratory Investigation 95:903.

Meaney DF, Smith DH (2011) Biomechanics of concussion. Clinics in Sports Medicine 30:19-31.

Miller JH, Gill C, Kuhn EN, Rocque BG, Menendez JY, O'Neill JA, Agee BS, Brown ST, Crowther M, Davis RD (2016) Predictors of delayed recovery following pediatric sports-related concussion: a case-control study. Journal of Neurosurgery: Pediatrics 17:491-496.

Minagar A, Alexander JS (2003) Blood-brain barrier disruption in multiple sclerosis. Multiple Sclerosis Journal 9:540-549.

Miyazono K (2000) Positive and negative regulation of TGF-beta signaling. Journal of Cell Science 113:1101-1109.

Montagne A, Barnes SR, Sweeney MD, Halliday MR, Sagare AP, Zhao Z, Toga AW, Jacobs RE, Liu CY, Amezcua L (2015) Blood-brain barrier breakdown in the aging human hippocampus. Neuron 85:296-302.

Morganti-Kossmann MC, Hans VH, Lenzlinger PM, Dubs R, Ludwig E, Trentz O, Kossmann T (1999) TGF-β is elevated in the CSF of patients with severe traumatic brain injuries and parallels blood-brain barrier function. Journal of Neurotrauma 16:617-628.

Morris R (1984) Developments of a water-maze procedure for studying spatial learning in the rat. Journal of Neuroscience Methods 11:47-60.

Mortezaee K, Khanlarkhani N, Beyer C, Zendedel A (2018) Inflammasome: its role in traumatic brain and spinal cord injury. Journal of Cellular Physiology 233:5160-5169.

Mortimer J, Van Duijn C, Chandra V, Fratiglioni L, Graves A, Heyman A, Jorm A, Kokmen E, Kondo K, Rocca WA (1991) Head trauma as a risk factor for Alzheimer's disease: a collaborative re-analysis of case-control studies. International Journal of Epidemiology 20:S28-S35.

Mychasiuk R, Farran A, Esser MJ (2014) Assessment of an experimental rodent model of pediatric mild traumatic brain injury. Journal of Neurotrauma 31:749-757.

Nag S, Venugopalan R, Stewart DJ (2007) Increased caveolin-1 expression precedes decreased expression of occludin and claudin-5 during blood–brain barrier breakdown. Acta Neuropathologica 114:459-469.

Nag S, Manias J, Stewart D (2009) Expression of endothelial phosphorylated caveolin-1 is increased in brain injury. Neuropathology and Applied Neurobiology 35:417-426.

Namjoshi DR, Good C, Cheng WH, Panenka W, Richards D, Cripton PA, Wellington CL (2013) Towards clinical management of traumatic brain injury: a review of models and mechanisms from a biomechanical perspective. Disease Models & Mechanisms 6:1325-1338.

Nimmerjahn A, Kirchhoff F, Helmchen F (2005) Resting microglial cells are highly dynamic surveillants of brain parenchyma in vivo. Science 308:1314-1318.

Noble JM, Hesdorffer DC (2013) Sport-related concussions: a review of epidemiology, challenges in diagnosis, and potential risk factors. Neuropsychology Review 23:273-284.

Oldendorf WH, Cornford ME, Brown WJ (1977) The large apparent work capability of the blood-brain barrier: a study of the mitochondrial content of capillary endothelial cells in brain and other tissues of the rat. Annals of Neurology 1:409-417.

Omalu BI, DeKosky ST, Minster RL, Kamboh MI, Hamilton RL, Wecht CH (2005) Chronic traumatic encephalopathy in a National Football League player. Neurosurgery 57:128-134.

Omalu BI, DeKosky ST, Hamilton RL, Minster RL, Kamboh MI, Shakir AM, Wecht CH (2006) Chronic traumatic encephalopathy in a national football league player: part II. Neurosurgery 59:1086-1093.

Ommaya AK, Gennarelli T (1974) Cerebral concussion and traumatic unconsciousness: correlation of experimental and clinical observations on blunt head injuries. Brain 97:633-654.

Ongali B, Nicolakakis N, Tong X-K, Aboulkassim T, Papadopoulos P, Rosa-Neto P, Lecrux C, Imboden H, Hamel E (2014) Angiotensin II type 1 receptor blocker losartan prevents and rescues cerebrovascular, neuropathological and cognitive deficits in an Alzheimer's disease model. Neurobiology of Disease 68:126-136.

Onyszchuk G, Al-Hafez B, He Y-Y, Bilgen M, Berman NE, Brooks WM (2007) A mouse model of sensorimotor controlled cortical impact: characterization using longitudinal magnetic resonance imaging, behavioral assessments and histology. Journal of Neuroscience Methods 160:187-196.

Paniak C, Reynolds S, Phillips K, Toller-Lobe G, Melnyk A, Nagy J (2002) Patient complaints within 1 month of mild traumatic brain injury: A controlled study. Archives of Clinical Neuropsychology 17:319-334.

Park JS, Svetkauskaite D, He Q, Kim J-Y, Strassheim D, Ishizaka A, Abraham E (2004) Involvement of toll-like receptors 2 and 4 in cellular activation by high mobility group box 1 protein. Journal of Biological Chemistry 279:7370-7377.

Patel RK, Prasad N, Kuwar R, Haldar D, Abdul-Muneer P (2017) Transforming growth factor-beta 1 signaling regulates neuroinflammation and apoptosis in mild traumatic brain injury. Brain, Behavior, and Immunity 64:244-258.

Pavlovic D, Pekic S, Stojanovic M, Popovic V (2019) Traumatic brain injury: neuropathological, neurocognitive and neurobehavioral sequelae. Pituitary 22:270-282.

Pechlivanova DM, Stoynev AG, Tchekalarova JD (2011) The effects of chronic losartan pretreatment on restraint stress-induced changes in motor activity, nociception and pentylenetetrazol generalized seizures in rats. Folia Medica 53:69-73.

Perron AD, Brady WJ, Huff JS (2001) Concussive convulsions: emergency department assessment and management of a frequently misunderstood entity. Academic Emergency Medicine 8:296-298.

Phillips DJ, Nguyen P, Adamides AA, Bye N, Rosenfeld JV, Kossmann T, Vallance S, Murray L, Morganti-Kossmann MC (2006) Activin a release into cerebrospinal fluid in a subset of patients with severe traumatic brain injury. Journal of Neurotrauma 23:1283-1294.

Prager O, Kamintsky L, Hasam-Henderson LA, Schoknecht K, Wuntke V, Papageorgiou I, Swolinsky J, Muoio V, Bar-Klein G, Vazana U (2019) Seizure-induced microvascular injury is associated with impaired neurovascular coupling and blood–brain barrier dysfunction. Epilepsia 60:322-336.

Rabender C, Mezzaroma E, Mauro AG, Mullangi R, Abbate A, Anscher M, Hart B, Mikkelsen R (2016) IPW-5371 Proves Effective as a Radiation Countermeasure by Mitigating Radiation-Induced Late Effects. Radiat Res 186:478-488.

Ritchie E, Emery C, Debert C (2018) Analysis of serum cortisol to predict recovery in paediatric sport-related concussion. Brain Injury 32:523-528.

Rodríguez-Baeza A, Reina-de la Torre F, Poca A, Martí M, Garnacho A (2003) Morphological features in human cortical brain microvessels after head injury: a three-dimensional and immunocytochemical study. The Anatomical Record Part A: Discoveries In Molecular, Cellular, And Evolutionary Biology: An Official Publication of The American Association of Anatomists 273:583-593.

Rolfe D, Brown GC (1997) Cellular energy utilization and molecular origin of standard metabolic rate in mammals. Physiological Reviews 77:731-758.

Roozenbeek B, Maas AI, Menon DK (2013) Changing patterns in the epidemiology of traumatic brain injury. Nature Reviews Neurology 9:231-236.

Rosenbaum SB, Lipton ML (2012) Embracing chaos: the scope and importance of clinical and pathological heterogeneity in mTBI. Brain Imaging and Behavior 6:255-282.

Rosenfeld JV, McFarlane AC, Bragge P, Armonda RA, Grimes JB, Ling GS (2013) Blast-related traumatic brain injury. The Lancet Neurology 12:882-893.

Rowson S, Duma SM (2013) Brain injury prediction: assessing the combined probability of concussion using linear and rotational head acceleration. Annals of Biomedical Engineering 41:873-882.

Rüber T, David B, Lüchters G, Nass RD, Friedman A, Surges R, Stöcker T, Weber B, Deichmann R, Schlaug G (2018) Evidence for peri-ictal blood–brain barrier dysfunction in patients with epilepsy. Brain 141:2952-2965.

Saatman KE, Feeko KJ, Pape RL, Raghupathi R (2006) Differential behavioral and histopathological responses to graded cortical impact injury in mice. Journal of Neurotrauma 23:1241-1253.

Saatman KE, Duhaime A-C, Bullock R, Maas AI, Valadka A, Manley GT (2008) Classification of traumatic brain injury for targeted therapies. Journal of Neurotrauma 25:719-738.

Santiago LA, Oh BC, Dash PK, Holcomb JB, Wade CE (2012) A clinical comparison of penetrating and blunt traumatic brain injuries. Brain Injury 26:107-125.

Saunders NR, Dziegielewska KM, Mollgard K, Habgood MD (2015) Markers for blood-brain barrier integrity: how appropriate is Evans blue in the twenty-first century and what are the alternatives? Frontiers in Neuroscience 9:385.

Scaffidi P, Misteli T, Bianchi ME (2002) Release of chromatin protein HMGB1 by necrotic cells triggers inflammation. Nature 418:191.

Sedlakova R, Shivers R, Del RM (1999) Ultrastructure of the blood-brain barrier in the rabbit. Journal of Submicroscopic Cytology and Pathology 31:149-161.

Seiffert E, Dreier JP, Ivens S, Bechmann I, Tomkins O, Heinemann U, Friedman A (2004) Lasting blood-brain barrier disruption induces epileptic focus in the rat somatosensory cortex. Journal of Neuroscience 24:7829-7836.

Senatorov VV, Friedman AR, Milikovsky DZ, Ofer J, Saar-Ashkenazy R, Charbash A, Jahan N, Chin G, Mihaly E, Lin JM (2019) Blood-brain barrier dysfunction in aging induces hyper-activation of TGF-beta signaling and chronic yet reversible neural dysfunction. BioRXiv:537431.

Sengupta P (2013) The laboratory rat: relating its age with human's. International Journal of Preventive Medicine 4:624.

Serlin Y, Shelef I, Knyazer B, Friedman A (2015) Anatomy and physiology of the blood–brain barrier. In: Seminars In Cell & Developmental Biology, pp 2-6: Elsevier.

Shapira Y, Setton D, Artru A, Shohami E (1993) Blood-brain barrier permeability, cerebral edema, and neurologic function after closed head injury in rats. Anesthesia and Analgesia 77:141-148.

Shehata N, Wiley J, Richea S, Benson BW, Duits L, Meeuwisse W (2009) Sport concussion assessment tool: baseline values for varsity collision sport athletes. British Journal of Sports Medicine 43:730-734.

Shen W-X, Chen J-H, Lu J-H, Peng Y-P, Qiu Y-H (2014) TGF-β1 protection against Aβ1–42-induced neuroinflammation and neurodegeneration in rats. International Journal of Molecular Sciences 15:22092-22108.

Shi Y, Massagué J (2003) Mechanisms of TGF-β signaling from cell membrane to the nucleus. Cell 113:685-700.

Shigemori Y, Katayama Y, Mori T, Maeda T, Kawamata T (2006) Matrix metalloproteinase-9 is associated with blood-brain barrier opening and brain edema formation after cortical contusion in rats. In: Brain Edema Xiii, pp 130-133: Springer.

Shlosberg D, Benifla M, Kaufer D, Friedman A (2010) Blood–brain barrier breakdown as a therapeutic target in traumatic brain injury. Nature Reviews Neurology 6:393.

Shohami E, Gallily R, Mechoulam R, Bass R, Ben-Hur T (1997) Cytokine production in the brain following closed head injury: dexanabinol (HU-211) is a novel TNF-α inhibitor and an effective neuroprotectant. Journal of Neuroimmunology 72:169-177.

Shultz SR, Bao F, Omana V, Chiu C, Brown A, Cain DP (2012) Repeated mild lateral fluid percussion brain injury in the rat causes cumulative long-term behavioral impairments, neuroinflammation, and cortical loss in an animal model of repeated concussion. Journal of Neurotrauma 29:281-294.

Simon DW, McGeachy MJ, Bayır H, Clark RS, Loane DJ, Kochanek PM (2017) The far-reaching scope of neuroinflammation after traumatic brain injury. Nature Reviews Neurology 13:171.

Slobounov S, Slobounov E, Sebastianelli W, Cao C, Newell K (2007) Differential rate of recovery in athletes after first and second concussion episodes. Neurosurgery 61:338-344; discussion 344.

Smeda JS, McGuire JJ (2007) Effects of poststroke losartan versus captopril treatment on myogenic and endothelial function in the cerebrovasculature of SHRsp. Stroke 38:1590-1596.

Smeda JS, Daneshtalab N (2011) The effects of poststroke captopril and losartan treatment on cerebral blood flow autoregulation in SHRsp with hemorrhagic stroke. Journal of Cerebral Blood Flow & Metabolism 31:476-485.

Smith DH, Meaney DF (2000) Axonal damage in traumatic brain injury. The Neuroscientist 6:483-495.

Smith DH, Soares HD, Pierce JS, Perlman KG, Saatman KE, Meaney DF, Dixon CE, McIntosh TK (1995) A model of parasagittal controlled cortical impact in the mouse: cognitive and histopathologic effects. Journal of Neurotrauma 12:169-178.

Stahel PF, Shohami E, Younis FM, Kariya K, Otto VI, Lenzlinger PM, Grosjean MB, Eugster H-P, Trentz O, Kossmann T (2000) Experimental closed head injury: analysis of neurological outcome, blood–brain barrier dysfunction, intracranial neutrophil infiltration, and neuronal cell death in mice deficient in genes for pro-inflammatory cytokines. Journal of Cerebral Blood Flow & Metabolism 20:369-380.

Statler KD, Alexander H, Vagni V, Holubkov R, Dixon CE, Clark RS, Jenkins L, Kochanek PM (2006) Isoflurane exerts neuroprotective actions at or near the time of severe traumatic brain injury. Brain Research 1076:216-224.

Stern RA, Daneshvar DH, Baugh CM, Seichepine DR, Montenigro PH, Riley DO, Fritts NG, Stamm JM, Robbins CA, McHale L (2013) Clinical presentation of chronic traumatic encephalopathy. Neurology 81:1122-1129.

Strauss KI, Barbe MF, Marshall RM, Raghupathi R, Mehta S, Narayan RK (2000) Prolonged cyclooxygenase-2 induction in neurons and glia following traumatic brain injury in the rat. Journal of Neurotrauma 17:695-711.

Strich SJ (1956) Diffuse degeneration of the cerebral white matter in severe dementia following head injury. Journal of Neurology, Neurosurgery, and Psychiatry 19:163.

Suliman HB, Piantadosi CA (2016) Mitochondrial quality control as a therapeutic target. Pharmacological Reviews 68:20-48.

Sweeney MD, Sagare AP, Zlokovic BV (2018) Blood–brain barrier breakdown in Alzheimer disease and other neurodegenerative disorders. Nature Reviews Neurology 14:133.

Tagge CA, Fisher AM, Minaeva OV, Gaudreau-Balderrama A, Moncaster JA, Zhang X-L, Wojnarowicz MW, Casey N, Lu H, Kokiko-Cochran ON (2018) Concussion, microvascular injury, and early tauopathy in young athletes after impact head injury and an impact concussion mouse model. Brain 141:422-458.

Tang Y-p, Noda Y, Hasegawa T, Nabeshima T (1997) A concussive-like brain injury model in mice (II): selective neuronal loss in the cortex and hippocampus. Journal of Neurotrauma 14:863-873.

Tanno H, Nockels RP, Pitts LH, Noble L (1992) Breakdown of the blood–brain barrier after fluid percussive brain injury in the rat. Part 1: distribution and time course of protein extravasation. Journal of Neurotrauma 9:21-32.

Teasdale G, Jennett B (1974) Assessment of coma and impaired consciousness: a practical scale. The Lancet 304:81-84.

Teasdale G, Maas A, Lecky F, Manley G, Stocchetti N, Murray G (2014) The Glasgow Coma Scale at 40 years: standing the test of time. The Lancet Neurology 13:844-854.

Tényi D, Gyimesi C, Horváth R, Kovács N, Ábrahám H, Darnai G, Fogarasi A, Büki A, Janszky J (2016) Concussive convulsions: a YouTube video analysis. Epilepsia 57:1310-1316.

Thompson HJ, Lifshitz J, Marklund N, Grady MS, Graham DI, Hovda DA, McIntosh TK (2005) Lateral fluid percussion brain injury: a 15-year review and evaluation. Journal of Neurotrauma 22:42-75.

Tomkins O, Friedman O, Ivens S, Reiffurth C, Major S, Dreier J, Heinemann U, Friedman A (2007) Blood–brain barrier disruption results in delayed functional and structural alterations in the rat neocortex. Neurobiology of Disease 25:367-377.

Tomkins O, Shelef I, Kaizerman I, Eliushin A, Afawi Z, Misk A, Gidon M, Cohen A, Zumsteg D, Friedman A (2008) Blood–brain barrier disruption in post-traumatic epilepsy. Journal of Neurology, Neurosurgery & Psychiatry 79:774-777.

Tortosa JG, Martínez-Lage JF, Poza M (2004) Bitemporal head crush injuries: clinical and radiological features of a distinctive type of head injury. Journal of Neurosurgery 100:645-651.

VA/DoD (2009) VA/DoD clinical practice guideline for management of concussion/mild traumatic brain injury. Journal of Rehabilitation Research & Development 46.

VA/DoD (2016) VA/DoD Clinical Practice Guideline for the Management of Concussion-Mild Traumatic Brain Injury. In: US Department of Veterans Affairs, Department of Defence.

Vorhees CV, Williams MT (2006) Morris water maze: procedures for assessing spatial and related forms of learning and memory. Nature Protocols 1:848.

Weinstein E, Turner M, Kuzma BB, Feuer H (2013) Second impact syndrome in football: new imaging and insights into a rare and devastating condition: case report. Journal of Neurosurgery: Pediatrics 11:331-334.

Weissberg I, Veksler R, Kamintsky L, Saar-Ashkenazy R, Milikovsky DZ, Shelef I, Friedman A (2014) Imaging blood-brain barrier dysfunction in football players. Journal of the American Medical Association Neurology 71:1453-1455.

Weissberg I, Wood L, Kamintsky L, Vazquez O, Milikovsky DZ, Alexander A, Oppenheim H, Ardizzone C, Becker A, Frigerio F (2015) Albumin induces excitatory synaptogenesis through astrocytic TGF-β/ALK5 signaling in a model of acquired epilepsy following blood–brain barrier dysfunction. Neurobiology of Disease 78:115-125.

Willer B, Leddy JJ (2006) Management of concussion and post-concussion syndrome. Current Treatment Options in Neurology 8:415-426.

Wojnarowicz MW, Fisher AM, Minaeva O, Goldstein LE (2017) Considerations for experimental animal models of concussion, traumatic brain injury, and chronic traumatic encephalopathy—these matters matter. Frontiers in Neurology 8:240.

Woodroofe M, Sarna G, Wadhwa M, Hayes G, Loughlin A, Tinker A, Cuzner M (1991) Detection of interleukin-1 and interleukin-6 in adult rat brain, following mechanical injury, by in vivo microdialysis: evidence of a role for microglia in cytokine production. Journal of Neuroimmunology 33:227-236.

Wrana JL (2000) Regulation of Smad activity. Cell 100:189-192.

Xiong Y, Mahmood A, Chopp M (2013) Animal models of traumatic brain injury. Nature Reviews Neuroscience 14:128.

Yagi K, Goto D, Hamamoto T, Takenoshita S, Kato M, Miyazono K (1999) Alternatively spliced variant of Smad2 lacking exon 3: Comparison with wild-type Smad2 and Smad3. Journal of Biological Chemistry 274:703-709.

Yang SH, Gangidine M, Pritts TA, Goodman MD, Lentsch AB (2013) Interleukin 6 mediates neuroinflammation and motor coordination deficits after mild traumatic brain injury and brief hypoxia in mice. Shock 40:471.

Yeung D, Manias JL, Stewart DJ, Nag S (2008) Decreased junctional adhesion molecule-A expression during blood–brain barrier breakdown. Acta Neuropathologica 115:635-642.

Yoo R-E, Choi SH, Oh B-M, Do Shin S, Lee EJ, Shin DJ, Jo SW, Kang KM, Yun TJ, Kim J-h (2019) Quantitative dynamic contrast-enhanced MR imaging shows widespread blood-brain barrier disruption in mild traumatic brain injury patients with post-concussion syndrome. European Radiology 29:1308-1317.

Zhang L, Yang KH, King AI (2004) A proposed injury threshold for mild traumatic brain injury. Journal of Biomechanical Engineering 126:226-236.

Zhang TL, Fu JL, Geng Z, Yang JJ, Sun XJ (2012) The neuroprotective effect of losartan through inhibiting AT1/ASK1/MKK4/JNK3 pathway following cerebral I/R in rat hippocampal CA1 region. CNS Neuroscience & Therapeutics 18:981-987.

Zhu Y, Yang G-Y, Ahlemeyer B, Pang L, Che X-M, Culmsee C, Klumpp S, Krieglstein J (2002) Transforming growth factor-β1 increases bad phosphorylation and protects neurons against damage. Journal of Neuroscience 22:3898-3909.

Zlokovic BV (2005) Neurovascular mechanisms of Alzheimer's neurodegeneration. Trends in Neurosciences 28:202-208.

Zlokovic BV (2011) Neurovascular pathways to neurodegeneration in Alzheimer's disease and other disorders. Nature Reviews Neuroscience 12:723.

Appendix A: Impact Apparatus

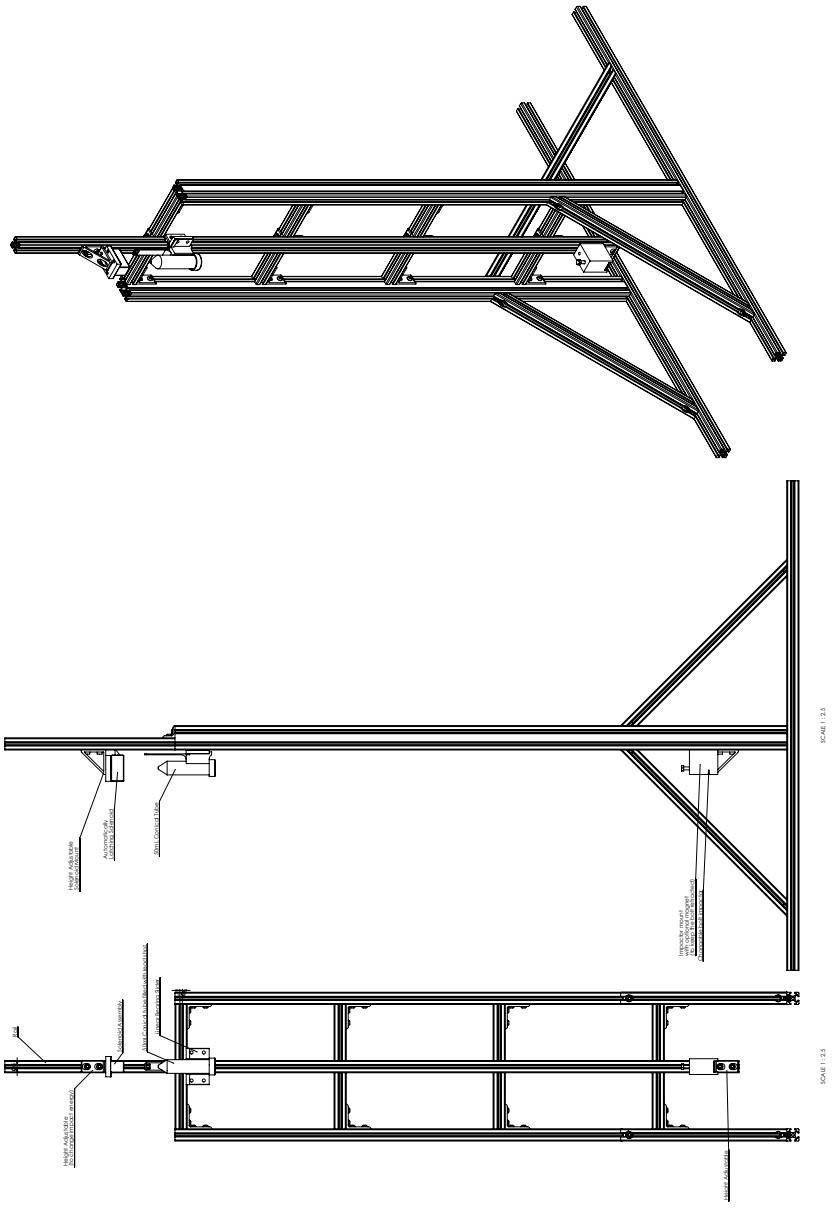

Figure A.1: Blueprint of impact apparatus used for administration of TBI

Appendix B: Individual Behavioural Task Scores Following Single Mild TBI

A

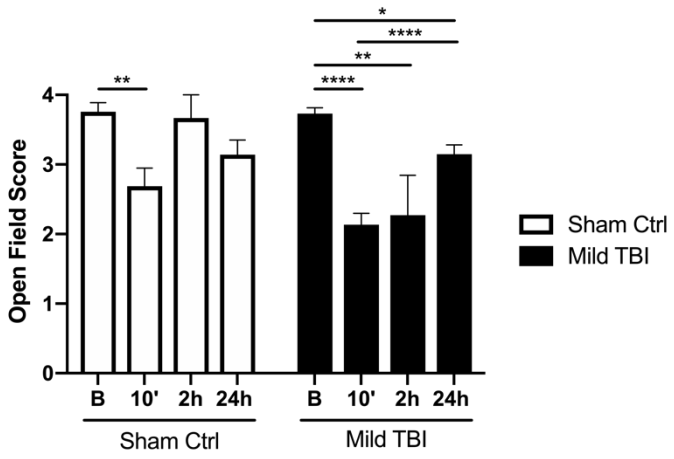

B

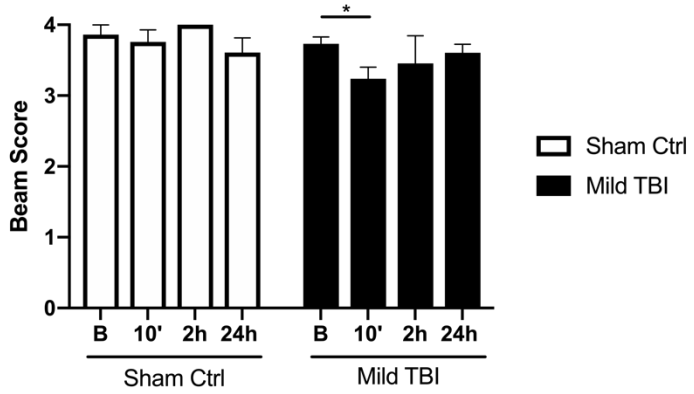

C

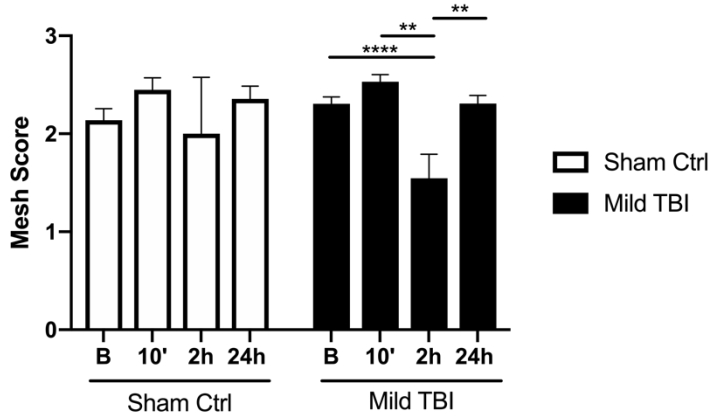

Figure B.1: Individual behavioural task breakdown following single mild TBI
Behaviour scores for individual behavioural tests (see Chapter 2, Table 2.1) used to form a combined neurological score. **(A)** Open field scores for sham control and single mild TBI animals are shown. Sham controls (n = 29) had decreased scores in the open field test 10 minutes after exposure to anesthesia (P = 0.0020) compared to baseline. No differences in open field scores were present when tested 2 hours (P = 0.9990; n = 3) or 24 hours (P = 0.1531; n = 28) after exposure to anesthesia compared to baseline. In contrast, mild TBI animals (n = 81) had a significant reduction in open field score 10 minutes (P < 0.0001), 2 hours (P = 0.0012; n = 11), and 24 hours (P = 0.0123; n = 81) after exposure to mild TBI compared to baseline. 24 hours post-impact, mild TBI animals had higher open field scores than 10 minutes post-impact (P = < 0.0001). **(B)** Beam walk scores for sham control and single mild TBI animals are shown. Sham controls did not differ in beam walk scoring when tested 10 minutes, 2 hours, or 24 hours after exposure to anesthesia compared to baseline (P = 0.7204). In contrast, mild TBI animals had a significant decrease in beam walk score 10 minutes (P = 0.0199) post-impact but did not differ 2 hours or 24 hours after exposure to mild TBI compared to baseline. **(C)** Inverted wire mesh scores for sham control and single mild TBI animals are shown. Sham controls did not differ in inverted wire mesh scoring when tested 10 minutes, 2 hours, or 24 hours after exposure to anesthesia compared to baseline (P = 0.2806). In contrast, mild TBI animals had a significant reduction in inverted wire mesh score 2 hours post-impact (P = 0.0035) but did not differ 10 minutes (P = 0.1534) or 24 hours (P > 0.9999) after exposure to mild TBI compared to baseline. 2 hours post-impact, inverted wire mesh scores were lower than at 10 minutes (P < 0.0001) or 24 hours (P = 0.0034) post-impact. Statistical analyses involved one-way ANOVA with Tukey's post-hoc test.

Appendix C: Percentage of Sensitive Animals Per Animal Order

A

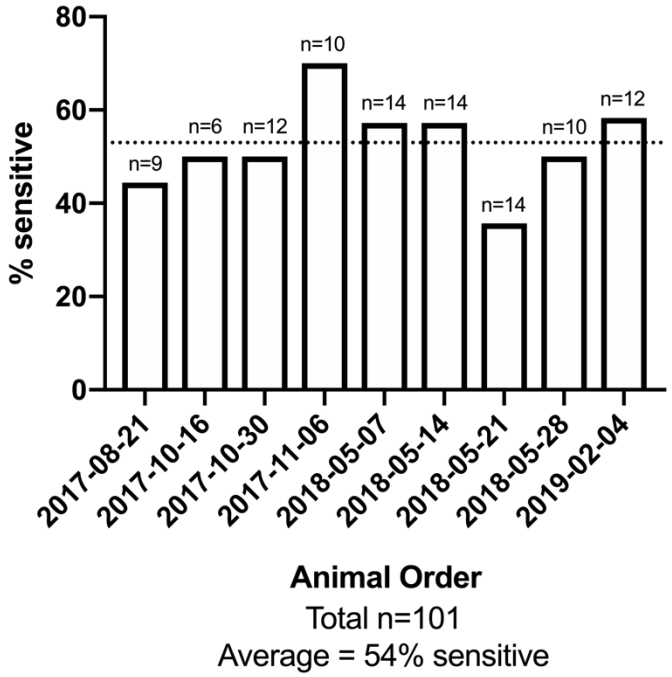

Figure C.1: Percentage of sensitive animals per animal order. (A) The percentage of animals that retrospectively met criteria for sensitivity are shown for various animal orders over time for the experiments described in this thesis. Sensitivity to rmTBI was reliably observed with each cohort of animals that underwent the rmTBI protocol.

Appendix D: Relative Sensitivity of Pressure-Sensitive Film

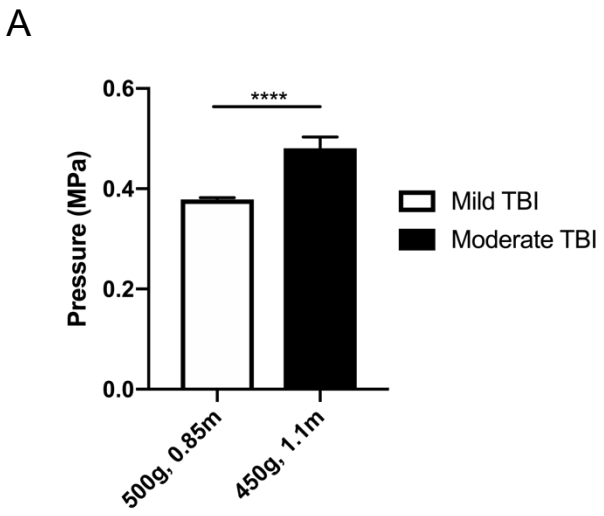

Figure D.1: Relative sensitivity of pressure sensitive film. (A) Pressure measurements for mild impacts (n = 191) with an impact mass of 500g and fall distance of 0.85m (as described in this thesis) are lower than pressure measurements for input parameters of 450g impact mass and 1.1m fall distance (model for moderate TBI, n = 44) ($P < 0.0001$). This data provides an indication of the relative sensitivity of the pressure film to impacts of varying impact parameters and injuries.

Appendix E: Corticosterone Response to Single Mild TBI Differs Between Sensitive and Resilient Animals

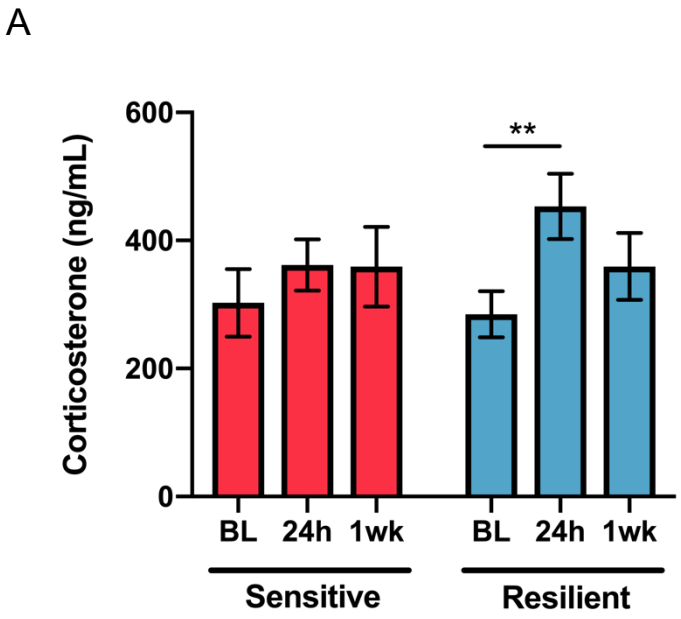

Figure E.1: Corticosterone response to single mild TBI differs between sensitive and resilient animals. (A) Serum was collected from sensitive (n = 12) and resilient (n = 16) animals at baseline, 24 hours after a single mild TBI, and 1 week after repetitive mild TBIs were administered and serum corticosterone levels were quantified. Sensitive animals did not differ in serum corticosterone levels 24 hours (P = 0.3667) or 1 week (P = 0.6755) post-impact compared to baseline. In contrast, serum corticosterone levels of resilient animals increased significantly after a single mild impact (P = 0.0027) compared to baseline, although did not differ one week after repetitive impacts were administered (P = 0.2522). Wilcoxon matched-pairs signed rank test was used for statistical analyses.